



Justus-Liebig-Universität Gießen

Klinik Für Neurologie



Evaluation of the Fibroblast growth factor receptor 1 (FGFR1) in Experimental Autoimmune Encephalomyelitis (EAE)

Inaugural Dissertation

Submitted

In partial fulfillment of the requirements
for the Dr. rer. nat. Degree
To the Faculty of Biology and Chemistry
Of the Justus Liebig University Giessen, Germany

By

Ranjithkumar Rajendran, M.Sc.

(29.07.1983)

From Karipatty,
Salem, Tamil Nadu, India

Giessen, 2014
Germany

Multiple Sclerosis Research Group

Klinik für Neurologie
Justus-Liebig-Universität Gießen
Prof. Dr. Manfred Kaps

First Supervisor:

Prof. Dr. Reinhard Lakes-Harlan

Faculty 8 Biology and Chemistry
Institute of Animal Physiology
Department of Integrative Sensory Physiology
Justus-Liebig-Universität Gießen, Germany

Second Supervisor:

PD Dr. med. Martin Berghoff

Faculty 11 Medicine
Multiple Sclerosis Research Group
Klinik für Neurologie
Justus-Liebig-Universität Gießen, Germany

Committee members:

Prof. Dr. med. Manfred Kaps

Department of Neurology
Justus-Liebig-University Giessen

Prof. Dr. rer. nat. Michael U. Martin

Immunology FB08 - Biology and Chemistry
Justus-Liebig-University Giessen

Date of the Doctoral Defense: 19.02.2015

I dedicate this Thesis
To my Family (esp. my Grandmother) and Friends
&
To a large extent the Mother Nature

I love you all dearly

Save the Soil



திருக்குறள்

அகர முதல எழுத்தெல்லாம் ஆதி
பகவன் முதற்றே உலகு

திருவள்ளுவர்

Tirukkural

*A, as its first of letters, every speech maintains; so the world has
the eternal God for its first*

Thiruvalluvar

DECLARATION

I hereby declare that the present thesis is my original work and that it has not been previously presented in this or any other university for any degree. I have also abided by the principles of good scientific conduct laid down in the charter of the Justus Liebig University of Giessen in carrying out the investigations described in the dissertation.

By

.....

Ranjithkumar Rajendran

Giessen, Germany

INDEX

INDEX.....	I
ABBREVIATIONS.....	IV
LIST OF FIGURES.....	V
LIST OF TABLES.....	VI
ABSTRACT.....	VII
 1 INTRODUCTION.....	 1
1.1 Multiple sclerosis (MS).....	1
1.1.1 Etiology of MS.....	1
1.1.2 MS symptoms.....	2
1.1.3 Subtypes of MS.....	3
1.1.4 MS pathology.....	3
1.1.5 MS diagnosis.....	5
1.1.6 MS treatment.....	7
1.2 Experimental autoimmune encephalomyelitis (EAE).....	8
1.3 Oligodendrocytes in MS and EAE.....	11
1.4 Fibroblast growth factors (FGFs).....	12
1.5 Fibroblast growth factor receptors (FGFR).....	14
1.6 Fibroblast growth factor/FGF receptor interaction.....	16
1.7 FGFR1 in oligodendrocyte lineage.....	18
1.8 FGF/FGFR1 in demyelinating disease MS and its animal model EAE.....	19
1.9 FGF/FGFR signalling in disease.....	20
1.10 FGFR inhibitors in clinical trials.....	21
 2 AIMS.....	 23
 3 MATERIALS AND METHODS.....	 24
3.1 MATERIALS.....	24
3.1.1 Animals.....	24
3.1.2 Cell lines.....	24
3.1.3 Primary antibodies.....	25
3.1.4 Secondary antibodies.....	26
3.1.5 Kits.....	26
3.1.6 Primers.....	26
3.1.7 Ladders.....	28

3.1.8 Chemicals	28
3.1.9 Laboratory consumables	29
3.1.10 Laboratory instruments	30
3.1.11 Buffers	32
3.2 METHODS	34
3.2.1 Animal experiment procedures.....	34
3.2.2 Molecular biology methods.....	37
3.2.3 Protein biochemistry.....	38
3.2.4 Histopathology and immunohistochemistry	39
3.2.5 Cell culture experiments	42
3.2.6 Statistics	44
4 RESULTS	45
4.1 Oligodendrocyte specific Fgfr1 knock down study.....	45
4.1.1 Genotype and phenotype confirmation.	45
4.1.2 Characterization of oligodendrocyte specific Fgfr1 signalling.....	46
4.1.3 Effect of Fgfr1 ablation in oligodendrocytes on Fgfr1 signal cascade	46
4.1.4 Effect of Fgfr1 ablation in oligodendrocytes on TrkB expression.....	46
4.1.5 Effect of Fgfr1 ablation in MBP expression in Fgfr1 ^{ind/-}	50
4.1.6 Effect of Fgfr1 ablation in oligodendrocytes on cell population	51
4.2 EAE in Fgfr1^{ind/-} and control mice	51
4.2.1 EAE scoring.....	51
4.2.2 Fgfr1 ^{ind/-} mice show a milder EAE disease course.....	53
4.2.3 Demyelination and axonal density in Fgfr1 ^{ind/-} mice	55
4.2.4 Inflammation in Fgfr1 ^{ind/-} mice	56
4.2.5 Altered pattern of cytokines expression in Fgfr1 ^{ind/-} mice spinal cord.....	63
4.2.6 Altered pattern of cytokines expression in Fgfr1 ^{ind/-} mice spleen	63
4.2.7 Chemokine and its receptor expression in Fgfr1 ^{ind/-} mice spinal cord.....	67
4.2.8 ERK and AKT phosphorylation in Fgfr1 ^{ind/-} mice spinal cord.....	68
4.2.9 BDNF and TrkB receptor expression.....	70
4.2.10 PLP and MBP expression	70
4.2.11 Ablation of Fgfr1 affects remyelination inhibitor expression	74
4.2.12 Deletion of Fgfr1 does not affect oligodendrocyte lineage cells.....	75
4.3 Milder EAE score in IFN β-1a treated Fgfr1^{ind/-} mice	79

4.4 <i>In vitro</i> experiments	80
4.4.1 The effects of Fgfr1 inhibition and IFN β -1a in oli-neu oligodendrocytes.....	80
5 DISCUSSION	82
5.1 Oligodendrocyte specific Fgfr1 knock out in C57Bl/6J mice	82
5.1.1 Fgfr1 deletion in oligodendrocytes does not result in phenotypic changes	82
5.1.2 Increased ERK and AKT phosphorylation in Fgfr1 ^{ind/-} mice	83
5.1.3 Increased TrkB expression in Fgfr ^{ind/-} mice spinal cord	84
5.2 Oligodendrocyte specific Fgfr1 inhibition reduces chronic EAE	85
5.2.1 Reduced immune cells in Fgfr1 ^{ind/-} mice.....	86
5.2.2 Decreased cytokines in Fgfr1 ^{ind/-} mice	87
5.2.3 Decreased chemokines in Fgfr1 ^{ind/-} mice	88
5.2.4 Increased neuronal growth factors in Fgfr1 ^{ind/-} mice.....	90
5.2.5 Decreased myelin inhibitors in Fgfr1 ^{ind/-} mice	91
5.3 IFN β -1a treatment milder the disease course of Fgfr1 ^{ind/-} mice	92
6 SUMMARY	94
ZUSAMMENFASSUNG	95
REFERENCES	96
ACKNOWLEDGEMENTS	105

ABBREVIATIONS

BBB	Blood Brain Barrier
BDNF	Brain-derived neurotrophic factor
BSA	Bovine serum albumin
CNS	Central nervous system
CSF	Cerebrospinal fluid
CX3CL	Chemokine (C-X3-C motif) Ligand 1 (Fractalkine)
CX3CR	Chemokine (C-X3-C motif) receptor 1
DNA	Deoxyribonucleic acid
EAE	Experimental autoimmune encephalomyelitis
ECL	Enhanced chemiluminescence
ERK	Extracellular signal-regulated kinases
FGF	Fibroblast growth factor
FGFR	Fibroblast growth factor receptor
Fgfr1 ^{ind/-}	Oligodendrocyte specific inducible Fgfr1 knockout
GA	Glatiramate acetate
GAPDH	Glyceraldehyde 3-phosphate dehydrogenase
h	hour
H and E	Hematoxylin and Eosin
IFN β -1a	Interferon β -1a
IL	Interleukins
iNOS	Inducible Nitric oxide synthase
LFB/PAS	Luxol fast blue/periodic acid Schiff
MBP	Myelin Basic protein
min	Minutes
MOG	Myelin oligodendrocyte glycoprotein
mRNA	Messenger Ribonucleic acid
MS	Multiple sclerosis
OPC	Oligodendrocyte progenitor cells
p.i	Post immunization
PBS	Phosphate buffered saline
PFA	Paraformaldehyde
PLP	Proteolipid protein
RT	Room temperature
RT-PCR	Real time-Polymerase chain reaction
SDS	Sodium dodecyl sulfate
TBS	Tris buffered saline
TBST	Tris buffered saline with Tween 20
TNF	Tumor necrosis factor
TrkB	Neurotrophic tyrosine kinase receptor, type 2

LIST OF FIGURES

Figure 1 Symptoms of Multiple sclerosis.....	2
Figure 2 Pathology of MS.....	4
Figure 3 Schematic diagram of MOG induced EAE mechanism.....	9
Figure 4 The FGF signalling system.....	13
Figure 5 The FGF structure.....	15
Figure 6 Structure and family members of FGF ligands.....	16
Figure 7 FGF signalling pathways.....	17
Figure 8 FGFR expression pattern in developing oligodendrocyte lineage.....	18
Figure 9 Fgfr1 conditional knockout creation and Fgfr1 knockout study.....	35
Figure 10 Experimental design of Fgfr1 conditional knockout creation, EAE induction.....	36
Figure 11 Experimental design of EAE induction and IFN β 1a treatment.....	37
Figure 12 Schematic procedure of H & E staining.....	40
Figure 13 Schematic procedure of Luxol fast Blue/PAS staining.....	41
Figure 14 Genotype confirmation of Fgfr1 lox and PLP cre locus.....	45
Figure 15 Fgfr expression in Fgfr1 ^{ind/-} mice CNS.....	47
Figure 16 Expression pattern of ERK and AKT phosphorylation.....	48
Figure 17 TrkB protein expression in different CNS region of control and Fgfr1 ^{ind/-}	49
Figure 18 Myelin basic protein expression in control and Fgfr1 ^{ind/-} mice.....	50
Figure 19 Olig2 (+) and nogoA (+) oligodendrocyte lineage cells.....	51
Figure 20 Clinical symptoms of MOG ₃₅₋₅₅ peptide induced EAE in Fgfr1 ^{ind/-} mice.....	52
Figure 21 Mean weight of control and Fgfr1 ^{ind/-} mice after MOG ₃₅₋₅₅ EAE induction.....	53
Figure 22 Conditional deletion of Fgfr1 in MOG ₃₅₋₅₅ induced EAE.....	54
Figure 23 Histopathological analysis of acute and chronic EAE (H and E).....	57
Figure 24 Histopathological analysis of acute and chronic EAE (LFB/PAS).....	58
Figure 25 Histopathological analysis of acute and chronic EAE (Silver).....	59
Figure 26 Immune cell infiltration in acute and chronic EAE spinal cord (T cells).....	60
Figure 27 Immune cell infiltration in acute and chronic EAE spinal cord (B cells).....	61
Figure 28 Immune cell infiltration in acute and chronic EAE spinal cord (Macrophages).....	62
Figure 29 Expression of proinflammatory cytokine in the spinal cord.....	64
Figure 30 Expression of proinflammatory cytokine in the spinal cord (iNOS and IL-12).....	65
Figure 31 Expression of proinflammatory cytokine in spleen.....	66
Figure 32 Expression of proinflammatory cytokine in spleen (iNOS and IL-12).....	67
Figure 33 Expression of the chemokine CX3CL1 and the receptor CX3CR1.....	68
Figure 34 ERK and AKT expression in chronic EAE mice spinal cord.....	69
Figure 35 Expression of BDNF and TrkB receptor in acute EAE.....	71

Figure 36 Expression of BDNF and TrkB receptor in chronic EAE	72
Figure 37 Expression of PLP and MBP in acute EAE	73
Figure 38 Expression of PLP and MBP in chronic EAE	73
Figure 39 MBP expression in tissue level in chronic EAE	74
Figure 40 Fgfr1 mRNA expression in acute and chronic EAE.....	75
Figure 41 Expression of the remyelination inhibitors.....	76
Figure 42 Oligodendrocyte lineage cell population in acute EAE mice.....	77
Figure 43 Olig2 (+) and nogoA (+) oligodendrocytes in chronic EAE	78
Figure 44 Effect of Interferon β -1a treatment in chronic EAE.....	79
Figure 45 Proliferation effect of Fgfr1 inhibition and IFN β -1b treatment in oli-neu cells.....	81
Figure 46 Cytotoxicity effect of Fgfr1 inhibition and IFN β -1b treatment in oli-neu cells.	81
Figure 47 ERK, STAT1 phosphorylation in Fgfr1 inhibition and IFN β -1b on oli-neu cells.	81

LIST OF TABLES

Table 1 The 2010 McDonald criteria for diagnosis of MS.	6
Table 2 Genomic deregulation of FGFR in solid tumors	20
Table 3 FGFR inhibitors in clinical development.	21
Table 4 Clinical characteristics of MOG ₃₅₋₅₅ -induced EAE in Fgfr1 ^{ind-/-} mice	55
Table 5 Histopathological analysis of spinal cord sections from EAE mice.	55
Table 6 Immune cells in spinal cord of EAE mice.	56
Table 7 Oligodendrocyte lineage cell population in EAE spinal cord.	75

ABSTRACT

Fibroblast growth factors (FGFs) exert diverse biological effects by binding and activation of specific fibroblast growth factor receptors (FGFRs). Recent studies on the function of FGF2 in MOG₃₅₋₅₅-induced experimental autoimmune encephalitis (EAE) showed that systemic deletion of FGF2 leads to a more severe disease course, increased lymphocyte and macrophage infiltration and decreased remyelination. In the present study the *in vivo* function of the corresponding receptor Fgfr1 was characterized using an oligodendrocyte-specific genetic approach. *Plp/CreER^T:Fgfr1^{fl/fl}* mice were administered tamoxifen to induce conditional Fgfr1 deletion in oligodendrocytes (referred to as Fgfr1^{ind/-}). In MOG₃₅₋₅₅-induced EAE the Fgfr1^{ind/-} mice show a delayed onset of disease, less maximum disease severity and enhanced recovery. Decreased lymphocyte and macrophage/microglia infiltration, and myelin and axon degeneration are found in Fgfr1^{ind/-} mice. In acute EAE downregulation of proinflammatory cytokines such as TNF- α , IL-1 β and IL-6, in chronic EAE downregulation of the CX3CL1/CX3CR1 pathway is seen in Fgfr1^{ind/-} mice. Furthermore, increased expression of BDNF, TrkB (neurotrophic tyrosine kinase receptor, type 2) and decreased expression of Lingo-1 are found in Fgfr1^{ind/-} mice. Fgfr1 ablation in oligodendrocytes showed increased TrkB expression in whole lysate of cortex and spinal cord. These data suggest that impaired signalling via oligodendroglial Fgfr1 has a beneficial effect on MOG₃₅₋₅₅-induced EAE. These findings on the oligodendroglial Fgfr1 pathway may offer a new target for developing therapy in multiple sclerosis.

1 INTRODUCTION

1.1 Multiple sclerosis (MS)

Multiple sclerosis was first depicted in 1838. The unnamed patient was French, the illustrator a Scotsman (Compston *et al.* 2005). In the six decades that followed, French and German physicians provided a coherent clinicopathological account of the disease (Compston *et al.* 2005). By the beginning of the 20th century, a disease that earlier had merited individual case reports had become one of the commonest reasons for admission to a neurological ward. Now multiple sclerosis is recognized throughout the world, with around 2.5 million and one hundred twenty thousand people in Germany affected individuals incurring costs in billions of dollars for health care. As MS became better recognized in the early part of 20th century, ideas began to formulate on its cause and the pathogenesis. Research over the last 50 years has illuminated mechanisms of tissue injury, and the therapeutics are which will surely culminate in the application of successful strategies both for limiting and repairing the damage has begun (Compston *et al.* 2005). MS mainly affects women in the age of third or fourth decade of life. The usual ratio is two females for one male (2F:M) (Goldenberg 2012). It is not always easy to determine the age at which symptoms of MS first develop. Some symptoms such as paraesthesia, are nonspecific and often so vague as easily to be overlooked. However, there is consensus for peak onset around 30 years of age (Compston *et al.* 2005, Wingerchuk and Carter 2014).

1.1.1 Etiology of MS

The specific cause (etiology) of MS has not yet been determined (Goldenberg 2012), several theories are plausible either immunologic, genetic, microbial or environmental factors. Although no definite cause of MS has yet been identified, substantial amounts of research point to a dual multifactorial influence of both genetics and environmental elements contributing to the development of the disease (Hoglund and Maghazachi 2014). Family studies support a genetic association, they also show that genetics alone are not enough to develop MS, as shown by homozygous twins not both acquiring disease. Studies have shown risk association during months of birth as spring births have higher risk of MS than autumn births and Vitamin D3 deficiency increases the risk of MS (Hoglund and Maghazachi 2014). Another risk factor with

strong association to MS is Epstein Barr Virus (EBV) infection. Many other factors have shown association with increased MS risk but are in need of further research to be conclusive. These include cigarette smoking, a diet rich in saturated but low in polyunsaturated fats, sex hormones, and socioeconomic status, among others. Viruses other than EBV have also been implicated in the etiology of MS (Hoglund and Maghazachi 2014).

1.1.2 MS symptoms

The clinical course of MS is as unpredictable as the symptoms that may occur but some patterns can usefully be defined (Compston *et al.* 2005). The most commonly affected sites to produce symptoms are the optic nerves, the cerebrum and the spinal cord. The major symptoms are shown in Figure 1. These will be affected in most patients at some stage in the illness. The spinal cord is predominantly involved in most patients with progressive MS, whether this occurs after a period of relapsing disease or from onset. Selective involvement of the optic nerves, cerebrum and brainstem may also progressive blindness, dementia, or ataxia (Compston *et al.* 2005).



Figure 1 Symptoms of Multiple sclerosis. Figure shows the major symptoms of MS in percentage. Walking difficulty, vision problems and numbness are widely observed symptoms. (source: multiplesclerosis.net)

MS shows a number of unpredictable symptoms including pain, tingling or burning sensations throughout the body, vision problems, mobility difficulties, muscle spasms or stiffness, slurred speech, impaired memory and cognitive function. The course of multiple sclerosis can be described in terms of relapses, remissions and chronic progression either from onset or after a period of remissions. Two major outcome measures usefully describe the clinical course and prognosis: the qualitative description, an expression of the interplay between relapses and progression; and the quantitative description, which refers to the accumulation of neurological deficits and is characterized as disability, impairment or loss of social functions.

1.1.3 Subtypes of MS

There are several MS subtypes by the terms of clinical course and disease pathology. (i) relapsing-remitting MS (RR-MS) clearly defined relapses with full recovery or with sequelae and residual deficits upon recovery; periods between disease relapses characterized by a lack of disease progression (approximately 85% patients have RR-MS) (Rangachari and Kuchroo 2013); (ii) secondary progressive MS (SP-MS), which is characterized by initial relapsing-remitting disease course followed by progression with or without occasional relapses, minor remissions, and plateaus; (iii) primary progressive MS (PP-MS), defined disease progression from onset with occasional plateaus and temporary minor improvements allowed (affects approximately 15% of people with MS); (iv) progressive-relapsing MS (PR-MS) is rare variant and shows progressive disease from onset, with clear acute relapses, with or without full recovery; periods between relapses characterized by continuing progression (Compston *et al.* 2005, Constantinescu *et al.* 2011).

1.1.4 MS pathology

Multiple sclerosis is an autoimmune chronic neuroinflammatory demyelinating disease of the central nervous system (Goldenberg 2012). Inflammation, demyelination and axonal loss are major pathological features of MS (Constantinescu *et al.* 2011). Multiple sclerosis has acute and chronic lesions. Active demyelination and inflammation with various immune cells are pathology of acute lesion, whereas in chronic lesions, significant loss of myelin with less inflammatory infiltrates and gliosis (Constantinescu *et al.* 2011, Milo and Miller 2014).

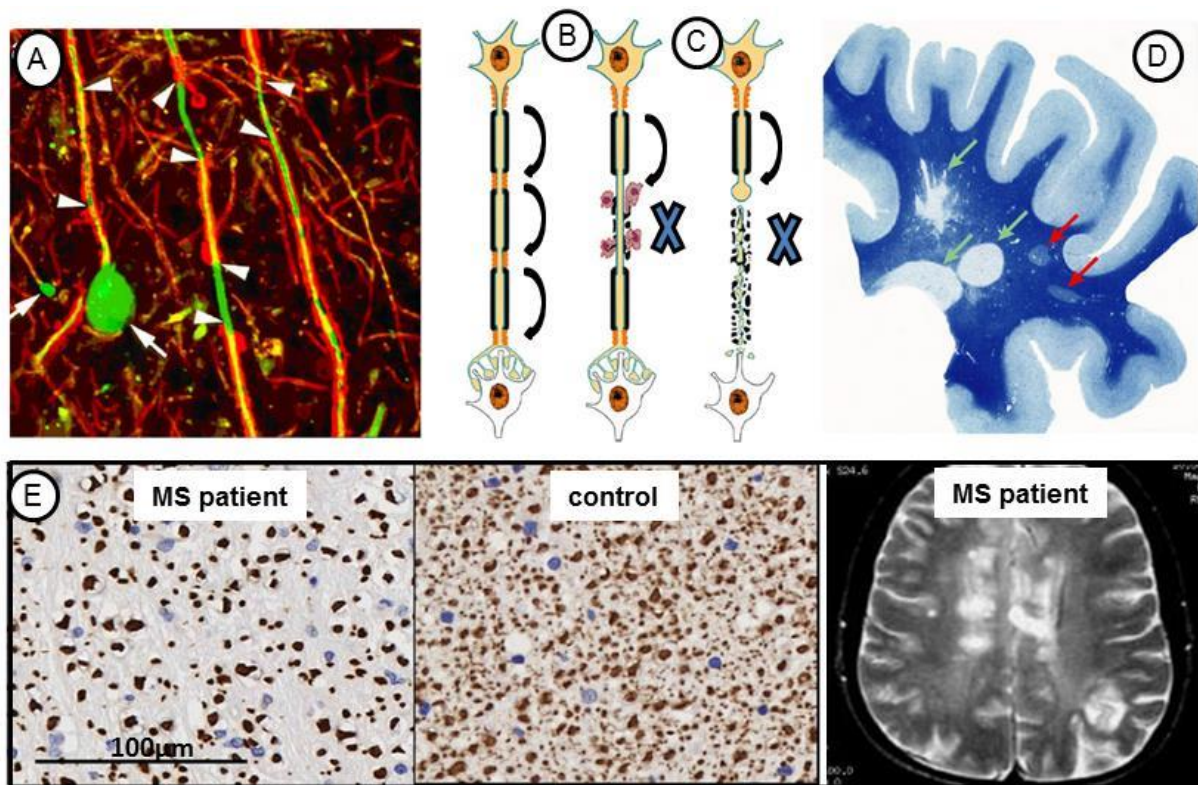


Figure 2 Pathology of MS. A) One of the axons ends in a large swelling (arrow) or axonal retraction bulb (arrow). B and C) schematic of axonal response during and following transection (Dutta and Trapp 2011). D) LFB staining reveal areas of myelination in the subcortical white matter. The green arrows indicate three areas from which the myelin stain is absent, representing three foci or plaques of chronic demyelination (Robin JM Franklin 2002). E) neurofilament stain of the lateral corticospinal tract of a patient with MS demonstrates extensive axonal loss compared to control tissue (Bø *et al.* 2013). MRI in a patient with multiple sclerosis demonstrates numerous white matter plaques in a callosal and pericallosal white matter distribution.

MS lesions can arise anywhere in the CNS. However, they show a predilection for the optic nerve, spinal cord, brain stem, and periventricular areas. Furthermore, brain tissue immediately adjacent to the subarachnoid space, i.e. subpial gray matter, is especially vulnerable to demyelination. Mild meningeal inflammation consisting of T and B lymphocytes, plasma cells and macrophages is common pathology of MS (Stadelmann *et al.* 2011). Reactive astrocytes may still be present at the lesion border; more prominent, however, a dense, fibrous gliosis. In contrast to these seemingly inert lesions, scattered macrophages digesting myelin products may be present at the lesion edge, mostly accompanied by scattered perivascular and parenchymal T cells, indicating ongoing myelin destruction. Accordingly, signs of

axonal damage are routinely found at the edge of slowly expanding lesions. In general, T cell lymphocytic infiltration decreases over time and is markedly reduced in late stage MS (Stadelmann *et al.* 2011). Early MS lesions mostly appear pale, but not completely devoid of myelin. Oligodendroglial cells are present in the lesions, often displaying an activated phenotype with signs of early remyelination.

Early MS lesions are more likely to be encountered in patients who have been biopsied for reasons of differential diagnosis, but may also be found at autopsy, especially in patients dying early in the disease course. The most studied lesions are “early active demyelinating” MS lesions where macrophages filled with minor, i.e. low abundance myelin proteins, such as myelin oligodendrocyte glycoprotein (MOG), cyclic nucleotide phosphodiesterase (CNPase) and myelin-associated glycoprotein (MAG) cover most or part of the lesion area (Stadelmann *et al.* 2011). Although demyelination as hallmark of MS is largely restricted to focal lesions, other aspects of pathology are less confined. Perivascular and also scattered parenchymal T cell infiltration and microglia activation are widespread in many MS patients, even in the chronic disease phase.

1.1.5 MS diagnosis

The diagnosis of MS is primarily with clinical symptoms and white matter lesions signs. There is no single laboratory test for MS diagnosis. Analysis of increased oligoclonal bands (OCBs) from the CSF is one step in MS diagnosis. MRI is the most sensitive test to detect and demonstrate MS lesions. It supports the diagnosis, estimates the lesion load and disease activity, measures brain atrophy and axonal loss (Milo and Miller 2014). Revised versions (2010) of McDonald criteria facilitate the diagnosis of MS (Table 1; Milo and Miller 2014). The diagnosis of MS is based on the evaluation of lesions in CNS (Figure 2) and alternative diagnosis.

PPMS May Be Diagnosed in subjects with: (Revisions to MS Diagnosis, Polman *et al.* 2010)

1. One year of disease progression (retrospectively or prospectively determined).
2. Plus 2 of the 3 following criteria^a:
 - A. Evidence for DIS in the brain based on ≥ 1 T2^b lesions in at least 1 area characteristic for MS (periventricular, juxtacortical, or infratentorial).
 - B. Evidence for DIS in the spinal cord based on ≥ 2 T2^b lesions in the cord.

C. Positive CSF (isoelectric focusing evidence of oligoclonal bands and/or elevated IgG index).

^a If a subject has a brainstem or spinal cord syndrome, all symptomatic lesions are excluded from the criteria.

^b Gadolinium enhancement of lesions is not required.

DIS = lesion dissemination in space; IgG = immunoglobulin G.

Table 1 The 2010 McDonald criteria for diagnosis of MS. (Revisions to MS diagnosis, Polman *et al.* 2010)

Clinical presentation	Additional data needed for MS diagnosis
≥ 2 attacks; objective clinical evidence of ≥ 2 lesions or objective clinical evidence of 1 lesion with reasonable historical evidence of a prior attack	None
≥ 2 attacks; objective clinical evidence of 1 lesion	Dissemination in space, demonstrated by: ≥ 1 T2 lesion in at least 2 of 4 MS-typical regions of the CNS (periventricular, juxtacortical, infratentorial, or spinal cord); or Await a further clinical attack implicating a different CNS site.
1 attack; objective clinical evidence of ≥ 2 lesions	Dissemination in time, demonstrated by: Simultaneous presence of asymptomatic gadolinium-enhancing and nonenhancing lesions at any time; or A new T2 and/or gadolinium-enhancing lesion(s) on follow-up MRI, irrespective of its timing with reference to a baseline scan; or Await a second clinical attack.
1 attack; objective clinical evidence of 1 lesion (clinically isolated syndrome)	Dissemination in space and time, demonstrated by: For DIS: ≥ 1 T2 lesion in at least 2 of 4 MS-typical regions of the CNS (periventricular, juxtacortical, infratentorial, or spinal cord); or Await a second clinical attack implicating a different CNS site; and For DIT: Simultaneous presence of asymptomatic gadolinium-enhancing and nonenhancing lesions at any time; or A new T2 and/or gadolinium-enhancing lesion(s) on follow-up MRI, irrespective of its timing with reference to a baseline scan; or Await a second clinical attack.
Insidious neurological progression suggestive of MS (PPMS)	1 year of disease progression (retrospectively or prospectively determined) plus 2 of 3 of the following criteria: <ol style="list-style-type: none"> 1. Evidence for DIS in the brain based on ≥ 1 T2 lesions in the MS-characteristic (periventricular, juxtacortical, or infratentorial) regions 2. Evidence for DIS in the spinal cord based on ≥ 2 T2 lesions in the cord 3. Positive CSF (isoelectric focusing evidence of oligoclonal bands and/or elevated IgG index)

1.1.6 MS treatment

There is no cure for MS, whereas disease modifying therapy (DMT) can reduce disease activity and progression of the disease (Goldenberg 2012). The first line of treatment was represented by β -Interferons (INF) and glatiramate acetate (GA) (Milo and Miller 2014). Currently, there are nine approved MS DMTs (interferon beta 1a/b, GA, natalizumab, fingolimod, alemtuzumab, dimethyl fumarate, mitoxantrone, teriflunomide) (Brück *et al.* 2012) with varying degrees of efficacy for reducing relapse risk and preserving neurological function, but their long-term benefits remain unclear. Moreover, available DMTs differ with respect to the route and frequency of administration, tolerability and likelihood of treatment adherence, common adverse effects, risk of major toxicity, and pregnancy-related risks (Wingerchuk and Carter 2014).

Five interferon beta preparations and glatiramer acetate (GA) are approved for relapsing MS (Milo and Miller 2014). Their mechanisms of action are not fully understood, but interferon beta reduces BBB disruption and modulates T-cell, B-cell, and cytokine functions, whereas GA regulates the shift of Th1 to Th2 cells. Mitoxantrone is a general immunosuppressive drug approved for rapidly worsening relapsing MS and is the only agent approved to treat secondary progressive MS. Natalizumab is a humanized monoclonal antibody that selectively targets the $\alpha 4$ subunit of the cell adhesion molecule “very late antigen 4” expressed on the surface of lymphocytes and monocytes (Brück *et al.* 2012).

Three oral DMTs are approved for relapsing MS: fingolimod, teriflunomide, and dimethyl fumarate/BG-12. Fingolimod is a once-daily oral medication approved for relapsing MS. It is a sphingosine-1-phosphate (S1P) agonist, binding to 4 of the 5 S1P receptor subtypes, but acts as a functional antagonist (Goldenberg 2012). Teriflunomide, a once-daily oral DMT, is the active metabolite of the rheumatoid arthritis drug leflunomide. It exerts immunological effects by inhibiting dihydroorotate dehydrogenase, an enzyme required for de novo pyrimidine synthesis in proliferating (but not resting) cells. Dimethyl fumarate (DMF) is a newly approved twice-daily oral DMT for relapsing MS. On ingestion, it is hydrolyzed to monomethyl fumarate, which is eliminated through respiration and has little hepatic or renal excretion. The mechanism of DMF action has not been completely elucidated, but it is known to activate the nuclear-related factor 2 transcriptional pathway, which reduces oxidative

cell stress, as well as to modulate nuclear factor κ B, which could have anti-inflammatory effects (Brück *et al.* 2012).

Emerging therapies include humanized monoclonal antibodies such as alemtuzumab (against CD52), Ocrelizumab (against CD20), Laquinimod (unknown mechanism) and daclizumab (against α subunit (CD25) on T cells) are in clinical trials for MS treatment (Wingerchuk and Carter 2014).

1.2 Experimental autoimmune encephalomyelitis (EAE)

Three different types of animal models are currently established for the exploration of pathologic patterns of demyelinating diseases, a) Theiler's murine encephalomyelitis virus (TMEV) model, b) cuprizone induced toxic model and c) EAE, which is the most common animal model for MS (Bittner *et al.* 2014). Experimental autoimmune encephalomyelitis is a common term referring to different models of CNS autoimmunity in vertebrate animals. EAE is a well-established animal model for MS which mimics pathology of human MS. Till end of 2014 around 7500 research articles were published with EAE models (Pubmed search EAE as key word).

In 1920s, Koritschoner and Schewinburg induced spinal cord inflammation in rabbits by inoculation with human spinal cord that is the origin of EAE. In 1930s, researchers attempted encephalitic complications associated with rabies vaccination by repetitive immunization of rhesus monkeys with CNS tissue (Gold *et al.* 2006). Since then EAE is classically induced by immunization of many different species, including mice, rat, rabbit, guinea pig, monkeys non-human primates with encephalitogenic antigens derived from CNS myelin related gene proteins mainly myelin oligodendrocyte glycoprotein (MOG), proteolipid protein (PLP) and myelin basic protein (MBP) (Rangachari and Kuchroo 2013, Milo and Miller 2014).

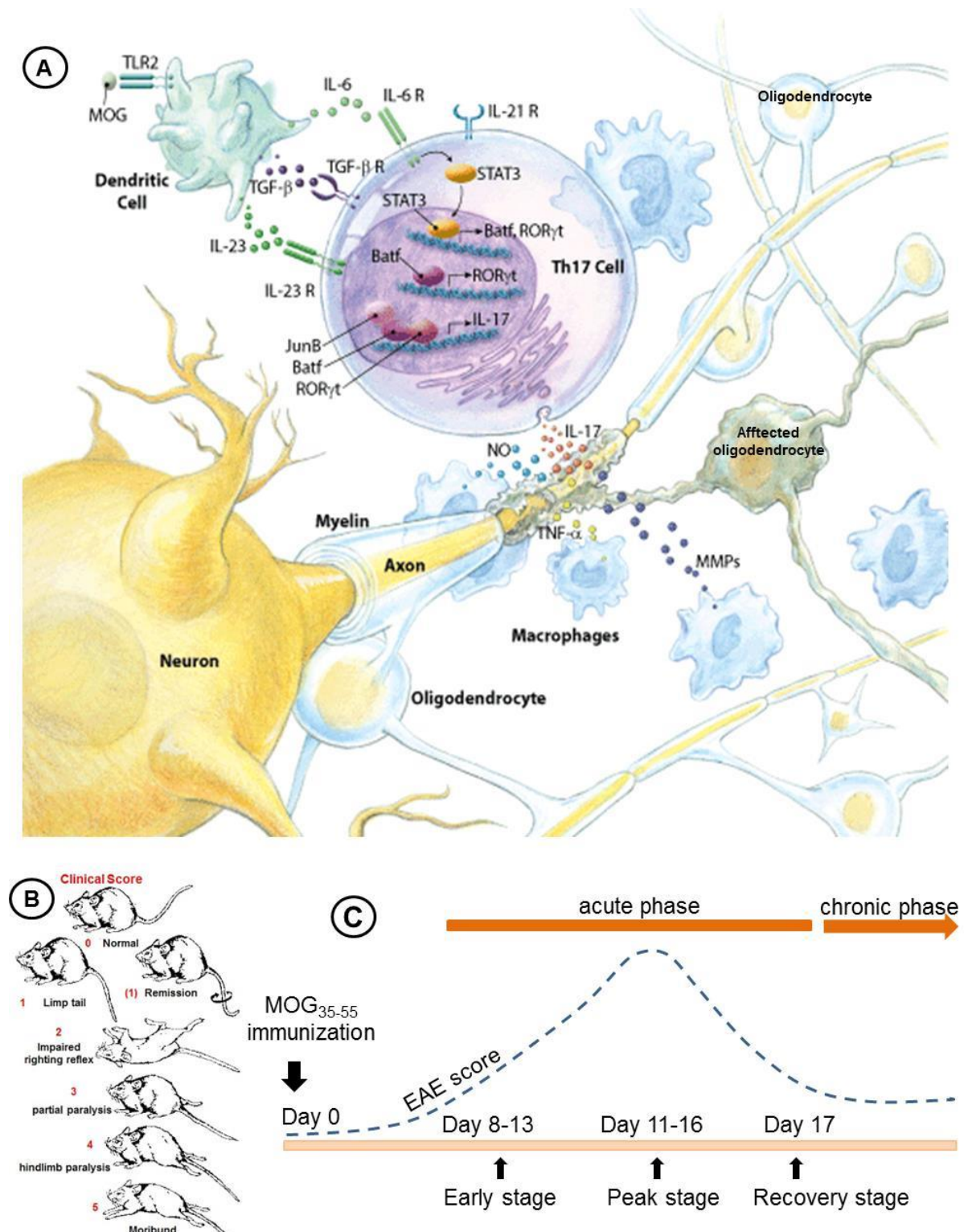


Figure 3 Schematic diagram of MOG induced EAE mechanism. A) Following induction of autoimmune conditions in mice using MOG₃₅₋₅₅ immunization, differentiated T- cells secrete proinflammatory cytokines such as TNF- α , IL-17, IL-6, IL-23, NO, TGF β and activated macrophages destroy myelin and damage oligodendrocytes (Cytokine technical resources, R and D Systems, Germany). B) Clinical course of EAE in mice model (Hooks Laboratory, EAE protocol). C) Experimental procedure of MOG EAE induction and expected EAE score.

A major difference between MS and EAE is that external immunization of myelin antigen is required in EAE. In EAE the inducible agent is well known whereas in MS the causative agent is not known. There are different models of EAE using in MS researchers in which each model shows different and distinct aspects of MS pathology. <http://www.jove.com/video/51275> provides the protocol for MOG EAE induction video (Bittner *et al.* 2014). Immunization of animals with myelin peptides induces the auto reactive inflammatory immune cells (T and B cells) and combination of complete Freund's adjuvant and pertussis toxin facilitate the blood brain barrier to allow the myelin activated immune cells into the CNS. Inflammatory immune cell infiltration occurs in CNS upon the entry of activated immune cells into the CNS (Figure 3). EAE disease onset starts 9-12 days post immunization and shows different clinical and pathological symptoms. The EAE clinical symptoms can be measured by the scale range of 1-5 (detailed in method section 3.2.1.7). MOG is unique myelin auto antigens that induce encephalitogenic T-cell response and also a demyelinating autoantibody response. Demyelinating anti-MOG antibodies augment disease severity and initiate extensive demyelination in T-cell-mediated brain inflammation in mouse, rat and primate EAE models (Gold *et al.* 2006).

In MOG-induced EAE, the lesions are in general characterized by massive global tissue injury (including axonal and neuronal damage) with very little primary demyelination and tissue damage is accomplished by T cells and activated macrophages (Gold *et al.* 2006). The limitation of EAE is a) sometimes, low disease incidence or weak symptoms might be an experimental challenge, b) disease severity can be varied with different amounts of peptide/mouse, c) age, gender, season of the year and environmental conditions within the animal facility are important factors that influence EAE susceptibility (Bittner *et al.* 2014).

Another method of EAE induction is adoptive transfer of myelin antigen activated myelin-specific T cells into the animals induces the disease in recipient animals. *In vitro*, myelin-antigen-specific T cells cultured in different conditions and adoptive transfer to the animals to investigate the effect of particular compounds (Rangachari and Kuchroo 2013, Milo and Miller 2014). MOG₃₅₋₅₅ peptides are the widely used antigen to induce EAE in mice and rats, PLP₁₃₉₋₁₅₁ also used to induce EAE. Mice immunized with PLP₁₃₉₋₁₅₁ developed splenic lymphocyte responses to PLP₁₇₈₋₁₉₁ that could induce EAE upon adoptive transfer. Further, MBP₈₄₋₁₀₄ peptide showed delayed

EAE responses (Rangachari and Kuchroo 2013). MOG₃₇₋₄₆ peptides also induce specific CD8⁺ T cell response in B6 mice. Other method of EAE induction is spontaneous induction of EAE on SJL/J mice. Wekerle *et al.* have developed spontaneous EAE by generating a MOG₉₂₋₁₀₆-specific TcR transgenic in SJL/J background (Rangachari and Kuchroo 2013). MOG₃₅₋₅₅ peptide induced EAE is the common and chronic form of EAE that did not show remittance. The dose of MOG₃₅₋₅₅ peptide influence the disease course of EAE, the high dose of MOG₃₅₋₅₅ peptide (300 µg) induces chronic non-relapsing EAE in C57/Bl6 mice, whereas lower doses of peptide (50 µg) shows relapsing-relapsing EAE (Rangachari and Kuchroo 2013).

1.3 Oligodendrocytes in MS and EAE

The central nervous system (CNS) is responsible for integrating information from and to the peripheral system and responds accordingly. CNS consists of two major anatomical parts such as spinal cord and brain. The nervous system is consisting of nerve cells and unique cells known as glial cells. These glial cells are non-neuronal cells that primarily support the protection and functions of the neurons. Oligodendrocytes are glial cells present in the CNS. In the CNS, oligodendrocytes produce myelin by the elaboration of the oligodendrocyte plasma membrane which wrap around in to the axons. This makes the myelin sheaths compact and multilamellar sheaths. Myelin is a lipoprotein ensheathment of the axons with the thickness of 1 µm and forming nodes of Ranvier. Myelin sheath protects the axons from the injury and increase the rate and efficacy of nerve conduction. A single oligodendrocyte can form myelin sheaths to more than one axon (up to 50) and renew its myelin sheaths three times within 24 h (Patel and Balabanov 2012). Impaired myelin formation or myelin sheath damage is the major pathology in MS and its animal model EAE (Bansal 2002). Demyelination process compromises the salutatory property of the axonal action potential and blocks the axonal conduction.

Besides protecting axons by the insulating myelin sheath, oligodendrocytes produce many neurotrophic factors (BDNF, GDNF, FGF) that are well known to promote the survival of neurons as well as advancing oligodendrocyte differentiation and myelination, especially during CNS myelin lesion and repair. Neuron-astrocyte-oligodendrocyte interaction loop involving astrocyte-produced trophic factors has also

been suggested for oligodendrocytes to achieve CNS myelination and protection. Oligodendrocytes play major roles in supporting axonal metabolism and oligodendrocyte impairment contributes to the onset and/or progression of neurodegeneration (Bankston *et al.* 2013).

Inflammatory demyelination process can be altering by the regulatory signals produced by the oligodendrocytes (Patel and Balabanov 2012). Invading macrophages (monocytes) and microglia remove the myelin from the axons. The specific mechanisms of oligodendrocyte injury involve immune cells, mainly T and B cells. Activated T cells produce inflammatory cytokines (IFN- γ and TNF- α), which affect oligodendrocytes and myelin sheaths. B cells in the lesion area produce antibodies against oligodendrocytes and myelin. Myelin oligodendrocyte glycoprotein (MOG) and galactocerebroside are the major targets of antibody-mediated cytotoxicity (Patel and Balabanov 2012).

Myelin repair process by oligodendrocytes largely fails, because the inability of oligodendrocyte progenitor cells (OPC) to proliferative or differentiate into myelin-producing cells. OPC are very sensitive to inflammatory cytokines compared to mature oligodendrocytes. Newly formed myelin is thinner and has shorter internodes than normal myelin. Demyelination and oligodendrocyte injury in MS and EAE are complex immune processes. Oligodendrocyte injury is the first stage of disease process in MS and EAE. So the protection of oligodendrocytes against injury resulted in the protection from MS and EAE. Till to date, there is no oligodendrocyte-based treatment for MS, however all the available disease-modifying agents providing little direct protection to oligodendrocytes and myelin sheaths (Patel and Balabanov 2012).

1.4 Fibroblast growth factors (FGFs)

Genetic location analysis showed that the human and mouse FGF family consist of seven FGF subfamilies, all members share homology and similar binding specificity to their respective receptors (Itoh and Ornitz 2008). FGF family members are classical signalling molecules which are extracellular secreted proteins mostly and they bind to the heparan sulfate proteoglycans (HSPGs). FGFs act in an autocrine or

paracrine fashion by interacting with high affinity and different degrees of specificity, with tyrosine kinase receptors (FGF receptors) present at the cell surface.

The 23 human and mouse FGF ligands can be subdivided into i) canonical (cFGFs), ii) intracellular (iFGFs), and iii) hormone like (hFGFs) subfamilies (Itoh and Ornitz, 2008). FGF15/19, FGF21, and FGF23 have reduced heparan binding affinity and act as a long distance as endocrine factor to regulate metabolism and these FGFs called “hormone-like” FGFs. Another set of FGFs (FGF11, 12, 13 and 14) are intracellular FGFs which are secreted by the cells intracellularly and they do not activate FGF receptors (Figure 4). These FGFs localized to the nucleus and interact with intracellular domains of voltage gated sodium channels (Itoh and Ornitz 2008). Fibroblast growth factors regulate a wide range of cellular functions, regulating proliferation, differentiation, survival, migration and differentiation of different cell types. FGF family consists of 23 members, out of this FGF 11, FGF 12, FGF 13 and FGF 14 was not function as FGF ligand, and is described as FGF homologous factors. FGF15 is not expressed in human.

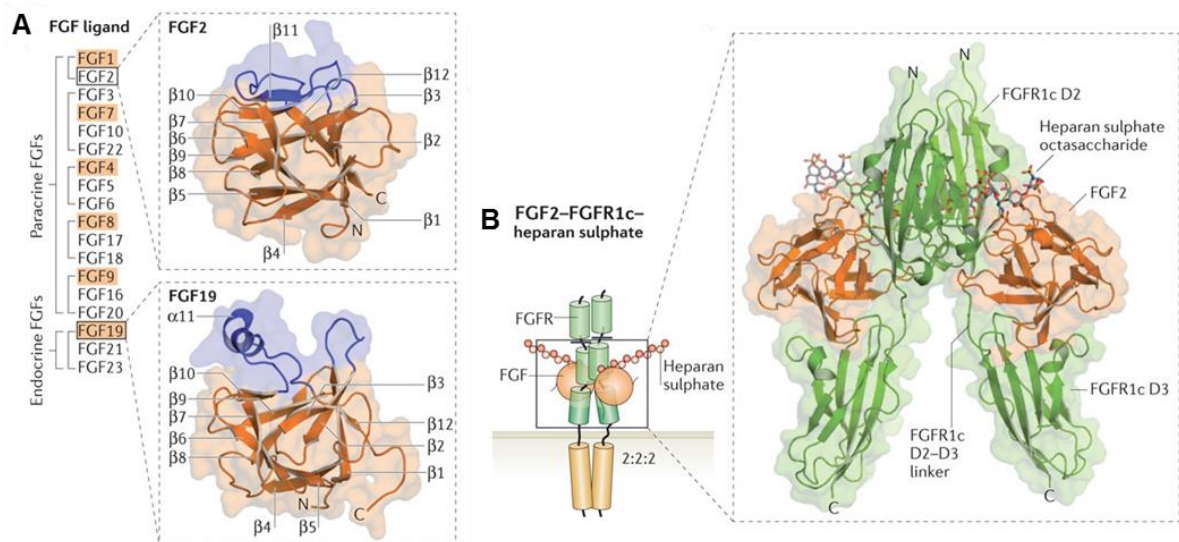


Figure 4 The FGF signalling system (Goetz and Mohammadi 2013) A) The 18 mammalian fibroblast growth factor (FGF) ligands are listed, grouped by subfamily and mode of action. The ligand which each subfamily is named after is boxed in orange. The crystal structures of FGF2, a prototypical paracrine FGF and FGF19, an endocrine FGF 14 are shown. B) The crystal structure of the ternary complex of FGF2, FGFR1c and heparan sulphate 4 as well as a schematic of the paracrine FGF signal transduction unit based on this structure are shown.

FGF-2 is considered to be one of the most controversial in terms of oligodendrocyte lineage and myelin repair. Administration of neutralizing antibodies against endogenous FGF2 reduces the rate of neural proliferation and development. In mice models FGF2 reduces inflammation by decreasing inflammatory cells such as macrophages, microglia, CD8 T cells (Ruffini *et al.* 2001, Rottlaender *et al.* 2011) and limited the CD44-mediated leukocyte migration (Jones *et al.* 2000). FGF activity is mediated through FGFR1, which is expressed in both embryonic and adult OPCs. FGF-2 affects the oligodendroglial cells and it arrests OPC differentiation *in vitro* and pathological conditions (Clemente *et al.* 2013).

1.5 Fibroblast growth factor receptors (FGFR)

There are four main FGF receptors (FGFR1 to 4) regulating FGF signals. Structurally FGF receptors have an extracellular domain, transmembrane domain and intracellular domain. The extracellular domain composed of three Immunoglobulin-like domains (IgGI-IgGIII), which facilitate FGF ligand to the receptor. The extracellular domain has an acid box (AB) domain and a heparin sulfate proteoglycans binding regions, which are regulating the receptor to the extracellular molecules, particularly cell adhesion molecules (CAMs). Extracellular and intracellular domains are joined with transmembrane domain. Following the transmembrane domain, the intracellular domain present inside the cell body, which has the tyrosine kinase domain (KI, KII), which contains the catalytic activity of the receptor. Transmembrane domain has the autophosphorylation sites which interact with intracellular substrates. The specificity and the tissue-specific alternative splice variant were determined by the half of the IgGIII which generate two isoforms, IIIb and IIIc which have very different ligand binding specificity (Zhang *et al.* 2006). The FGFR1 splice forms IIIa, IIIb and IIIc were differentiated by the third part of the third Ig-like domain (Figure 5).

FGFR1 is composed of an extracellular ligand-binding domain, a unique transmembrane domain, and a catalytic (tyrosine kinase) cytosolic domain. The extracellular region (with the N-terminus) contains a signal peptide (amino acids (aa) 1-21), 3 immunoglobulin-like loops (aa: 25-119, 158-246, and 255-357 according to Swiss-Prot), with an acidic box (seven glutamic acids in 127-133) between IgI and

IgII, a CHD (Cell adhesion molecule (CAM) homology domain) in 151-170, and an heparin-binding domain in the beginning of the IgII (aa 166-177); this extracellular region is followed by a transmembrane domain (aa 377-397) and an intracellular domain composed of a juxtamembrane domain, which serves as a binding site for phosphotyrosine binding (PTB) domains of proteins such as FRS2, and a tyrosine kinase domain (aa 478-767) (two kinase domains interrupted by a short kinase insert of 14 amino acids), and a C-terminal tail. A part of the C-terminal tail of FGFR1 containing 28 amino acids binds the SH2 domain of PLCG (PLC gamma) (Figure 5 and 6).

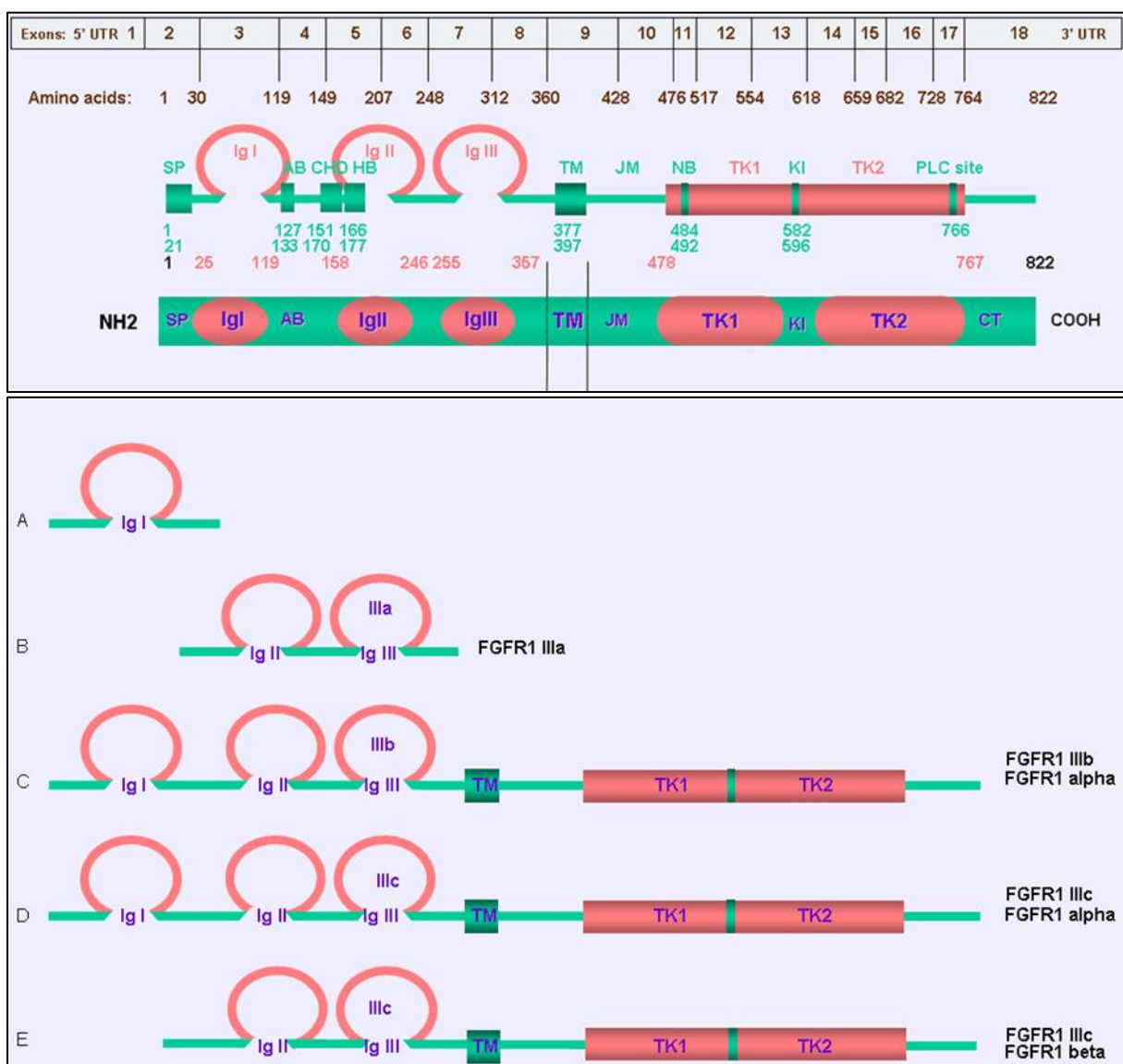


Figure 5 The FGF receptor 1 structure. IgG domain and cytoplasmic tyrosine kinase domain is attached by transmembrane domain (top box). Soluble form of FGFR1 showed (A and B). Membrane attached complete form of Fgfr1 showed in C, D, and E. Adapted from Johnson and Williams 1993, and Splice Center data.

Phosphorylation of tyrosine 766 is the interactive item with PLC gamma (Itoh *et al.* 1990, Johnson and Williams, 1993). The five tyrosine autophosphorylation sites in the catalytic core of FGFR1 are phosphorylated by a precisely controlled and ordered reaction. The rate of catalysis of two substrates is enhanced by 50- and 500-fold after autophosphorylation of Y653 and Y654, respectively, in the activation loop of FGFR1 (Furdui *et al.* 2006).

1.6 Fibroblast growth factor/FGF receptor interaction

FGF/FGF receptor interaction downstream regulates multiple signalling pathways involving various cellular functions such as proliferation, migration and differentiation (Figure 7). Following ligand binding and receptor dimerization, the kinase domains transphosphorylate each other, leading to the docking of adaptor proteins and the activation of four key downstream pathways: RAS-RAF-MAPK, PI3K-AKT, signal transducer and activator of transcription (STAT) and phospholipase C γ (PLC γ) (Turner and Grose 2010).



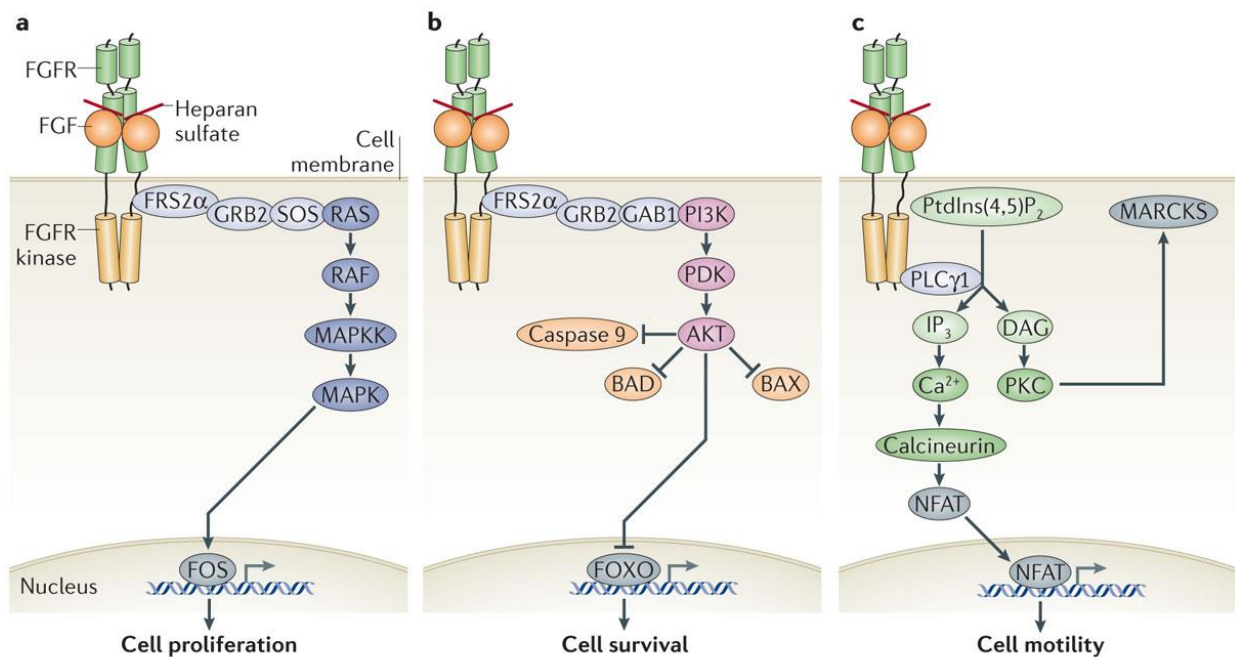
LIGANDS			RECEPTORS			
Scheme	Family	Members	FGFR	Isoforms	Scheme	
	cFGFs	FGF3	1, 2	IIIb		
		FGF4	FGF4	1, 2, 3, 4		IIIc
			FGF6	1, 2, 4		
			FGF5	FGF1		1, 2, 3, 4
		FGF2		1, 2, 3, 4		
		FGF5		1, 2		IIIc
		FGF8	FGF8	1, 2, 3, 4		IIIc
			FGF17	1, 2, 3, 4		
			FGF18	2, 3, 4		
		FGF9	FGF9	2, 3		IIIb, IIIc
			FGF16	2, 3		IIIc
			FGF20	1, 2, 3, 4		IIIb, IIIc
	FGF10	FGF7	2, 4	IIIb		
		FGF10	1, 2			
		FGF22	1, 2			
	hFGFs	FGF15/19	FGF15/19	1, 2, 3, 4		IIIb, IIIc
			FGF21	1, 2, 3, 4		
			FGF23	1, 2, 3, 4		
	iFGFs	FGF11	FGF11			
			FGF12			
			FGF13			
			FGF14			

Figure 6 Structure and family members of FGF ligands and the respective FGF receptor subtype's specificity (Guillemot and Zimmer 2011). FGFR numbers depicted in bold letters indicate high-affinity binding to the ligand in the same line; in plain letters they indicate intermediate affinity binding, and in italic they indicate lower affinity binding.



Nature Reviews | Molecular Cell Biology

Figure 7 FGF signalling pathways (Goetz and Mohammadi, Nat Rev Mol Cell Biol, 2013). Binding of fibroblast growth factor (FGF) to the FGF receptor (FGFR) induces FGFR dimerization, which juxtaposes the intracellular Tyrosine kinase domains of the receptors so that kinase activation by transphosphorylation can occur. The outcome of FGF/FGFR1 pathway is primarily cell proliferation (a) but can also lead to cell differentiation (b), cell migration (c) or another cellular response.

The major pathway, which is mediated by FGF/FGFR signalling is the proliferative pathway MAPK/ERK signalling cascade which resulted in the activation of various transcriptional factors such as Ets protein, AP1, GATA proteins, and CREB. The second pathway, the PLCg/Ca²⁺ pathway is activated by FGF/FGFR interaction, which stimulate neurite outgrowth by FGF2 (Doherty and Walsh, 1996). The other pathway, which is mediated by FGF/FGFR signalling is PI3 kinase/AKT pathway, which regulate cell proliferation and survival. FGF/FGFR signalling involve in multiple developmental processes in embryogenesis such as implantation, gastrulation, somitogenesis, body plan formation, morphogenesis and organogenesis (Belov and Mohammadi 2013).

1.7 FGFR1 in oligodendrocyte lineage

FGF receptor expression in oligodendrocyte lineage is distinct in different stage of oligodendrocyte lineage. FGFR1 is expressed in all stages of oligodendrocyte lineage cells. FGFR2 is expressed in mature oligodendrocytes. FGFR3 is expressed in early and late progenitors. FGFR4 is not expressed by any stage of oligodendrocyte lineage cells. FGF2 up-regulates FGFR1 in early and late progenitors whereas downregulates FGFR2 in mature oligodendrocytes (dotted line the Figure 8). FGFR1 in early progenitors stimulate proliferation and migration. FGFR1 mRNA has been detected in preprogenitors by PCR (Bansal 2003). Exposure of FGF-2 to terminally differentiating oligodendrocytes resulted in i) down regulation of myelin specific gene expression such as myelin basic protein, proteolipid protein, ii) increases in the length of cellular process iii) cell cycle re-entry without finishing mitosis, iv) importantly altering the expression patterns of low and high affinity FGF receptors (Bansal and Pfeiffer 1997). FGFR1 expression increases in the oligodendrocyte lineage and the predominant is FGF receptor 1 transcript variant alpha (FGFR-1 α). Expression of FGFR1 level in astrocytes is different compared to oligodendrocytes lineages, as astrocytes express more FGF receptor-1 β (Bansal *et al.* 1996).

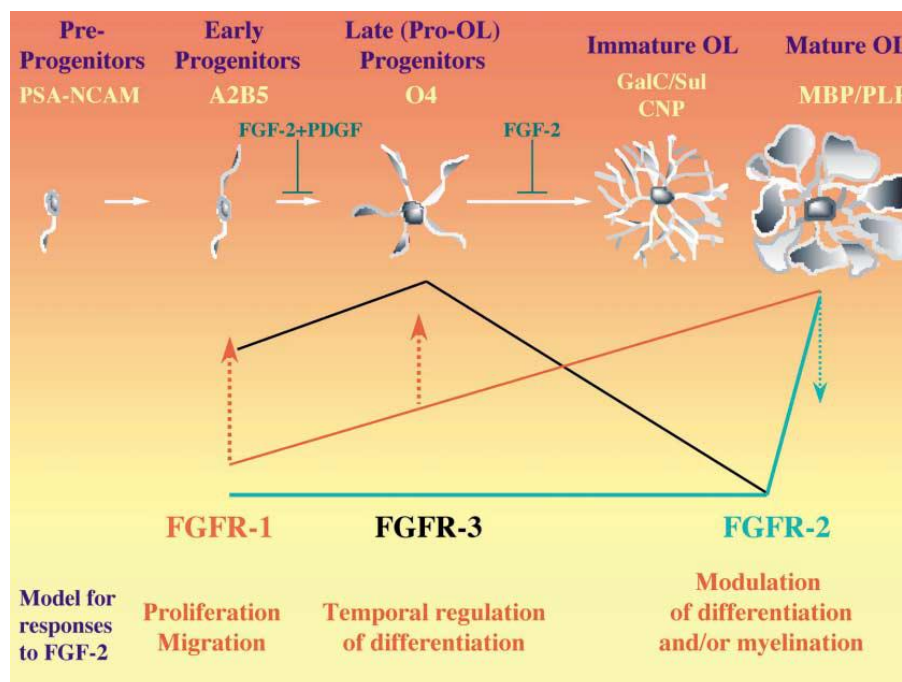


Figure 8 FGFR expression pattern in developing oligodendrocyte lineage with stage specific cell marker (Pfeiffer *et al.* 1993, Bansal 2002). Inhibition of early or late progenitors by FGF2 is shown.

1.8 FGF/FGFR1 in demyelinating disease MS and its animal model EAE

In vitro and *in vivo* data suggest that FGF2 plays a role in demyelinating pathologies. The most common demyelinating disease is multiple sclerosis (MS). In postmortem brain tissue from patients with multiple sclerosis, FGF2 is expressed in active lesions and in the periplaque of chronic lesions (Clemente *et al.* 2011). Furthermore, high levels of FGF2 protein expression are found during relapse in serum (Harirchian *et al.* 2012) and cerebrospinal fluid (CSF) (Sarchielli *et al.* 2008). *In vitro* activation of the FGF2/FGFR1 pathway results in downregulation of myelin proteins (Fortin *et al.* 2005). In MOG₃₅₋₅₅-induced experimental autoimmune encephalomyelitis (EAE), the most widely used animal model of multiple sclerosis, FGF2 ablation leads to a more severe disease course, increased lymphocyte and macrophage infiltration and decreased remyelination (Rottlaender *et al.* 2011). This finding is supported by a FGF2 gene therapy study in EAE resulting in less disease severity, reduced lymphocyte and macrophage infiltration and an increased number of myelin-forming oligodendrocytes (Ruffini *et al.* 2001). These data support an important role of FGF2 in multiple sclerosis and EAE.

The function of the corresponding receptor FGFR1 in multiple sclerosis and EAE is not well- defined. FGFR1 is present on oligodendrocytes, astrocytes and neurons in humans (Galvez-Contreras *et al.* 2012) and rodents (Reuss *et al.* 2003). However, it is also expressed on lymphocytes, macrophages and microglia in rats (Liu *et al.* 1998). In patients with multiple sclerosis FGFR1 is upregulated in oligodendrocyte precursor cells in active lesions, chronic-active and chronic-inactive lesions (Clemente *et al.* 2011). In rats FGFR1 is expressed on macrophages/activated microglia in the acute phase of EAE (Liu *et al.* 1998).

Butt and Dinsdale (2005) showed the raised FGF2 induces disruption of mature oligodendrocytes and severe loss of myelin. Moreover, they showed the aberrant accumulation of immature oligodendrocytes in the pre myelinating phenotype in FGF2 treatment. And they demonstrated that increased FGF2 induces demyelination in the adult rat CNS (Butt and Dinsdale, 2005). FGF treated mice in EAE model showed abrogate demyelination (Ruffini *et al.* 2001). In cuprizone mediated non-immune demyelination-remyelination model, FGF2 expression level was increased during both demyelination and remyelination (Gudi *et al.* 2011). Depending on the

oligodendrocyte developmental stage and level of concentration, FGF2 has both positive and negative effects.

1.9 FGF/FGFR signalling in disease

FGF receptor signalling mediating major cancer types in human beings. FGFR1 amplification is involved in breast, lung, squamous cell carcinoma, esophageal, ovarian and osteosarcoma (Dienstmann *et al.* 2014). Table 2 shows the involvement of FGFR1 in various cancer types in human beings. FGF signalling involved in many metabolic processes such as phosphate and vitamin D homeostasis, cholesterol and bile acid homeostasis, and glucose/lipid metabolism (Belov and Mohammadi 2013). Endocrine FGFs also involved in metabolic disorders such as chronic kidney disease, obesity and insulin resistance (Belov and Mohammadi 2013). Whereas, FGF/FGFR pathway implicated in the protection of neurons against neurotoxins and FGF have been shown to protect neurons by down-regulating the expression of the chemokine receptor CXCR4, activating cell-survival signalling and inhibiting the internalization of HIV-1 coded proteins (Sanders *et al.* 2000, Bachis *et al.* 2003). At least three genetic disorders can be attributed to mutations in FGFR1: Kallman's syndrome, ostroglophonic dysplasia and Pfeiffer's syndrome. Pathological Fgfr1 signalling also occurs in various malignancies (Beenken and Mohammadi 2009) (Table 2).

Table 2 Genomic deregulation of FGFR in tumors (Dienstmann *et al.* 2014). FGFR1 amplification and mutations involved in various cancer types in human beings.

Aberration		Tumor
FGFR1	Amplification	Breast (hormone receptor positive)
		Lung (squamous cell carcinoma)
		Lung (small cell)
		Head and neck (squamous cell carcinoma)
		Esophageal (squamous cell carcinoma)
		Ovarian
		Osteosarcoma
FGFR2	Amplification	Breast (triple-negative)
	Mutation	Gastric Endometrial
FGFR3	Mutation	Bladder (muscle-invasive)
		Glioblastoma
FGFR4	Amplification	Colorectal
	Mutation	Rhabdomyosarcoma

1.10 FGFR inhibitors in clinical trails

FGFR are receptor tyrosine kinases (RTKs) that regulate proliferation, differentiation and signalling processes in various cell types. Recently there are tyrosine kinase inhibitors (TKI) in cancer and autoimmune disease clinical trials (Mirschafiey *et al.* 2014). TKIs are a class of chemotherapy medications that block, or inhibit the enzyme tyrosine kinase. Imatinib, sorafenib, dasatinib, sunitinib, nilotinib, gefitinib, erlotinib, bosutinib, lapatinib, pazopanib and regorafenib are the TKI in clinical studies (Mirschafiey *et al.* 2014). All these inhibitors are ATP inhibitors at the catalytic binding site of tyrosine kinase and they differ from each other in the spectrum of targeted kinases, pharmacokinetics and substance specific adverse side effects (Hartmann *et al.* 2009). Imatinib, sunitinib, lestaurtinib (CEP-701), sorafenib (nexavar) and masitinib (AB1010) shows effects in MS and EAE study (Mirschafiey *et al.* 2014).

Table 3 FGFR inhibitors in clinical development. (Daniele *et al.* 2012, Dienstmann *et al.* 2014).

Compound	Company	Target	Clinical development (indication)
<i>Small-molecule tyrosine kinase inhibitors: mixed pharmacology</i>			
Brivanib	Bristol-Myers Squibb	FGFR, VEGFR	Phase III (CRC, HCC, liver)
Dovitinib	Novartis	FGFR, PDGFR, VEGFR, FLT3, c-KIT	Phase III (RCC)
Lenvatinib	Eisai	FGFR, PDGFR, VEGFR	Phase III (melanoma, thyroid)
Masitinib	AB Science	FGFR3, PDGFR, c-KIT	Phase III (GIST, melanoma, MM, pancreatic)
Nintedanib	Boehringer Ingelheim	FGFR, PDGFR, VEGFR	Phase III (NSCLC, ovarian)
Pazopanib	GlaxoSmithKline	FGFR1, FGFR3, VEGFR, PDGFR, c-KIT	Phase III (breast, lung, ovarian, RCC, STS)
PI-88	Progen	FGF1, FGF2, VEGF	Phase III (HCC, liver)
Regorafenib	Bayer	FGFR, PDGFR, VEGFR, c-KIT, RET	Phase III (GIST, CRC)
TSU 68	Pfizer	FGFR, KDR, PDGFR, VEGFR2	Phase III (HCC)
ENMD-2076	Entremed	FGFR1, KDR, FGFR2, PDGFR, VEGFR, FLT3, c-KIT, Aurora K, FLT3	Phase II (ovarian)
Ponatinib	Ariad	FGFR, PDGFR, VEGFR	Phase II (AML, CML)
E3810	Eisai	FGFR1, VEGFR	Phase I (solid tumors)
PBI-05204	Phoenix Bio	FGF2, AKT, NF- κ B, p70S6K	Phase I (solid tumors)
<i>Small-molecule tyrosine kinase inhibitors: FGFR selective</i>			
AZD4547	AstraZeneca	FGFR1–3	Phase II (breast, gastric)
BGJ398	Novartis	FGFR1–3	Phase I (solid tumors)
LY2874455	Eli Lilly	FGFR1–4	Phase I (solid tumors)
<i>FGFR antibodies</i>			
RG7444	Roche	FGFR3	Phase I (MM)
<i>FGF-ligand traps</i>			
FP-1039	Five Prime Therapeutics	FGF1, FGF2, FGF4	Phase II (endometrial)

There are various knockdown studies and selective pharmacological inhibition in preclinical models conclude that FGFRs as attractive targets for the therapeutic intervention in cancer studies (Dienstmann *et al.* 2014) (Table 3). Most FGFR inhibitors currently in development are small molecule kinase inhibitors of the ATP-binding domain. Selective FGFR tyrosine kinase inhibitors, monoclonal antibody that bind to the extracellular domain of FGFRs and block FGF ligand, thereby blocking FGFR dimerization and downstream activation are also in clinical testing.

2 AIMS

Based on the recent findings on the function of FGF2 in EAE it was hypothesized that deletion of oligodendroglial Fgfr1 would result in a more severe disease course, increased inflammation and neurodegeneration. Aim of the study was to characterize and evaluate the role of oligodendrocyte specific Fgfr1 in experimental autoimmune encephalomyelitis, an animal model of multiple sclerosis.

The objectives of this study are

1. To evaluate the role of oligodendrocyte specific Fgfr1 in EAE (Inflammation, demyelination, axons, cytokines, chemokines and growth factor expression).
2. To characterize the role of oligodendrocyte specific Fgfr1 signalling pathway in C57Bl/6J mice.
3. To evaluate the *in vitro* role of oligodendrocyte specific Fgfr1 and IFN- β in oligodendrocyte proliferation and cytotoxicity.

3 MATERIALS AND METHODS

3.1 MATERIALS

3.1.1 Animals

3.1.1.1 Mice provider

Mice line	Supplier	Animal facility
<i>Fgfr1^{fl/fl}</i>	The Jackson Laboratories, Bar Harbor, ME, USA	JLU, Central Animal facility, Frankfurter straÙe, Giessen, Germany.
<i>PLP CreER^T</i>		
C57BL/6J		

3.1.1.2 Genetic background of mice strains

Mouse strain	Administration	Abbreviation	Genotype
<i>Plp/CreER^T:Fgfr1^{fl/fl}</i>	Vehicle (sunflower oil + ethanol)	Control	Homozygous
<i>Plp/CreER^T:Fgfr1^{fl/fl}</i>	Tamoxifen	<i>Fgfr1^{ind/-}</i>	Homozygous

Tamoxifen was injected to 4 weeks old *Plp/CreER^T:Fgfr1^{fl/fl}* female mice for 5 consecutive days to create the conditional knockout of *Fgfr1* in oligodendrocyte lineage. Sunflower oil with ethanol without Tamoxifen was injected in age, gender matched mice from similar line (control).

3.1.2 Cell lines

Cell Line	Provider
Oli-neu	Neurologie Klinikum, MS Research group, Gießen

3.1.3 Primary antibodies

Name	Host	Reactivity	Mol. Weight	Method	Artikle Nr	Manufacturer
Anti-pStat1	Rabbit	H, M, R	84/91 kDa	WB	9171s	Cell Signaling Tech, MA, USA
Anti-Stat1	Rabbit	H, M, R, MK	84/91 kDa	WB	9172	Cell Signaling Tech, MA, USA
Anti-CNPase	Mouse	H, M, R	46/48 kDa	WB	ab6319	Abcam, UK
Anti-MBP	Mouse	H, M, R, G	33 kDa	WB	ab62631	Abcam, UK
Anti-PLP	Rabbit	H, M	26/30 kDa	WB	ab28486	Abcam, UK
Anti-pERK p-44/42	Rabbit	H M R Hm Mk	44, 42	WB	4370s	Cell Signaling Tech, MA, USA
Anti-Erk 1/2	Rabbit	H, M, R, MK	42/44 kDa	WB	9102	Cell Signaling Tech, MA, USA
Anti-Akt	Rabbit	H, M, R, MK	60 kDa	WB	9272	Cell Signaling Tech, MA, USA
Anti-pAkt (Ser473)	Rabbit	H, M, R, MK	60 kDa	WB	4060s	Cell Signaling Tech, MA, USA
Anti-Flg (C-15) (FGFR1)	Rabbit	H, M, R	110 kDa	WB	sc-121	Santa Cruz Biotech, CA, USA
Anti-Bek (C-17) (FGFR2)	Rabbit	H, M, R	120 kDa	WB	sc-122	Santa Cruz Biotech, CA, USA
Anti-GAPDH	Mouse	Ca, H, M, R	38 kDa	WB	MAB374	Chemicon/ Millipore, CA; USA
Anti-Trk B (794):sc12	Rabbit	H, M, R	145 kDa	WB	sc-12	Santa Cruz Biotech, CA, USA
Anti-BDNF	Rabbit	H, M, R	17, 13 kD	WB	sc-546	Santa Cruz Biotech, CA, USA
Anti pFGFR1 Mac 3	Rabbit	H M, R	~145 kDa	WB	06-1433	Millipore, CA; USA
Clone M3/84 B220	Rat	M	staining	IHC	553322	Pharmingen, USA
clone RA3-6B2	Rat	H, M	staining	IHC	557390	Pharmingen, USA
CD3, clone CD3-12	Rat	M	staining	IHC	MCA 1477	Serotec, UK
Olig-2	Rabbit	M	staining	IHC	18953	IBL, Japan
Nogo A H300	Rabbit	H, M	staining	IHC	Sc 25660	Santa cruz Biotech, CA, USA
MBP	Rabbit	M, R	staining	IHC	62301	Dako, Germany
SMI 32	Mouse	H, M.	staining	IHC	SMI32	SMI

3.1.4 Secondary antibodies

Antibody	Host	Artikle Nr	Manufacturer
Anti-Rabbit-HRP	Goat	sc-2004	Santa Cruz Biotech, CA, USA
Anti-Mouse-HRP	Donkey	sc-2318	Santa Cruz Biotech, CA, USA

3.1.5 Kits

Kit	Manufacturer	Artikle Nr	Method
BCA Protein Assay Kit	Pierce® Thermo Scientific, IL, USA	23225	Protein quantification
Cell Proliferation reagent WST-1	Roche Applied Science, Mannheim, Germany	11644807001	Proliferation assay
Cytotoxicity detection kit (LDH)	Roche Applied Science, Mannheim, Germany	11644793001	Cytotoxicity assay
DirectPCR Lysis Reagent (Tail)	Peqlab, Erlangen, Germany	31-121-T	DNA isolation
iTaq™ Universal SYBR® Green qPCR Master Mix	Bio-Rad, CA, USA	172-5124	PCR
QuantiTect® Reverse Transcription Kit	Qiagen GmbH, Hilden, Germany	205310	Reverse Transcription
SuperSignal® West Pico Chemiluminescent substrate	Thermo Scientific, IL, USA	34077	Western Blot
Total RNA Isolation Kit NucleoSpin RNA II	Macherey-Nagel, Düren, Germany	740955,3	RNA Isolation

3.1.6 Primers

Primers were designed using NCBI primer designing tool and all primers were purchased from Eurofins Genomics, Ebersberg, Germany.

3.1.6.1 Primers used for genotyping

Gene (Primer)	5' —→ 3' Sequence
PLP Cre PCR	PLP transgene forward GCGGTCTGGCAGTAAAACTATC
	PLP transgene reverse GTGAAACAGCATTGCTGTCACTT
	Cre Internal primer forward CTAGGCCACAGAATTGAAAGATCT
	Cre Internal primer reverse GTAGGTGGAAATTCTAGCATCATCC
Fgfr1 lox	Forward GGACTGGGATAGCAAGTCTCTA
	Reverse GTGGATCTCTGTGAGCCTGAG

3.1.6.2 Primers used for analysis

Primer	5' → 3' Sequence
TNF- α	Forward CGGTCCCCAAAGGGATGAGAAGT
	Reverse ACGACGTGGGCTACAGGCTT
IL-1 β	Forward TACCTGTGGCCTTGGGCCTCAA
	Reverse GCTTGGGATCCACACTCTCCAGCT
IL-6	Forward CTCTGCAAGAGACTTCCA
	Reverse AGTCTCCTCTCCGGACTT
IL-12	Forward AGACCACAGATGACATGGTGA
	Reverse ACGACGTGGGCTACAGGCTT
iNOS	Forward TTGGAGGCCTTGTGTCAGCCCT
	Reverse AAGGCAGCGGGCACATGCAA
BDNF	Forward AAGGGCCAGGTCTGTTAAGC
	Reverse GGTAAGAGAGCCAGCCACTG
TrkB	Forward TGACGCAGTCGCAGATGCTG
	Reverse TTTCCTGTACATGATGCTCTCTGG
GAPDH	Forward GGATGGGTCCTCATGCTCAC
	Reverse TGGTGCTGCAAGTCAGAGCAG
TGF- β	Forward CTCCTGCTGCTTTCTCCCTC
	Reverse GTGGGGTCTCCCAAGGAAAG
SEMA3A	Forward GGATGGGTCCTCATGCTCAC
	Reverse TGGTGCTGCAAGTCAGAGCAG
Lingo1	Forward TCATCAGGTGAGCGAGAGGA
	Reverse CAGTACCAGCAGGAGGATGG
FGF2	Forward GGCTGCTGGCTTCTAAGTGT
	Reverse ACTGGAGTATTTCCGTGACCG
Fgfr1	Forward CAGATGCACTCCCATCCTCG
	Reverse GGGAGCTACAGGGTTTGGTT
PLP	Forward GAGCAAAGTCAGCCGCAAAA
	Reverse CAAGCCCATGTCTTTGGCAC
MBP	Forward TCCATCGGGCGCTTCTTTAG
	Reverse TCTCGTGTGTGAGTCCTTGC
CX3CR1	Forward CTGCTCAGGACCTCACCATGT
	Reverse ATGTCGCCCCAAATAACAGGC
CX3CL1	Forward GCGACAAGATGACCTCACGA
	Reverse TGTCGTCTCCAGGACAATGG

3.1.7 Ladders

Marker	Manufacturer
PageRuler™ Plus Prestained Protein Ladder	Fermentas, Invitrogen, Carlsbad, USA
Fluorescent Long Range DNA Ladder	Jena Bioscience, Jena, Germany

3.1.8 Chemicals

Compound	Manufacturer
10x PBS for cell culture (DPBS)	Lonza, Köln, Germany
2-Mercaptoethanol	Sigma-Aldrich, Steinheim, Germany
2-Propanol	Sigma-Aldrich, Steinheim, Germany
3% Hydrogen peroxide	Carl Roth, Karlsruhe, Germany
Acetic acid	Merck, Darmstadt, Germany
Agarose	Bioline GmbH, Luckenwalde, Germany
Ammonium Persulphate (APS)	Carl Roth, Karlsruhe, Germany
Bovine Serum Albumin (BSA)	Merck, Darmstadt, Germany
Bromophenol Blue	Neolab, Heidelberg, Germany
Citric acid	Merck, Darmstadt, Germany
complete Freund's adjuvant	Sigma, Steinheim, Germany
Distilled water (Ecostrain®)	Braun, Melsungen, Germany
Dimethylsulfoxide (DMSO)	Carl Roth, Karlsruhe, Germany
Disodium-hydrogen-phosphate	Merck, Darmstadt, Germany
DNase	Qiagen, Hilden, Germany
EDTA	Carl Roth, Karlsruhe, Germany
Eosin	Merck, Darmstadt, Germany
Eosin	Carl Roth, Karlsruhe, Germany
Ethanol 100%	Sigma-Aldrich, Steinheim, Germany
FBS	PAA Laboratories, Pasching, Austria
Glycerol	Carl Roth, Karlsruhe, Germany
Glycin	Merck, Darmstadt, Germany
Glyzerin	Carl Roth, Karlsruhe, Germany
Hematoxylin	Carl Roth, Karlsruhe, Germany
Isopropanol	Merck, Darmstadt, Germany
Ketamine	Inersa Arzneimittel GmbH, Freiberg, Germany
Luxol-Fast-Blue	Sigma-Aldrich, Steinheim, Germany
Magnesiumsulfate (MgSO ₄)	Sigma Aldrich, Tachfkirchen, Germany
Methanol	Merck, Darmstadt, Germany
MOG ₃₅₋₅₅	Charité Berlin, Berlin, Germany
<i>Mycobacterium tuberculosis</i>	Difco Microbiology, Michigan, USA
NP40	US Biologicals, MA, Germany
Paraformaldehyde (PFA)	Sigma Aldrich, Taufkirchen, Germany
Pertussis Toxin	Calbiochem, Darmstadt, Germany
Poly-L-Lysine	Sigma-Aldrich, Steinheim, Germany
Potassium chloride (KCL)	Merck, Darmstadt, Germany

Potassiumdihydrogenphosphate	Merck, Darmstadt, Germany
Protease Inhibitor cocktail	Roche, Mannheim, Germany
Proteinase K	Sigma-Aldrich, Missouri, USA
RNAse free water	Millipore corporation, MA, USA
Rotiphorese Gel (30% acrylamide mix)	Carl Roth, Karlsruhe, Germany
Sodium chloride (NaCl)	Carl Roth, Karlsruhe, Germany
Sodium-dihydrogen-phosphate	Merck, Darmstadt, Germany
Sodium hydrogen carbonate (NaHCO ₃)	Merck, Darmstadt, Germany
Sodiumdodecylsulfate (SDS)	Neolab, Heidelberg, Germany
Sodiumazid (NaN ₃)	Merck, Darmstadt, Germany
Sunflower oil	Sigma-Aldrich, Steinheim, Germany
Tamoxifen	Sigma-Aldrich, Steinheim, Germany
TEMED	Carl Roth, Karlsruhe, Germany
Tris HCl	Carl Roth, Karlsruhe, Germany
Tris. acetat-EDTA buffer (TAE) 10x	Carl Roth, Karlsruhe, Germany
Trishdroxymethyl aminomethan (Tris)	Carl Roth, Karlsruhe, Germany
Tryphanblue	Carl Roth, Karlsruhe, Germany
Trypsin (2.5g/l)	Gibco, Invitrogen, Carlsbad, USA
Tween 20	Merck, Darmstadt, Germany
Xylazin 2%	CEVA Tiergesundheits GmbH, Düsseldorf, Germany

3.1.9 Laboratory consumables

Consumables	Manufacturer
Cellstar® 6 Well and 24 well Cell Culture Plate	GreinerBioOne, Frickenhausen, Germany
Cellstar® Plastikpipettes (5 ml, 10 ml)	GreinerBioOne, Frickenhausen, Germany
Cellstar® U-shape with Lid, TC-Plate, 96 well, sterile	GreinerBioOne, Frickenhausen, Germany
Cellstar® Flat bottom with Lid, TC-Plate, 96 well, sterile	GreinerBioOne, Frickenhausen, Germany
Cellstar® 75 cm ² Cell cultur flasks	GreinerBioOne, Frickenhausen, Germany
Cellstar® 125 cm ² Cell cultur flasks	GreinerBioOne, Frickenhausen, Germany
Cell scrapper	GreinerBioOne, Frickenhausen, Germany
Cryobox 136x136x130 mm	Ratiolab GmbH, Dreieich, Germany
Cryo Tube™ vials (1,8 mL; 4,5 mL)	Sarstedt AG & Co, Nümbrecht, Germany
Falcon tubes (15ml, 50ml)	Becton Dickinson, Heidelberg, Germany
Glass Pasteur pipettes 150 mm	Brand, Wertheim, Germany
Ministart single use filter (0,2 µm, 0,45 µm)	Sartorius Stedim Biotech GmbH, Göttingen, Germany

Nitra-Tex® powder free gloves	B. Braun Melsungen AG, Germany
Parafilm	Pechiney Plastic packaging, Menasha, WI
Pipette tips without filter (10 µL, 100 µL, 1000 µL)	Sarstedt AG & Co, Nümbrecht, Germany
Eppendorf tubes 1,5 mL, 2mL	Eppendorf Vertrieb Deutschland GmbH, Wesseling-Berzdorf, Germany
Eppendorf tubes 1,5 mL, 2mL (PCR clean- pyrogen & DNase free)	Nerbe Plus GmbH, Winsen (Luhe), Germany
Sterile PCR- clean pyrogen & DNase free with filter (10, 100, 200, 1000µl)	Nerbe Plus GmbH, Winsen (Luhe), Germany
Tissue culture dishes steril 35,0 /10mm	GreinerBioOne, Frickenhausen, Germany
UV-Spectroscopic cuvettes (RNA quantification)	BioRad, München, Germany
Falcon® Plastic pipettes 10ml, 5ml	Becton Dickinson, Heidelberg, Germany
Glasswares (different sorts)	Fisherbrand; IDL; Schott&Gen; Simax
Syringe 25ml for BSA	B. Braun Melsungen AG, Germany
Nitrocellulose membrane	GE Healthcare, Amersham™ Hybond ECL, Buckinghamshire, UK
PCR Tube, cap-strips	Applied Biosystems, Darmstadt, Germany

3.1.10 Laboratory instruments

Instrument	Manufacturer
Arpege 75, Liquid nitrogen tank	Air Liquide Medical GmbH, Düsseldorf, Germany
Axioplan 2 Fluorescence Microscope	Carl Zeiss, Jena, Germany
BEP 2000 Advance (ELISA-Reader)	Dade Behring Marburg GmbH, Marburg, Germany
Centrifuge type 2-6 Easia shaker Medgenix diagnostics	Sigma-Aldrich Chemie GmbH, Taufkirchen, Germany
Centrifuge Universal 32 R	Hettich GmbH, Kirchlingen, Germany
ELISA-Reader Multiscan EX	Thermo electron corporation, Langenselbold, Germany
Fusion FX7 chemiluminescence system	Peqlab Biotechnologie GmbH, Erlangen, Germany
Hettich centrifuge (cooling)	Hettich GmbH, Kirchlingen, Germany

Light Microscope for cell culture	Carl Zeiss Microscopy GmbH, Oberkochen Germany
Magnetic stirrer	IKA® Werke GmbH, Staufen, Germany
Nalgene™ Cryo 1°C Freezing container	Nalgene®, Germany
Nanophotometer	Implen GmbH, München, Germany
Neubauer improved cell chamber	Brand, Wertheim, Germany
Neubauer improved Haemocytometer	Brand, Wertheim, Germany
Nuaire™ Biological Safety Cabinets Class II type A/B3 (Sterilbank)	INTEGRA Biosciences GmbH, Fernwald, Germany
pH-Meter	Mettler Toledo GmbH, Giessen, Germany
Pipette boy	INTEGRA Biosciences GmbH, Fernwald, Germany
Power pack	Peqlab Biotechnologie GmbH, Erlangen, Germany
Refrigerators and freezers	Different companies
Rotamax 120 (Shaker)	Heidolph Instruments GmbH & Co. KG, Schwabach, Germany
Sanyo Incu-safe incubator for cell culture	Ewald Innovationstechnik GmbH, Bad Nenndorf, Germany
SmartSpec™ Plus Spectrophotometer	BioRad, München, Germany
StepOne® Real-Time PCR system	Applied Biosystems, Darmstadt, Germany
Surgical instruments	Various companies
Table top centrifuge EBA 20	Hettich GmbH, Kirchlingen, Germany
Table top centrifuge micro 120	Hettich GmbH, Kirchlingen, Germany
TissueRuptor	Qiagen Instruments, Hombrechtikon, Switzerland
Trans-Blot® SD Semi-dry transfer cell	BIO RAD, München, Germany
Trans-Blot® SD Semi-dry transfer cell	BioRad, München, Germany
Vortexer vortex-Genie2	Heidolph Instruments GmbH & Co. KG, Schwabach, Germany
Water bath	Memmert GmbH + Co.KG, Germany
Weighing balance	Sartorius Stedim Biotech GmbH, Göttingen, Germany
Western blotting system	BioRad, München, Germany

3.1.11 Buffers

Buffer	Components	Volume
1X SDS-PAGE Running Buffer	Rotiphorese [®] 10X Running Buffer	100 ml
	H ₂ O	900 ml
10x PBS (1 Liter) pH 7.4	137 mM NaCl	80 g
	2 mM KH ₂ PO ₄	2.4 g
	2.7 mM KCl	2 g
	10 mM Na ₂ HPO ₄	14.4 g
	H ₂ O	1000 ml
10x TBS (1 Liter) pH 7.2 to 7.6	Tris	24.2 g
	NaCl	87.7 g
	H ₂ O	1000 ml
1x TBS-Tween (TBST) (1 Liter)	1x TBS	1000 ml
	0.1% Tween®20	1 ml
Lysis Buffer (250ml) pH 7.4	NaCl	2.19 g
	Tris	0.61 g
	EDTA	0.07 g
	Glycerol	25 ml
	NP40	2.5 ml
	NaN ₃	0.025 g
6x SDS-PAGE Loading Buffer	60 mM Tris-HCl (pH 6.8)	36 ml
	2% SDS	60 ml
	0.01% Bromophenol blue	60 mg
	10% Glycerol	60 ml
	ddH ₂ O	144 ml
	β-Mercaptoethanol	65 µl/ml
SDS-PAGE Transfer buffer (1 Liter)	10x Running buffer	100 ml
	Methanol	200 ml
	ddH ₂ O	700 ml
Blocking buffer (5% BSA) Bovine Serum Albumin	BSA fraction V	5 g
	TBST	100 ml
10x Trypsin EDTA	10x Trypsin	5 ml
	ddH ₂ O	45 ml
10% Ammonium Persulfate (APS)	APS	1 g
	ddH ₂ O	10 ml
10% Sodiumdodecylsulfate (SDS)	SDS	1 g
	ddH ₂ O	10 ml

3.2.12 Softwares

Fusion Bio1D software (Peqlab, Erlangen, Germany)

Microsoft Office Professional Plus 2010 (Microsoft corporation, USA)

SigmaPlot 10 software (Systat, San Jose, CA, USA)

Systat 12 software (Systat, San Jose, CA, USA)

Image J software (Image J 1.47d, National Institute of Health, USA)

StepOne RealTime PCR Software v2.1 (Applied Biosystems, Darmstadt, Germany)

Graph Pad Prism Software Version 5.01 (GraphPad Software, Inc. CA, USA).

3.2 METHODS

3.2.1 Animal experiment procedures

3.2.1.1 Mice

Fgfr1^{-/-}geflox flox (*B6.129S4-Fgfr1*^{tm5.1Sor}/*J*), Plp-creER^T (*B6.Cg-Tg(Plp1-cre/ER*^T*)3Pop/J*) and C57BL/6 mice were purchased from The Jackson Laboratories (Bar Harbor, ME, USA). *Fgfr1*^{-/-}geflox flox (*B6.129S4-Fgfr1*^{tm5.1Sor}/*J*) mice were crossbred with Plp-creER^T (*B6.Cg-Tg(Plp1-cre/ER*^T*)3Pop/J*) mice and backcrossed to C57BL/6J for at least 10 generations (Final mice line: *B6.Cg-Tg(Plp1-cre/ER*^T*)3Pop Fgfr1*^{tm5.1Sor}). Mice were bred and grown in JLU-central animal facility, Frankfurter Straße 110, Gießen, Germany. All animal experiments were carried out in JLU central animal facility and analyzed in the Neurochemisches Labor, Department of Neurology, Gießen, Germany.

3.2.1.2 Preparation of mice genomic DNA for genotyping

The genotype was controlled by PCR (DirectPCR-Tail, Peqlab, Erlangen, Germany) using *Fgfr1*^{lox} and Plp cre locus and confirmed by agarose gel electrophoresis. A small portion of (1 mm) tail or the ear from each mice were lysed in 200µl of Direct PCR tail reagent with proteinase K for 5-15 hours at 55 °C to digest the tissues and then for 45 minutes at 80 °C to deactivate Proteinase K. The tail lysate was centrifuged for 10 seconds and 1 µl has been used for genotyping PCR.

3.2.1.3 Genotyping and identification of locus

Genomic DNA from all mice (1 µl) was used in SYBR Green PCR and the primers for *Fgfr1* and PLP/Cre locus were used (sections 3.2.1.4 and 3.2.1.5). Amplified PCR product was run in 1.5% agarose gel electrophoresis in 120v for 45 min (BioRad electrophoresis chamber) and bands were determined in Fusion Fx7 chemiluminescence system (PEQLAB, Erlangen, Germany).

3.2.1.4 PCR master mix:

Fgfr1 Locus		PLP Cre Locus	
10 µl SYBR Green master mix		10 µl SYBR Green master mix	
7 µl H ₂ O		5 µl H ₂ O	
1 µl Forward Primer (Fgfr1)		1 µl Forward Primer (PLP)	
1 µl Reverse Primer (Fgfr1)		1 µl Reverse Primer (PLP)	
1 µl genomic DNA		1 µl genomic DNA	
		1 µl Forward Primer (CRE)	
		1 µl Forward Primer (CRE)	
Total reaction	20 µl		20 µl

3.2.1.5 Genotyping PCR thermal profile:

<i>Fgfr1 locus</i>				<i>PLP Cre Locus</i>			
	Temp	Time	cycles	Temp	Time	cycles	
Denaturing	95° C	5 min	35x	95°C	5 min	35x	
Denaturing	95°C	30 s		95°C	30 s		
Annealing	64°C	1 min		51°C	1 min		
Elongation	72°C	1 min		72°C	1 min		
				72°C	2 min		

3.2.1.6 Fgfr1 conditional knockout creation

To induce cre recombinase mediated deletion of Fgfr1 in oligodendrocytes, four weeks old *Plp/CreER^T:Fgfr1^{fl/fl}* (B6.Cg-Tg(Plp1-cre/ER^T)3Pop *Fgfr1^{tm5.1Sor}*) female mice were injected with 1 mg of tamoxifen i.p. (Sigma-Aldrich, Steinheim, Germany) in 100 µl sunflower oil/ethanol (Sigma-Aldrich, Steinheim, Germany) over 5 consecutive days (later referred as Fgfr1^{ind/-} in this thesis) (Figure 9). Control mice of the same genotype received a sunflower oil/ethanol mixture. All animal experiments were approved by the local state authorities of Hesse, Giessen, Germany (GI 2008).



Figure 9 Fgfr1 conditional knockout creation and tissue collection for Fgfr1 knockout study.

3.2.1.7 Induction and clinical scoring of MOG₃₅₋₅₅-induced EAE

Mice were anesthetized for ~45 seconds by isoflurane and then EAE induction was done. EAE was induced in 8-12 weeks old female *B6.Cg-Tg(Plp1-cre/ER^T)3Pop Fgfr1^{tm5.1Sor}* conditional knockout (*Fgfr1^{ind/-}* Tamoxifen, n = 13) and control mice (oil/ethanol vehicle, n = 13). Subcutaneous injection of 300 µg myelin oligodendrocyte glycoprotein peptide (MOG₃₅₋₅₅; MOG peptide amino acids - MEVGWYRSPFSRVVHLYRNGK; Charité Hospital, Berlin, Germany) emulsified in complete Freund's adjuvant (Sigma, Steinheim, Germany) containing 10 mg/ml *Mycobacterium tuberculosis* (Difco, Michigan, USA) were injected in 4 flanks. Intraperitoneal injections of 300 ng pertussis toxin (Calbiochem, Darmstadt, Germany) were done during immunization and 48 hours later. The clinical disease course was monitored daily until day 19 (acute phase) and until day 62 (chronic phase) (Figure 10). The EAE disease course was evaluated using a scale that ranged from 0 to 5: 0 = normal, 0.5 = distal tail weakness, 1 = complete tail weakness, 1.5 = mild hind limb weakness, 2 = ascending hind limb weakness, 2.5 = severe hind limb weakness, 3 = hind limb paralysis, 3.5 = hind limb paralysis and forelimb weakness, 4 = tetraparesis, 4.5 = tetraplegia and incontinence, to 5 = moribund/death. Three independent experiments were done.

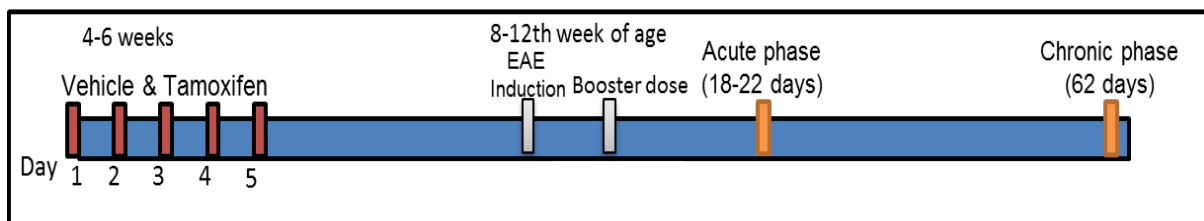


Figure 10 Experimental design of *Fgfr1* conditional knockout creation, EAE induction, and clinical scoring till acute and chronic phase.

3.2.1.8 EAE induction and Interferon beta-1a treatment (prevention study)

EAE were induced as described in paragraph 1.5 and preventive treatment of Interferon beta 1a (IFN β-1a) were done. Post immunization with MOG peptide, control and *Fgfr1^{ind/-}* mice subcutaneously injected with 1µg/ml IFN β-1a (Merck Serono) from day 0 till day 7 p.i. (Figure 11). Mice were monitored till day 62 for EAE scoring as described in section 3.2.1.7.

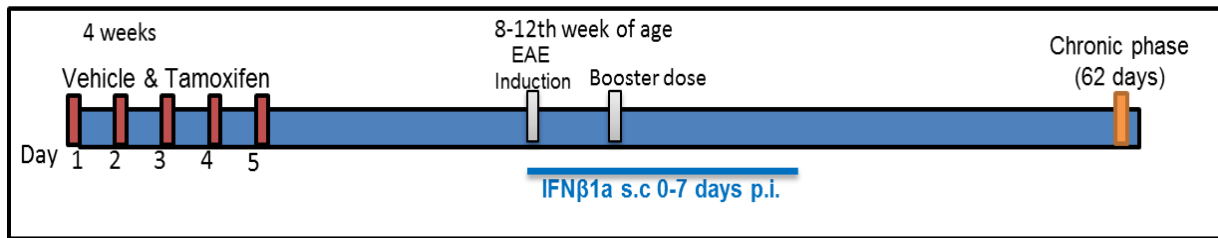


Figure 11 Experimental design of *Fgfr1* conditional knockout creation, EAE induction, IFN β -1a treatment and clinical scoring till chronic phase.

3.2.2 Molecular biology methods

3.2.2.1 RNA isolation

At day 19 (acute phase) and day 62 (chronic phase) after EAE induction, mice were euthanized with CO₂. The spinal cords and the spleens were removed, snap frozen in liquid nitrogen. The total RNA was isolated using NucleoSpin RNA II kit (Macherey-Nagel, Düren, Germany) as manufacturer instructions. Briefly, frozen spleen and spinal cord were taken and RA1 lysis buffer with β -mercaptoethanol were added according to the weight of each tissue samples and homogenized with Tissue ruptor (Qiagen Instruments, Hombrechtikon, Switzerland). Lysate were added to NucleoSpin filter in collection tube and centrifuged for 11000g for 1 minute and flow through were mixed with 70% ethanol and then added to NucleoSpin RNA II column followed by 11000g for 30 seconds centrifugation. rDNase mixer were added to the column and washed with wash buffer RA2 and RA3 then total RNA was eluted with 50 μ l RNase free water. Total RNA concentration was quantified in SmartSpec spectrophotometer.

3.2.2.2 Reverse transcription and cDNA synthesis

cDNA was synthesized from 1 μ g/ml of total RNA using the QuantiTect[®] Reverse Transcription Kit (Qiagen GmbH, Hilden, Germany). In 20 μ l of diluted 1 μ g/ml of total RNA 3 μ l genomic DNA wipeout buffer was added and incubated at 42 °C for 2 minutes, then cDNA synthesis master mix (5x RT buffer - 4 μ l, RT Primer - 1 μ l, RT master mix - 1 μ l) was added followed by incubation at 42 °C for 30 minutes and 95 °C for 3 minutes. Synthesized cDNA were stored -20 or -80 °C until use.

3.2.2.3 Relative real time-PCR quantification

Quantitative PCR detection of gene expression in the spinal cord and spleen were measured using iTaqTM Universal SYBR[®] Green qPCR Master Mix (Bio-Rad, CA, USA) by 40 cycles at an annealing temperature of 60 °C in the StepOne[®] Real-Time PCR system (Applied Biosystems, Darmstadt, Germany). Primers were designed by NCBI nucleotide Primer designing tool and primers were synthesized in Eurofins-Genomics (Eurofins MWG Synthesis GmbH, Ebersberg, Germany). The quantification of target genes was done using the primers listed on table and the PCR composition of 10 µl Mastermix (iTaQTM Universal SYBR[®] Green), 1 µl forward primer, 1 µl reverse primer, 7 µl H₂O and 1 µl of cDNA. GAPDH was used as the internal control gene, and the comparative $\Delta\Delta CT$ method ($\Delta CT = \text{target gene} - \text{housekeeping gene}$; $\Delta\Delta CT = 2^{-\Delta CT}$) was used to evaluate the relative quantification of gene expression.

3.2.3 Protein biochemistry

3.2.3.1 Protein extraction and quantification

Mice for knockout study (Figure 9), acute and chronic EAE (Figure 10) were euthunized by CO₂ and different CNS tissues (spinal cord, brain stem, cortex, cerebellum, hippocampus, rest of the brain) were separated. Tissues were homogenized in lysis buffer (150 mM NaCl, 20 mM Tris HCl, 1 mM EDTA, 10% glycerol, 1% NP40, 0.01% sodium azide) with Tissue ruptor (Qiagen Instruments, Hombrechtikon, Switzerland). The lysate were centrifuged at 4 °C for 30 minutes at 14000 rpm and supernatant were collected. The amount of protein was estimated using BCA assay as manufacturer instructions (Pierce[®] BCA Protein Assay Kit, Thermo Scientific, IL, USA). Briefly 25 µl of 1:10 diluted protein samples were taken as triplicate in 96 well flat bottom plate and 200 µl of Reaction Reagent was added and incubated for 30 minutes at 37 °C. The plate was measured in ELISA reader at the nanometer range of 540 nm. Measured protein level was normalized to 2 µg/µl concentrations in lysis buffer and stored at -20 °C until use.

3.2.3.2 SDS-PAGE and western blot

Protein loading buffer 6x was added to 30 µl of protein sample (60 µg) and boiled for 5 minutes at 95 °C. Normalized protein was loaded and separated by 10% SDS-PAGE (Rotiphorese® Gel 30, 10x SDS-PAGE, Carl Roth GmbH, Karlsruhe, Germany), transferred (Trans Blot, semi dry transfer cell, BioRad) to a nitrocellulose membrane (GE Healthcare, Amersham™ Hybond ECL, Buckinghamshire, UK) and blocked with 5% BSA for 1 hour. The membranes were incubated overnight at 4 °C with the primary antibodies diluted in 1x TBST buffer and washed with TBST for 5 minutes for 3 times. Membranes were then incubated for 1 hour at 4 °C with secondary antibody diluted in 1x TBST followed by 3 times TBST wash for each 5 minutes. Then membranes were developed using Super Signal West Pico chemiluminescent substrate (Thermo, Pierce Biotechnology, Rockford, IL, USA) in Fusion Fx7 chemiluminescence system (PEQLAB, Erlangen, Germany). GAPDH was used as a loading control; proteins were analyzed by use of the Fusion Bio1D software (PEQLAB, Erlangen, Germany).

3.2.4 Histopathology and immunohistochemistry

3.2.4.1 Mice perfusion

Intraperitoneal injection of ketamin and xylazin was done in *Fgfr1^{ind/-}* mice and controls for anesthesia, mice were transcardially perfused with 4% paraformaldehyde at day 18-19 (acute phase) and day 62 (chronic phase) after EAE induction. The spinal cord and brain were removed and embedded in paraffin blocks. Spinal cord and brain tissues were fixed and sections were made with 1 µm in thickness for histopathology and immunohistochemistry.

3.2.4.2 Histology

For histopathology, paraffin sections were evaluated for inflammatory infiltrates (hematoxylin and eosin stain), demyelination (Luxol fast blue/periodic acid-Schiff stain) and axonal density (Bielschowsky staining). Histological evaluation was done with a light microscope (Carl Zeiss, Germany).

3.2.4.3 Hematoxylin and Eosin staining (H & E)

Inflammation in the spinal cord in acute and chronic EAE was analyzed by H & E staining. Briefly, slides were incubated in xylene for deparafination followed by ethanol hydration. Then slides were stained in Hematoxylin for 5 minutes, washed with water and then stained in eosin for 5 minutes. Slides were mounted with mounting medium in glass cover slip after dehydration and xylene rinses. Detailed procedure is presented in schematic diagram (Figure 12).

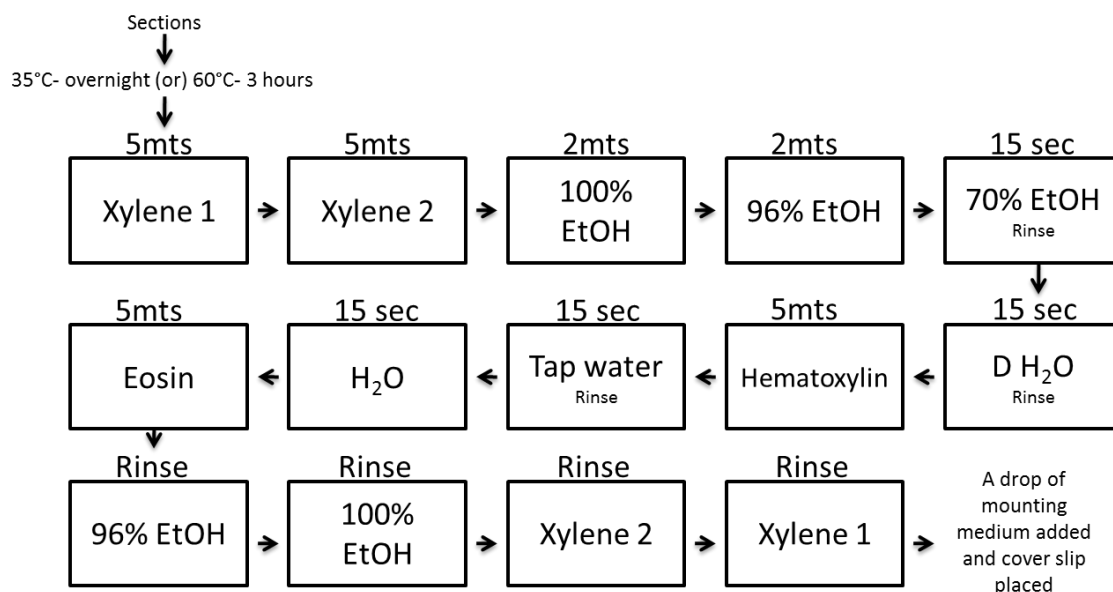


Figure 12 Schematic procedure of H & E staining.

3.2.4.4 Luxol fast blue/periodic acid-schiff stain (LFB / PAS)

Demyelination in acute and chronic EAE spinal cord was analyzed by LFB/PAS staining. Tissue sections were deparafinized with xylene and then hydrated in ethanol followed by overnight incubation in luxol fast blue stain at 56 °C. Slides were mounted with mounting medium in glass cover slip after hydration and xylene rinses. Detailed procedure is presented in schematic diagram (Figure 13). The final % value for demyelination was calculated using equation listed below:

$$\text{Demyelinated area (\%)} = \frac{\text{Demyelinated area in white matter}}{\text{Total white matter area}} \times 100$$

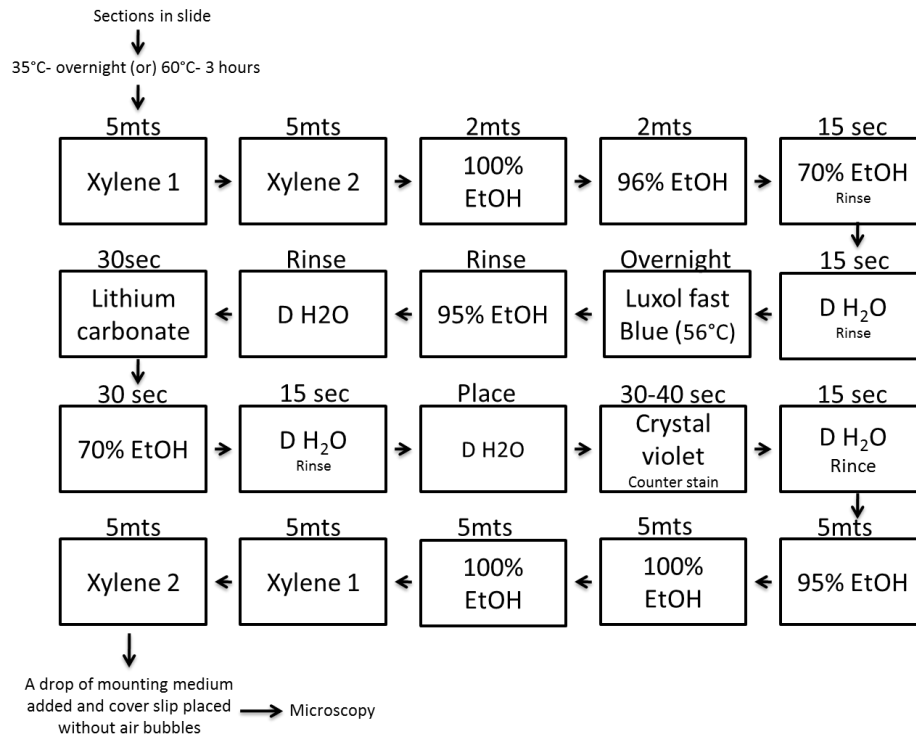


Figure 13 Schematic procedure of Luxol fast blue/PAS staining.

3.2.4.5 Bielschowsky (Silver staining)

Axonal density in acute and chronic EAE spinal cord was analyzed by Bielschowsky-silver staining. Deparaffinized and hydrated sections were incubated with 20% silver nitrate (AgNO_3 , Roth) for 20 minutes in dark and the reaction was stop by water wash. Then the sections were incubated for 2 minutes in 2% Na-Thiosulfate (Sigma Aldrich) followed by water wash. Sections were dehydrated in ethanol and mounted with cover glass.

3.2.4.6 Immunohistochemistry

For immunohistochemistry, sections were deparaffinized in xylene, hydrated, endogenous peroxidase was blocked for 10 minutes with 3% hydrogen peroxide and pretreated with citrate buffer (10 mM, pH 6) over 5 minutes for 3 times. Paraffin sections were incubated with 10% FCS and stained overnight for activated microglia-macrophage (Mac 3, clone M3/84, 1:200, Pharmingen, San Diego, CA, USA), activated B cells (B220, clone RA3-6B2, 1:200, Pharmingen, San Diego, CA, USA), and T cells (CD3, clone CD3-12, 1:150, Serotec, Oxford, UK). Quantitative analysis

of oligodendrocyte populations in the spinal cord and brain cortex region was performed by olig2, nogoA immunostaining (olig 2, 1:300, IBL, Gunma, Japan; nogoA, 1:300, Santa Cruz Biotech, CA, USA). Respective secondary antibodies (Mac 3-goat anti-rat, 1:100, B220-goat anti-rat 1:200, CD3 and olig2, nogoA-goat anti-rabbit-1:250) and avidin-biotin method was used and the signals were detected with DAB. Microscopic images were captured using a Zeiss light microscope (Germany) and analyzed using the Axio vision software.

3.2.5 Cell culture experiments

Oli-Neu (mice oligodendrocyte adherent cell line) was used in this study. Cell line was cultured at 37 °C in 5% CO₂. Oli-neu cell line were maintained in DMEM medium supplemented with B27 supplement (Invitrogen), 0.011% sodium pyruvate, 500 nM Tri-Iodo-L-Thyronine, 520 nM L-Thyroxine. Poly-L-Lysine was coated in 75 cm² culture flask for at least 5 hours or overnight and washed with 1x PBS for 3 times before use. Plates were stored at 4 °C until use. Oli-neu cells were seeded in the Poly-L-Lysine coated flask and above 80% confluent flasks were used for experiments. Cell lines were passaged by 1x PBS wash followed by 1% Trypsin at 37 °C for 1 minute incubation.

3.2.5.1 Fgfr1 inhibition and stimulants in oligodendrocyte cell line

PD166866, a potent Fgfr1 tyrosine kinase inhibitor was used in this study. PD166866 was dissolved in DMSO and above 80% confluent cells were treated with 10 µM concentration of PD166866 for 2-3 hours. Interferon β-1a (IFN β-1a, 400 ng/ml, Rabiff) and Interferon β-1b (IFN β-1b, 500 ng/ml, Betaferon) were used to analyze the impact of both Interferon β-(1a and b) and Fgfr1 ablation in oligodendrocyte and neuronal cell line.

3.2.5.2 Cell proliferation assay

Oli-neu oligodendrocyte cells were seeded in 96 well plates (poly-L-lysine coated) in a final volume of 100 µl/well (1x10⁵ cells/ml), maintained in culture until the cells tightly adhere to the bottom of the plates. Then the old medium was removed and

the cells were incubated for 24 hours with fresh medium containing FGF (20 ng/ml), PD166866 (10 μ M), IFN β -1a (400 ng/ml, Rabiff), IFN β -1b (500 ng/ml, Betaferon), IFN β -1a + PD166866 and IFN β -1b + PD166866. Then 10 μ l of WST-1 reagent (Cell proliferation reagent WST-1, Roche applied science, Indianapolis, IN) was added in each well and the assay was carried out as mentioned in the instructions provided by the manufacturer. Plates were shaken thoroughly for 1 minute on a shaker and incubated for 4 hours at standard cell culture conditions. The colour developed from the soluble formazan dye cleaved from the tetrazolium salt WST-1 was measured at an absorbance of 420-480 nm in an ELISA reader. 100 μ l of assay medium was taken as blank control for measuring the background absorbance. All experiments were carried out in triplicates. To calculate proliferation, mean absorbance was calculated and background absorbance (medium alone) subtracted from each value. The percentage of specific proliferation was quantified using the following calculation:

$$\% \text{ Proliferation} = (\text{experimental release} / \text{spontaneous release}) \times 100.$$

3.2.5.3 Cell cytotoxicity assay

Possible cytotoxicity effects of Fgfr1, IFN β -1a and IFN β -1b in oli-neu cells were measured using LDH cytotoxicity assay according to the manufacturer's instructions (Roche applied science, Indianapolis, IN). Cells were seeded in optically clear flat-bottomed 96 well plates in the concentration of 1×10^5 cells/ml. 100 μ l of this suspension is filled in the 96 well plates. Then, old medium was discarded and 200 μ l medium containing FGF, PD166866, IFN β -1a, IFN β -1b was added and incubated for another 24 hours at standard cell culture conditions. Assay medium was used as background control, 100 μ l cell suspensions and 100 μ l assay medium as low control. To determine the maximum amount of LDH enzyme activity, 2% Triton-X 100 was used as high control. After 24 hours, the plate was centrifuged at 250 g for 10 minutes. From this, 100 μ l supernatant was transferred into new 96-well plates and 100 μ l assay reagent was added and incubated for 30 minutes at room temperature in dark. The amount of color produced due to the release of LDH enzyme was read in 490 nm in an ELISA reader. All the assays were carried out in triplicates, average absorbance values of the triplicates were calculated and background control subtracted. Cytotoxicity (%) was calculated as follows: $\% \text{ Cytotoxicity} = [(\text{Experimental value} - \text{low control value}) / (\text{High control value} - \text{low control value})] \times 100$

3.2.5.4 Protein extraction

Oli-neu cells were grown in Poly-L-Lysine coated 75 cm² culture flask above 80% confluence. Culture medium was removed from the cells then fresh medium was added with respective treatments (10 μ M PD166866) for 2-3 hours. Cells were stimulated with 25 ng/ml basic FGF, IFN β -1a and or IFN β -1b with or without Fgfr1 inhibition (10 μ M PD166866) for 5 minutes. Then medium was removed from the culture medium and washed with cold 1x PBS followed by trypsination. Cells were scraped from the flask and centrifuged for 3500 rpm, 15 minutes at 4 °C. Supernatant was discarded and cell pellet were lysed with lysis buffer and incubated in ice for 30 minutes. Then the cell lysate was centrifuged at 14000 rpm in 4 °C for 30 minutes, supernatant were collected and stored at -20 °C until analysis.

3.2.5.5 Protein quantification and western blot

Protein quantification (BSA protein assay), SDS-PAGE and western blot procedure were followed as described in sections 3.2.3.1 and 3.2.3.2.

3.2.6 Statistics

All analyses were performed blinded to the genotype. All mice and samples were included into the analysis. Statistical analysis for differences between the genotypes in the clinical course and histological data was performed using the Mann-Whitney U test. T-test was used to analyze reverse transcription-PCR and protein data. Unpaired t-tests were used for other experiments. Statistical significance was set at $P \leq 0.05$. Statistical analysis was performed using GraphPad Prism version 4.00 for Windows (GraphPad Software, San Diego, California, USA) and Systat 12 software (Systat, San Jose, CA, USA). Graphs were prepared using the Sigmaplot 10 software (Systat, San Jose, CA, USA) and GraphPad Prism version 4.00 for Windows (GraphPad Software, San Diego, California, USA). Values are expressed as mean \pm standard error of mean. P values of * $P < 0.05$, ** $P < 0.005$, *** $P < 0.001$ were considered as significant.

4 RESULTS

4.1 Oligodendrocyte specific Fgfr1 knock down study

4.1.1 Conditional deletion of oligodendrocyte specific Fgfr1 in C57BL/6J mice: genotype and phenotype confirmation

Complete deletion of Fgfr1 is lethal in embryonic day 6-10. Fgfr1 conditional knockout is the appropriate method to study the role of Fgfr1 in specific cell type or in tissue. Tamoxifen inducible Cre mediated deletion of Fgfr1 in oligodendrocyte under PLP promoter achieved in *B6.Cg-Tg(Plp1-cre/ER^T)3Pop Fgfr1^{tm5.1Sor}* mice line. Mice with floxed Fgfr1 was mated with transgenic mice expressing Cre recombinase under the control of PLP promoter which is specific to oligodendrocytes. This PLP promoter allows excision of floxed alleles (Fgfr1) in oligodendrocyte lineage cells in CNS. Genotype was confirmed with primers for PLP Cre and Fgfr1 loxP (Figure 14). There were no effect on mortality, body weight, and specific phenotype changes were observed in Fgfr1 conditional knockout mice.

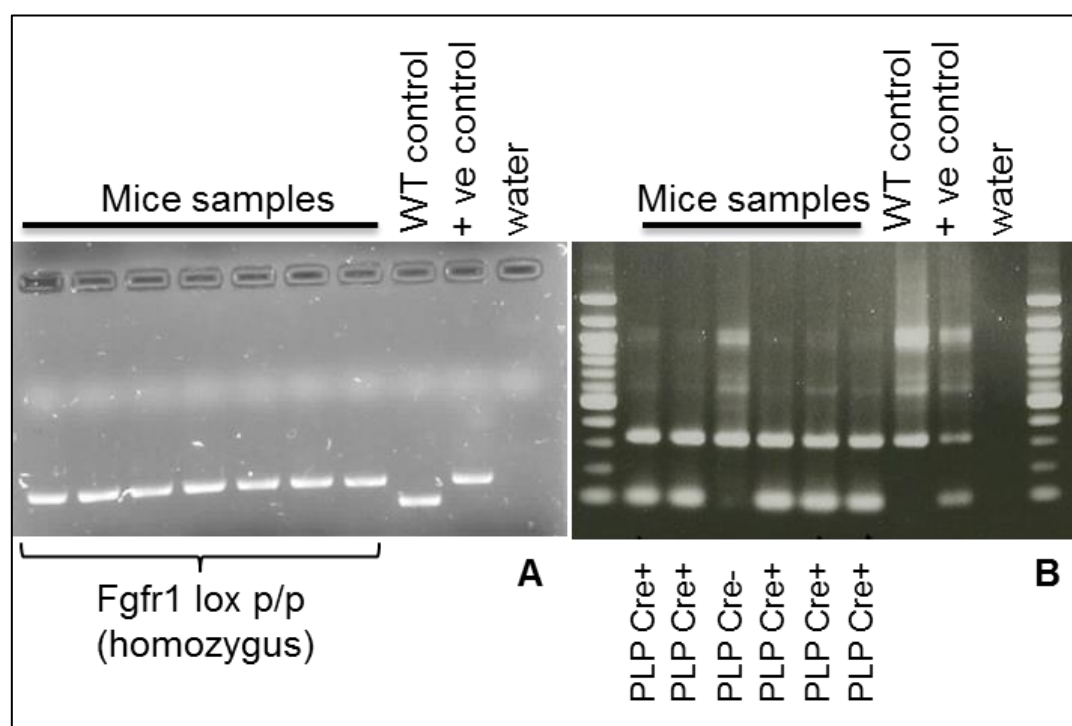


Figure 14 Genotype confirmation of Fgfr1 lox and PLP Cre locus from mice tail complete DNA by PCR. Mice tails were lyzed with direct tail lysis buffer and genotype was carried with Fgfr1 lox (A) and PLP Cre locus (B). PCR amplified products were confirmed with agarose gel electrophoresis. Representative agarose gel images were shown. WT: wild type C57Bl/6J control, +ve: positive control.

4.1.2 Characterization of oligodendrocyte specific Fgfr1 signalling in C57Bl/6J mice

To characterize the role of oligodendrocyte specific Fgfr1, Tamoxifen inducible Cre mediated deletion of Fgfr1 was achieved in 4 weeks old female mice (*B6.Cg-Tg(Plp1-cre/ER^T)3Pop Fgfr1^{tm5.1Sor}: Fgfr1^{lox+ve} and Cre^{+ve} mice*). Four weeks old *B6.Cg-Tg(Plp1-cre/ER^T)3Pop Fgfr1^{tm5.1Sor}* mice were injected with Tamoxifen for 5 consecutive days (referred as Fgfr1^{ind/-}). 15 days later Tamoxifen injection, spinal cord and CNS tissues were removed and analyzed by western blot. Whole lysate of cortex and spinal cord from control and Fgfr1^{ind/-} mice shows the same level of Fgfr1 (cortex $P = 0.8845$, spinal cord $P = 0.2711$) and Fgfr2 (cortex $P = 0.1417$, spinal cord $P = 0.3052$) expression (Figure 15 A and B). Three bands of different splice variant have been observed for Fgfr2 in cortex and spinal cord (Figure 15 A and B). There was no compensatory up-regulation of Fgfr2 expression detected in Fgfr1^{ind/-} mice spinal cord by western blot analysis.

4.1.3 Effect of Fgfr1 ablation in oligodendrocytes on Fgfr1 signal cascade

Fgfr1 signal cascade mainly involved in ERK and AKT pathways which enhance the proliferation and survival respectively. To analyze the effect of oligodendrocyte specific Fgfr1 ablation in the Fgfr1 signalling pathways, whole lysates of cortex and spinal cord were analyzed from control and Fgfr1^{ind/-} mice. There were increased expression of ERK and AKT phosphorylation was seen in cortex (pERK: $P = 0.6563$, pAKT: $P = 0.259$) but not significant (Figure 16 A) and spinal cord (pERK: $P = 0.029$, pAKT: $P = 0.045$) of Fgfr1^{ind/-} mice compared to control mice (Figure 16 B).

4.1.4 Effect of Fgfr1 ablation in oligodendrocytes on TrkB expression

To analyze the influence of oligodendrocyte specific Fgfr1 on TrkB expression, whole protein lysates of cortex, spinal cord, cerebellum and brainstem from control and Fgfr1^{ind/-} mice were analyzed by western blot. Increased expression of TrkB was observed in cortex ($P \leq 0.05$) and spinal cord ($P = 0.073$) of Fgfr1^{ind/-} mice (Figure 17 A and B). There was no regulation in TrkB expression in Fgfr1^{ind/-} mice cerebellum ($P = 0.31$), whereas down regulation of TrkB expression was seen in Fgfr1^{ind/-} brainstem ($P \leq 0.0001$).

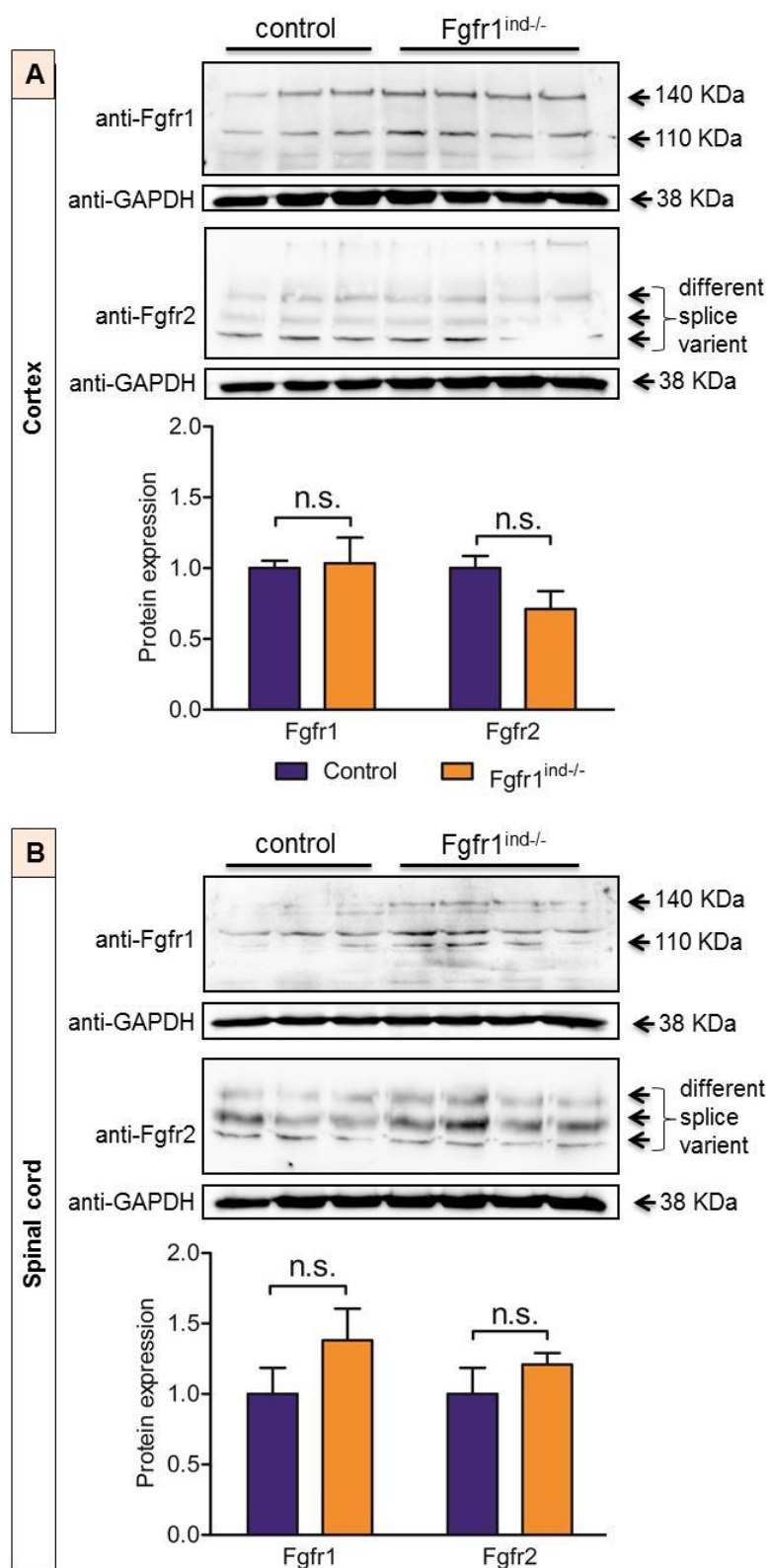


Figure 15 Fgfr's expression in Fgfr1^{ind/-} mice CNS. Whole protein lysate of cortex and spinal cord were checked in western blot for Fgfr1 and Fgfr2 expression. There is no difference in the expression of Fgfr1 and Fgfr2 in Fgfr1^{ind/-} cortex (A) and spinal cord (B) whole lysate. Fgfr1 with 110 and 140 kDa, and Fgfr2 show 3 bands of different splice variants (120 and nearby). Representative blot and quantification were shown. n.s. = not significant. Values are expressed as mean \pm standard error of mean.

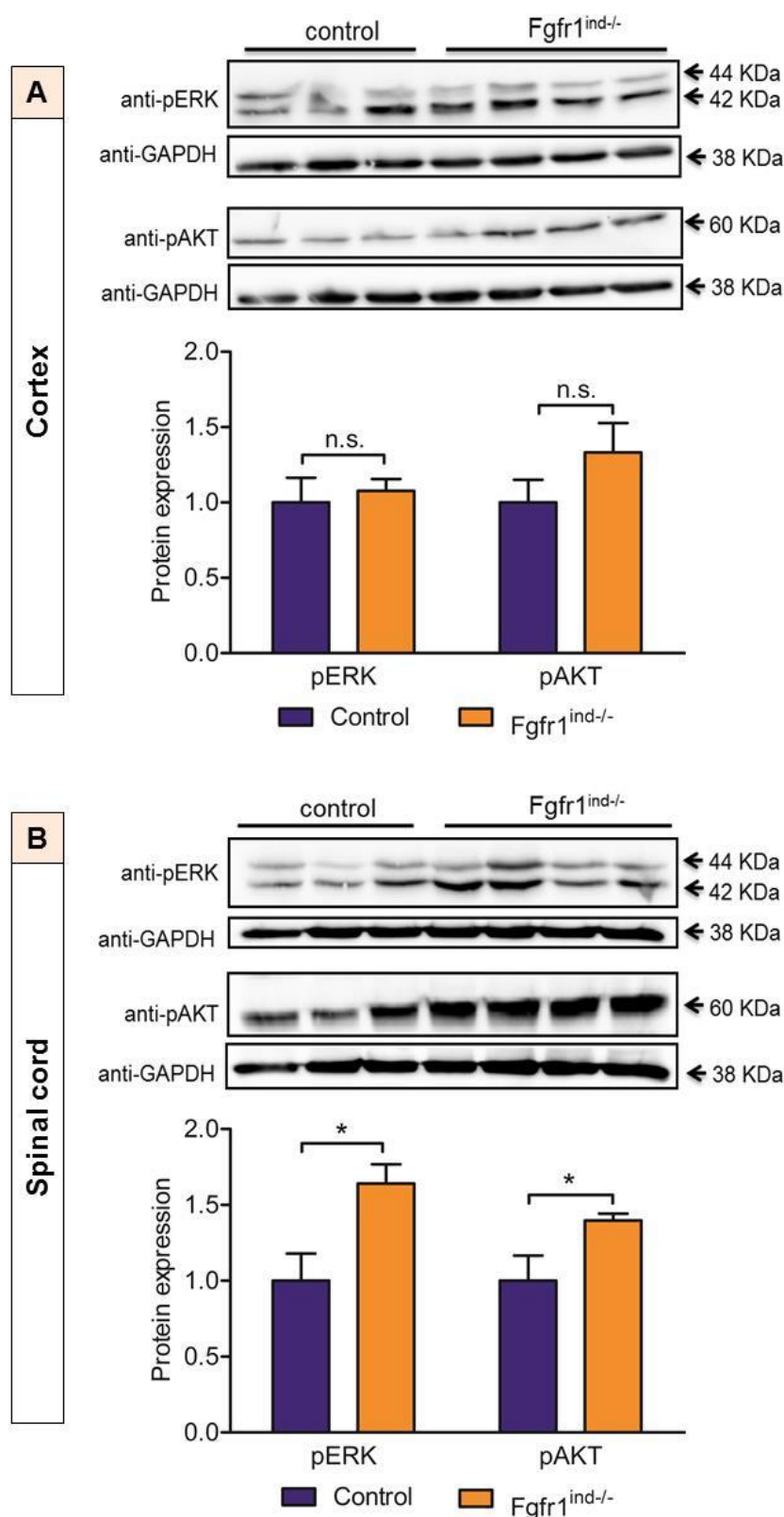


Figure 16 Expression pattern of ERK and AKT phosphorylation in control and Fgfr1^{ind/-} mice cortex and spinal cord. Representative blot and quantification were shown. Phosphorylation of ERK and AKT in cortex showed no regulation (A). Increased expression of ERK and AKT phosphorylation were seen in spinal cord of Fgfr1^{ind/-} mice (B). P values of * $P < 0.05$, ** $P < 0.005$, *** $P < 0.001$ were considered as significant. Values are expressed as mean \pm standard error of mean.

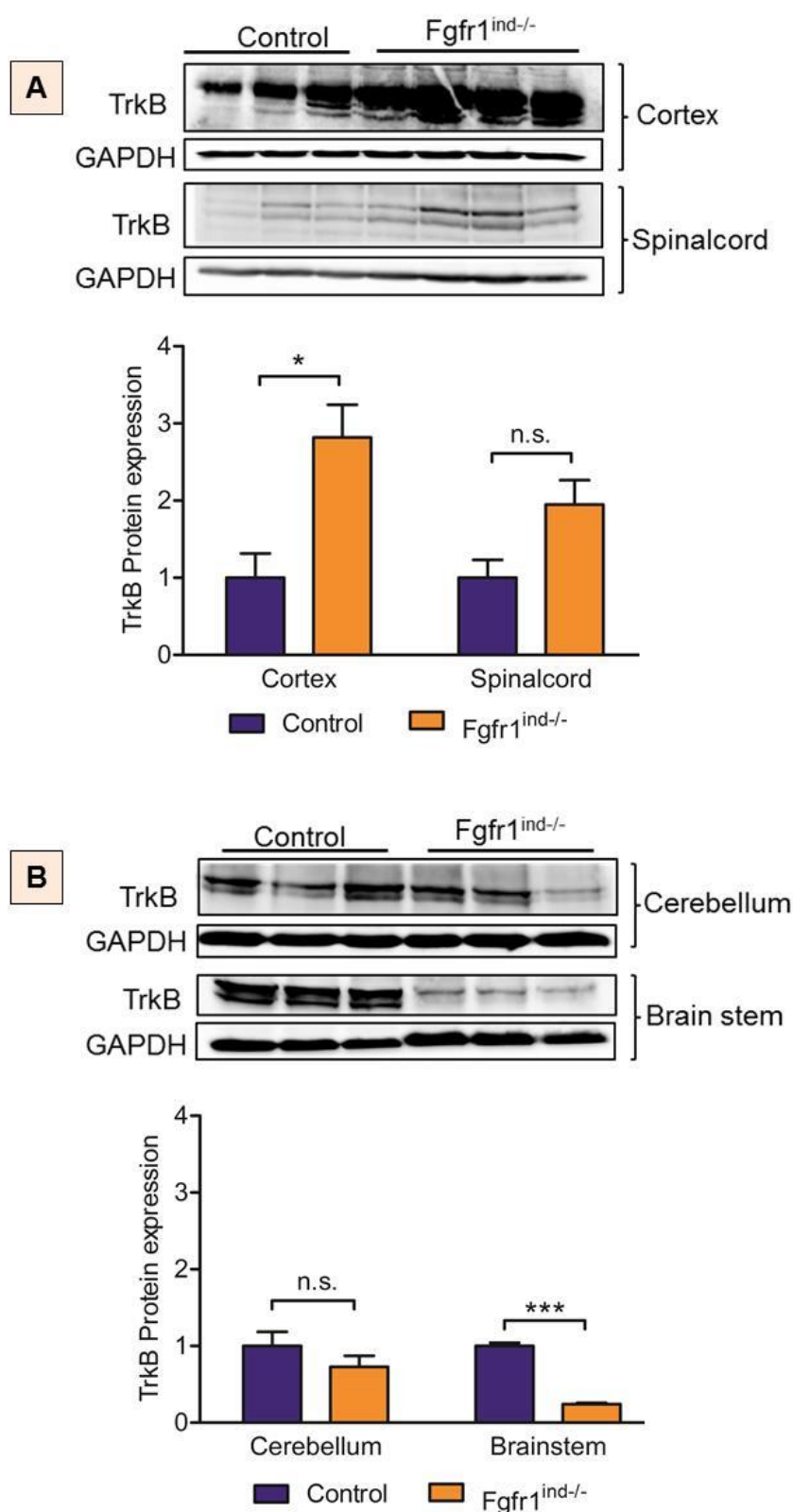


Figure 17 TrkB protein expression in different CNS region of control and Fgfr1^{ind/-}. Proteins were isolated from CNS region (cortex, spinal cord, cerebellum and brainstem) and analyzed for TrkB protein expression by western blot. Representative blots and respective quantification were shown (A: cortex and spinal cord, B: cerebellum and brain stem). *P* values of * *P* < 0.05, ** *P* < 0.005, *** *P* < 0.001 were considered as significant. Values are expressed as mean ± standard error of mean.

4.1.5 Effect of Fgfr1 ablation in MBP expression in Fgfr1^{ind/-}

To analyze the effect of oligodendrocyte specific Fgfr1 ablation in MBP expression in tissue level, spinal cord from control and Fgfr1^{ind/-} mice was perfused and immunostained with MBP antibody and analyzed semi quantitatively. There were no differences in the expression of MBP in tissue level was seen in spinal cord of Fgfr1^{ind/-} mice compared to control mice (Figure 18).

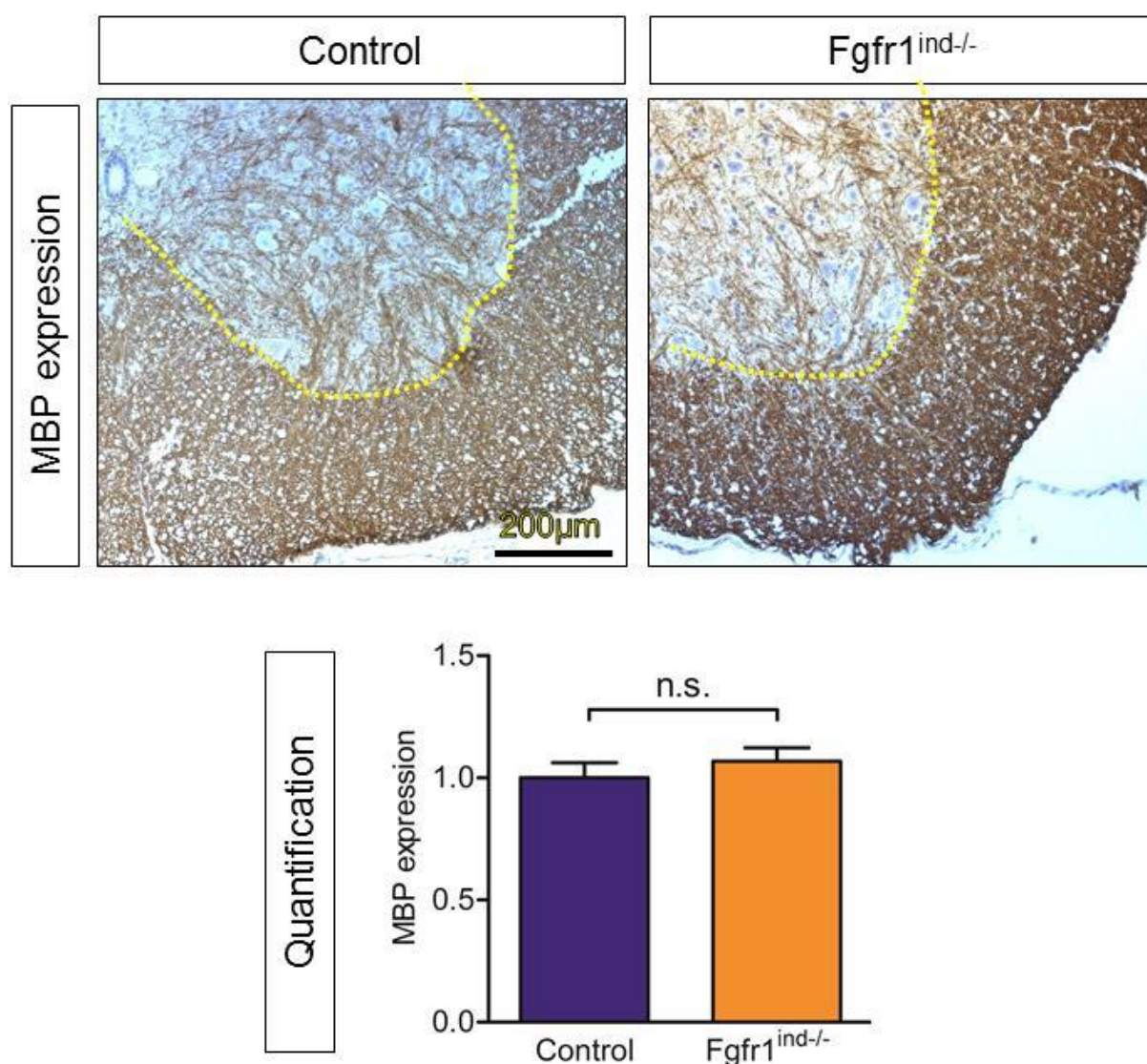


Figure 18 Myelin basic protein expressions in control and Fgfr1^{ind/-} mice. Immunohistochemistry analysis shows there were no differences in the expression of MBP in control and Fgfr1^{ind/-} mice spinal cord. n.s. = not significant. Values are expressed as mean ± standard error of mean.

4.1.6 Effect of Fgfr1 ablation in oligodendrocytes on cell population

To analyze the effect of oligodendrocyte specific Fgfr1 ablation on oligodendrocyte cell population, olig2 and nogo A positive oligodendrocyte lineage cells were counted from control and Fgfr1^{ind/-} mice spinal cord by immunohistochemistry. There were no differences in the olig 2 and nogo A positive oligodendrocyte lineage cell population in Fgfr1^{ind/-} mice spinal cord compared to control mice (Figure 19).

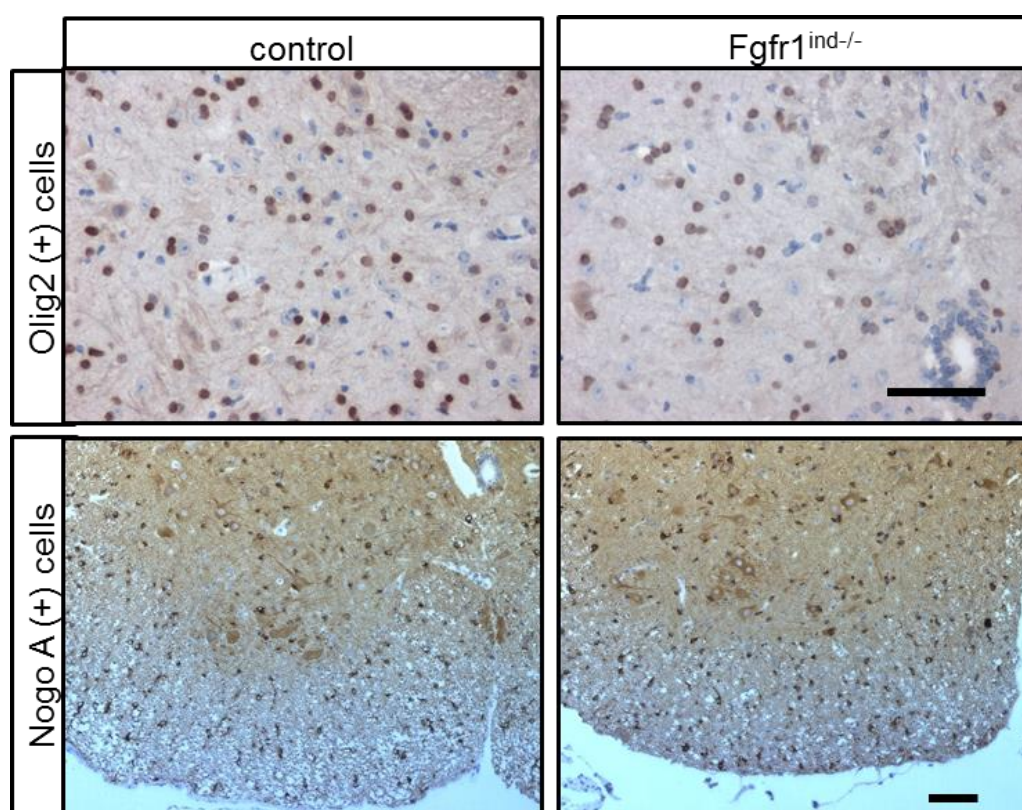


Figure 19 Olig 2 and nogoA positive oligodendrocyte lineage cells in control and Fgfr1^{ind/-} mice spinal cord. There are no differences in the number of olig2 and nogoA positive oligodendrocyte cell population in spinal cord of Fgfr1^{ind/-} mice.

4.2 EAE in Fgfr1^{ind/-} and control mice

4.2.1 EAE scoring

EAE was induced in control and Fgfr1^{ind/-} mice with MOG₃₅₋₅₅ peptide. All mice were monitored and scored EAE clinical symptoms. Both mice groups show distinct clinical symptom and EAE score were evaluated as described in method section 3.2.1.7. Figure 20 shows the clinical symptoms of EAE mice.

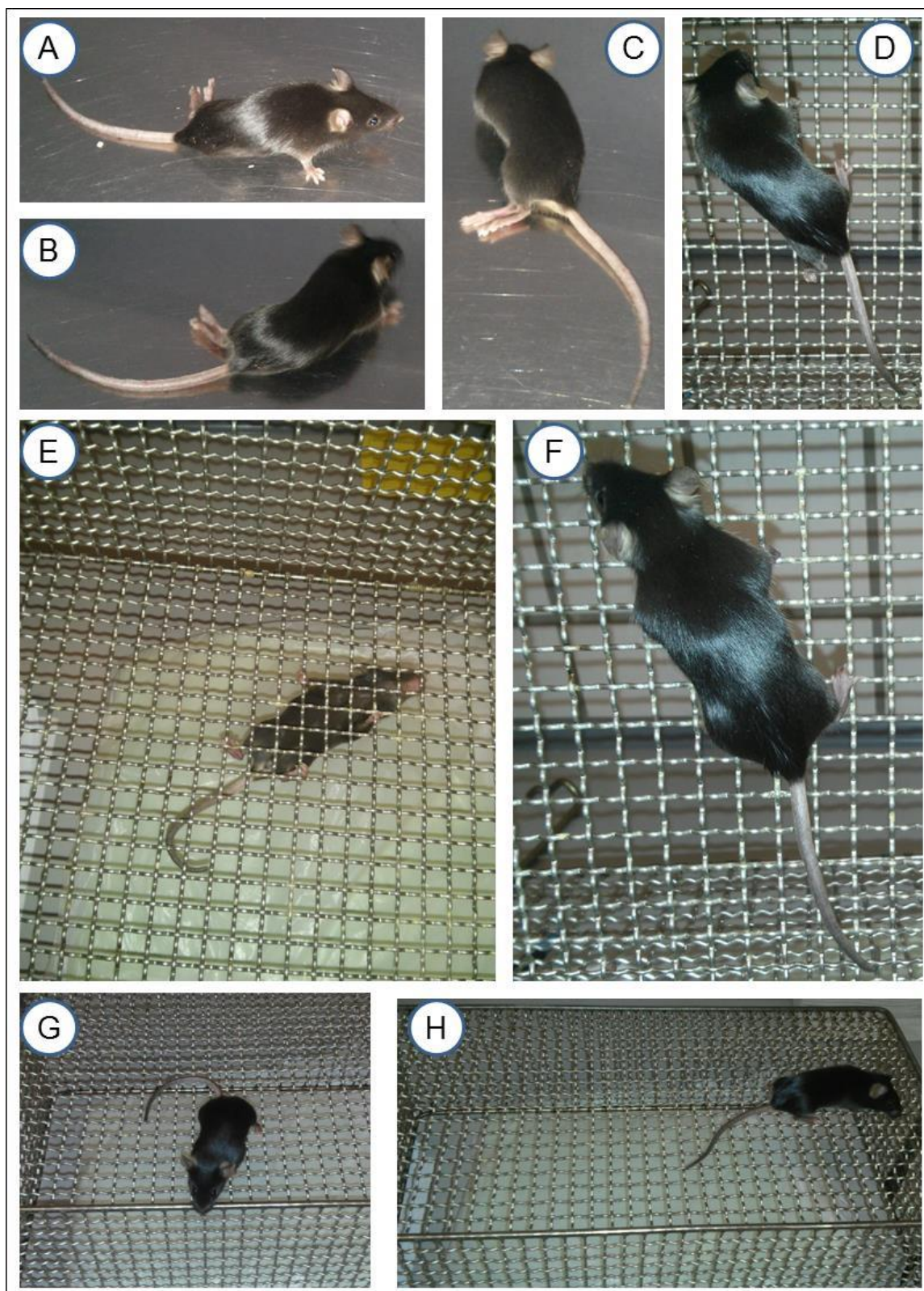


Figure 20 Clinical symptoms of MOG₃₅₋₅₅ peptide induced EAE in control mice. Tail and hind limb paralysis and mild fore limb weakness of EAE mice shown in plain (A-C) and net surface (D-H).

4.2.2 Fgfr1^{ind/-} mice show a milder EAE disease course

Mice with oligodendroglial Fgfr1 deletion (Fgfr1^{ind/-}) were analyzed for their susceptibility to MOG₃₅₋₅₅ peptide EAE induction. EAE was induced in 13 eight to twelve-week-old female Fgfr1^{ind/-} mice and compared with 13 age- and sex-matched controls. There were no differences in body weight between Fgfr1^{ind/-} and control mice (Figure 21). Figure 22 and table 4 shows the summary of the EAE score in control and Fgfr1^{ind/-} mice. The onset of clinical symptoms was on day 10.0 ± 0.24 in controls and on day 11.5 ± 0.21 in Fgfr1^{ind/-} mice ($P < 0.001$). The mean maximum disease score was less in Fgfr1^{ind/-} mice ($P \leq 0.05$). From day 33 p.i. (with exception of days 47 and 48) Fgfr1^{ind/-} mice showed a milder disease course than controls ($P \leq 0.05$). In this disease phase, Fgfr1^{ind/-} mice presented with a mild paraparesis whereas controls still suffered from a severe paraparesis. Also, the cumulative EAE score was higher in controls ($P \leq 0.05$; Figure 22 B). Disease incidence was 100%. No effect of gene deletion on mortality was observed.

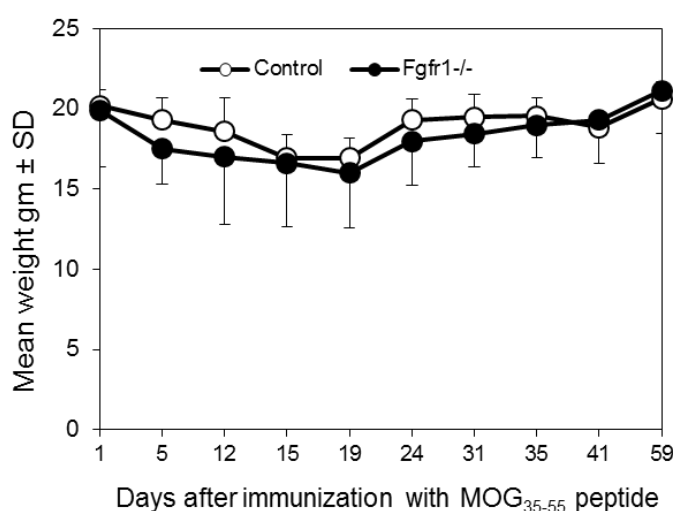


Figure 21 Mean weights of control and Fgfr1^{ind/-} mice after MOG₃₅₋₅₅ EAE induction. Both mice group showed weight loss in acute phase of the EAE disease and later in chronic phase, both mice group gained weight.

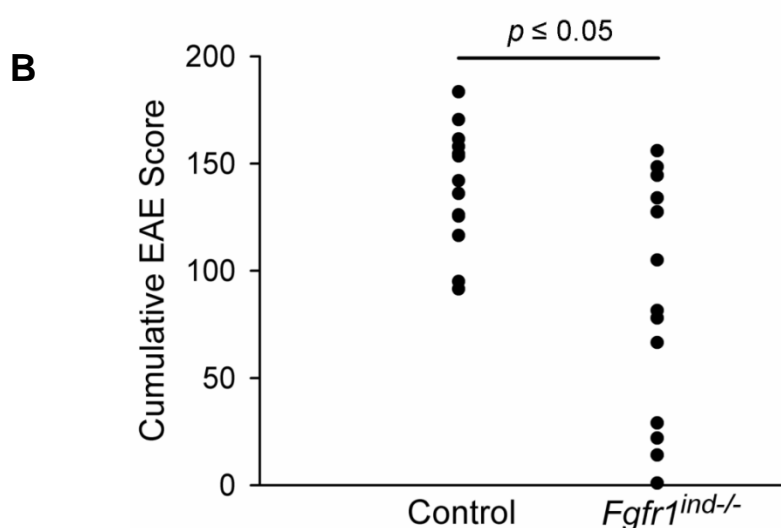
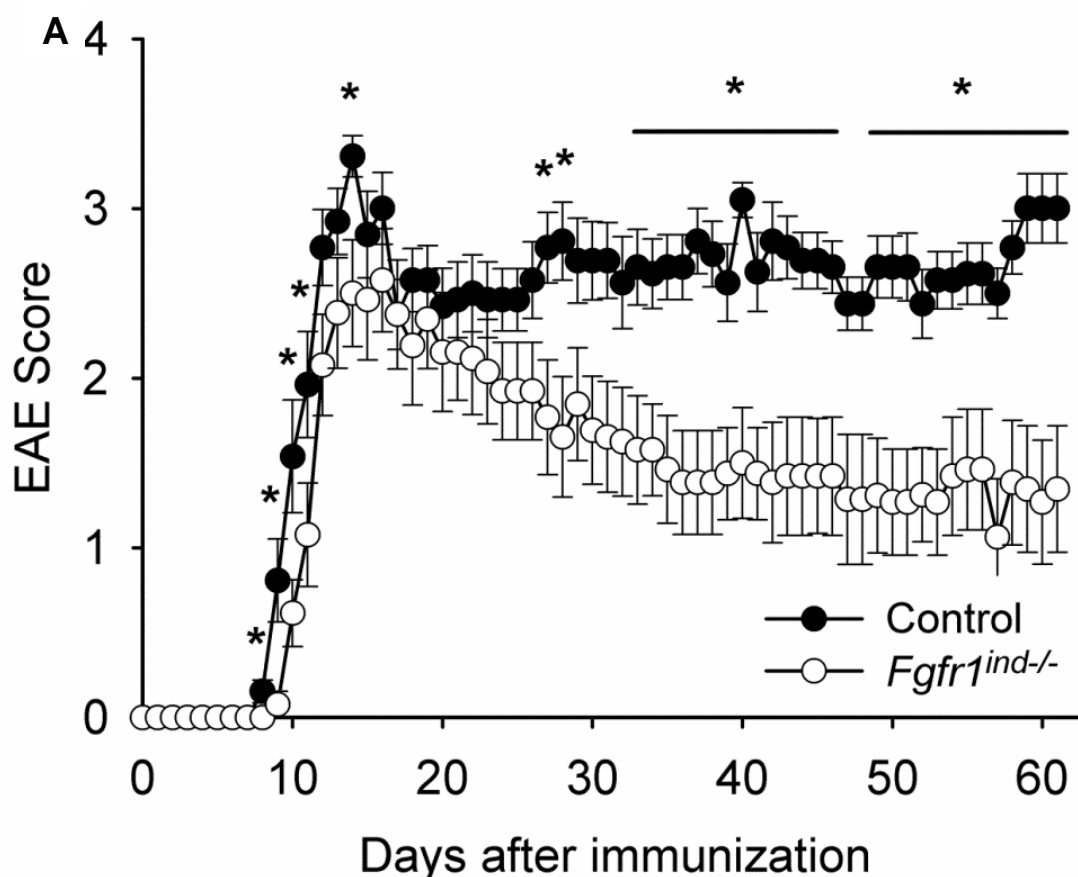


Figure 22 Conditional deletion of *Fgfr1* in oligodendrocyte suppresses the MOG₃₅₋₅₅ induced EAE. A) *Fgfr1*^{ind-/-} mice showed a delayed onset of disease ($P < 0.001$). Milder disease course was found in *Fgfr1* conditional knockout mice, until day 27 p.i. Whereas from day 28 onwards, conditional *Fgfr1*^{ind-/-} mice showed significant milder disease course ($P < 0.001$) till the end of chronic phase. B) Cumulative score of chronic EAE till day 62 p.i. was less in *Fgfr1*^{ind-/-} mice ($P < 0.001$). $n = 13$, data are presented as mean \pm SEM.

Table 4 Clinical characteristics of MOG₃₅₋₅₅-induced EAE in Fgfr1^{ind/-} mice

Mice	Number	Incidence	EAE clinical score				Mortality
			Disease onset (day)	Maximum score	Day 19	Day 62	
control	13	100%	9.9 ± 0.2	4.5	3.0 ± 0.2	3.0 ± 0.2	Nil
Fgfr1 ^{ind/-}	13	100%	11.4 ± 0.2	4.0	2.5 ± 0.3	1.3 ± 0.3	Nil

Conditional deletion of Fgfr1 in oligodendrocyte lineage showed late onset of EAE clinical sign. Whereas from day 19 p.i. Fgfr1^{ind/-} mice showed milder disease course till end of the experiment.

4.2.3 Reduced demyelination and increased axonal density in Fgfr1^{ind/-} mice

The differences in the clinical course were most evident for the chronic phase of EAE (Figure 22, Table 4 and 5). As the next step, Fgfr1^{ind/-} mice were assessed for their susceptibility to demyelination and axonal density in spinal cord white matter. Demyelination was evaluated by Luxol fast blue staining and axonal density by Bielschowsky staining. In the acute phase no difference in demyelination was observed between Fgfr1^{ind/-} mice and controls (Figure 24 A, B and C). At this time point, axonal density was higher in Fgfr1^{ind/-} mice than in controls ($P \leq 0.05$) (Figure 25 A, B and C). In the chronic phase Fgfr1^{ind/-} mice showed less demyelination ($P \leq 0.05$; Figure 24 D, E and F) and a higher axonal density ($P \leq 0.05$; Figure 25 D, E and F).

Table 5 Histopathological analysis of spinal cord from EAE mice.

Pathology	Day 19		P-value	Day 62		P-value
	control	Fgfr1 ^{ind/-}		control	Fgfr1 ^{ind/-}	
Inflammatory index	1.83 ± 0.8	0.97 ± 0.4	$P = 0.4147$	2.4 ± 0.4	1.01 ± 0.4	$P = 0.0163$
Demyelination (%)	5.76 ± 1.4	7.02 ± 3.1	$P = 0.7353$	29.7 ± 10.6	5.6 ± 9.8	$P = 0.0453$
Axonal density (%)	44.93 ± 3.2	73.07 ± 2.1	$P = 0.002$	23.8 ± 11.8	63.7 ± 17.2	$P = 0.030$

Blinded quantification of inflammation (H & E), demyelination by LFB/PAS and axonal density (silver staining) in spinal cord of controls and Fgfr1^{ind/-} mice in EAE. Data are presented as mean ± SEM.

4.2.4 Inflammation in $Fgfr1^{ind/-}$ mice is characterized by reduced numbers of lymphocytes and macrophages/microglia

To study the underlying cellular mechanisms that drive demyelination and axonal damage, the degree of inflammation was analyzed in spinal cord white matter lesions on H&E stained sections of $Fgfr1^{ind/-}$ mice and littermate controls. In the acute phase the inflammatory index was not different between $Fgfr1^{ind/-}$ mice and controls (Figure 23 A, B and C), whereas in the chronic phase the inflammatory index was reduced in $Fgfr1^{ind/-}$ mice ($P \leq 0.05$; Figure 23 D, E and F). With regard to cellular infiltration the number of CD3 (+) T cells was not affected by $Fgfr1$ deletion in the acute phase of EAE (Figure 26 A, B and C). However, the number of B220 (+) B cells ($P \leq 0.05$; Figure 27 A, B and C) and Mac3 (+) cells ($P \leq 0.05$; Figure 28 A, B and C) was reduced in $Fgfr1^{ind/-}$ mice compared to controls. In the chronic phase a reduction of CD3 (+) T cells ($P \leq 0.05$; Figure 26 D, E and F), B220 (+) B cells ($P \leq 0.05$; Figure 27 D, E and F) and Mac3 (+) cells ($P \leq 0.05$; Figure 28 D, E and F) was observed compared with controls. Table 6 shows the summary of immune cell infiltration in acute and chronic EAE spinal cord.

Table 6 Immune cell infiltrations in spinal cord of EAE mice.

Disease pathology	Acute EAE			Chronic EAE		
	control	$Fgfr1^{ind/-}$	P -value	control	$Fgfr1^{ind/-}$	P -value
CD3 (+) T cells	624 \pm 200	284 \pm 80	$P = 0.19$	160 \pm 43	27 \pm 9	$P \leq 0.05$
B220 (+) B cells	625 \pm 128	164 \pm 56	$P \leq 0.05$	273 \pm 51	48 \pm 16	$P \leq 0.05$
Mac3 (+) Macrophages	2455 \pm 306	1080 \pm 68	$P \leq 0.05$	1650 \pm 465	243 \pm 47	$P \leq 0.05$

Blinded quantification of immune cell infiltration of T cells, B cells and macrophages in spinal cord of controls and $Fgfr1^{ind/-}$ mice in acute and chronic EAE. Data are presented as mean \pm SEM.

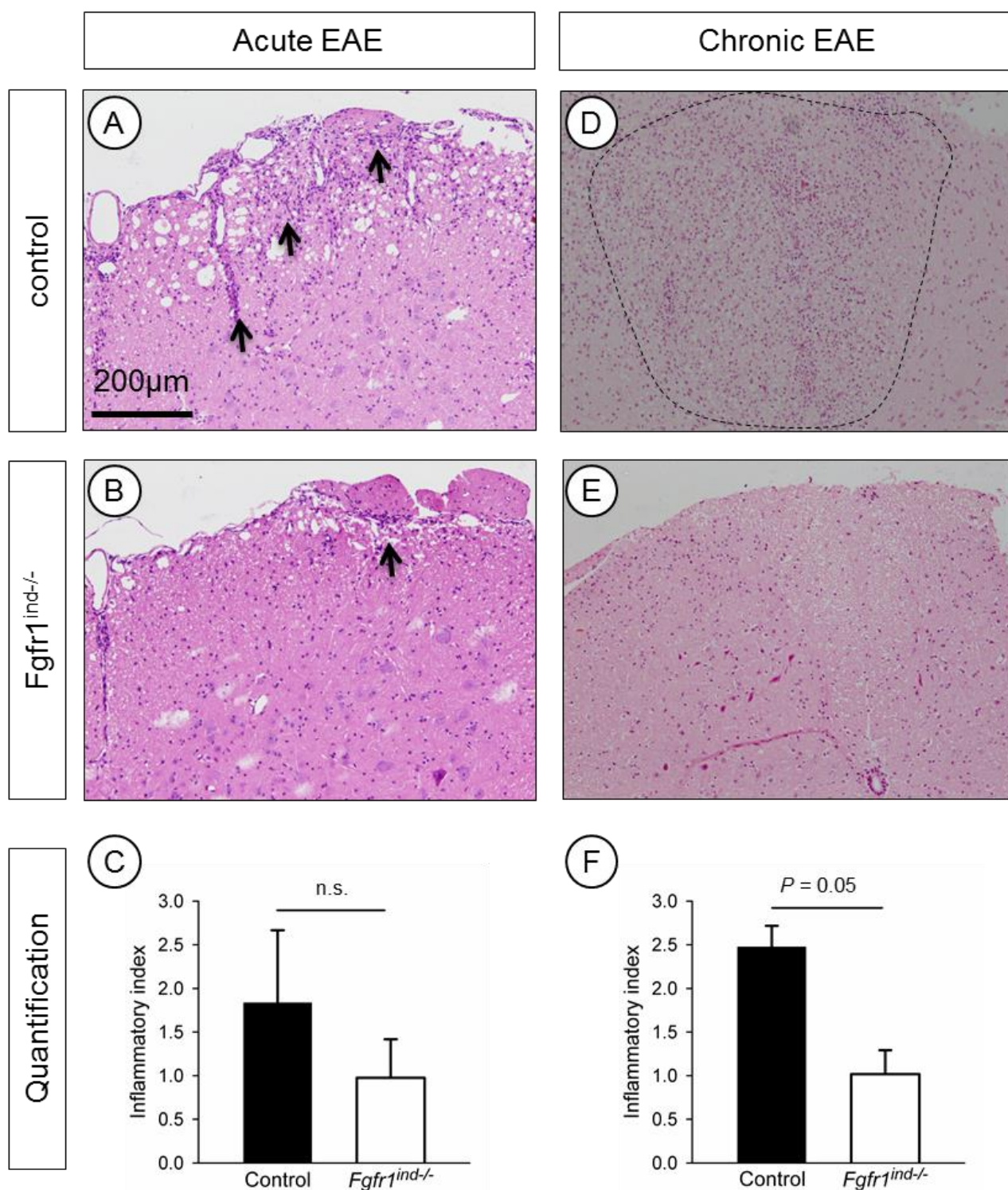


Figure 23 Histopathological analysis of acute and chronic EAE (H and E). Inflammatory index in the spinal cord sections of acute (A, B and C) and chronic (D, E and F) EAE in controls (A, D) and $Fgfr1^{ind/-}$ mice (B, E). Representative images of spinal cord sections are shown. The inflammatory index (C and F) was less in $Fgfr1^{ind/-}$ mice compared to control. Bar: 200 μ m. n = 3, data are presented as mean \pm SEM.

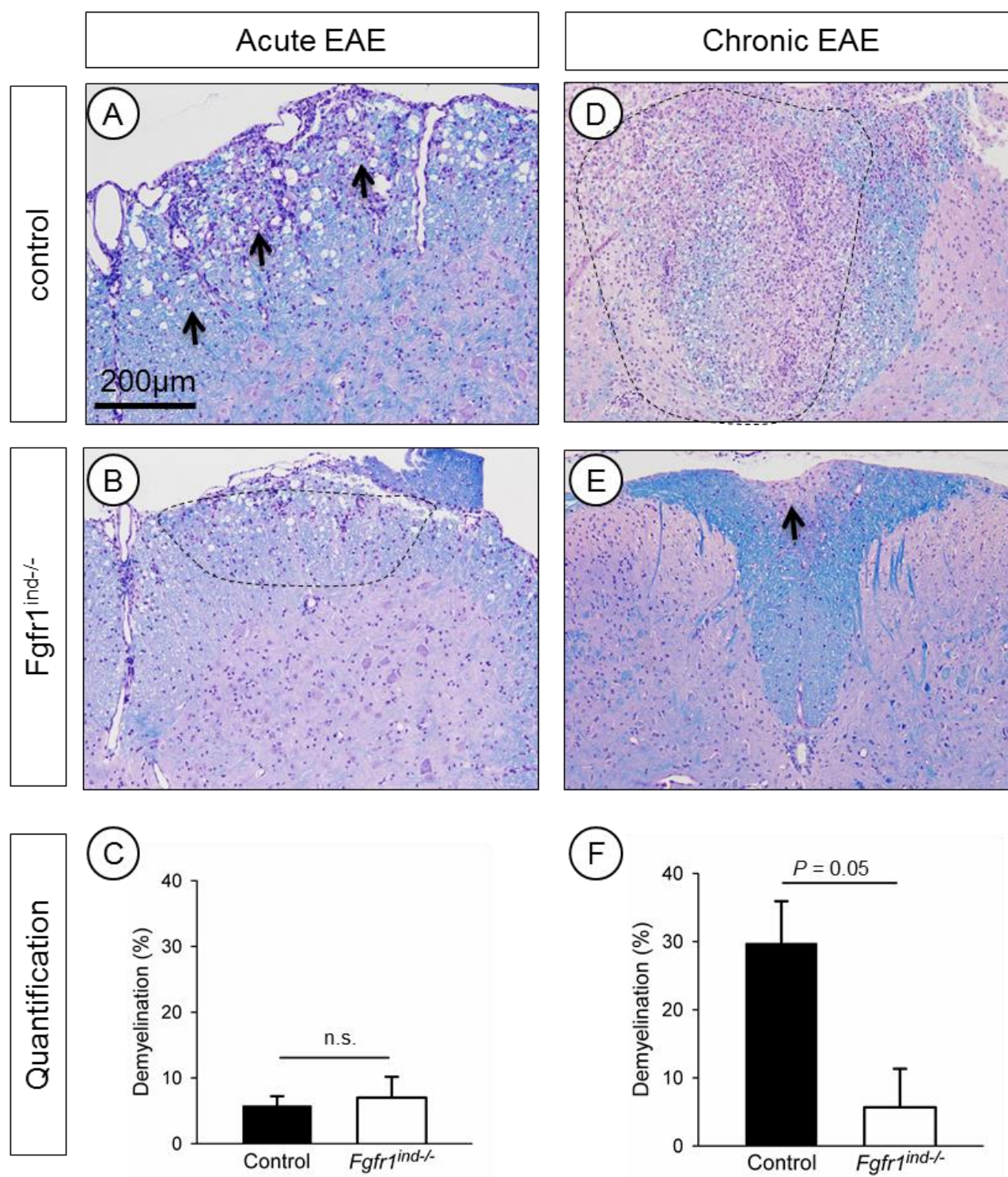


Figure 24 Histopathological analysis of acute and chronic EAE (LFB/PAS). Demyelination in the spinal cord sections of acute (A, B and C) and chronic (D, E and F) EAE in controls (A, D) and *Fgfr1*^{ind/-} mice (B, E). Representative images of spinal cord sections are shown. The percentage of demyelination (F) was less in *Fgfr1*^{ind/-} mice compared to control in chronic EAE. Bar: 200 μ m. n = 3, data are presented as mean \pm SEM.

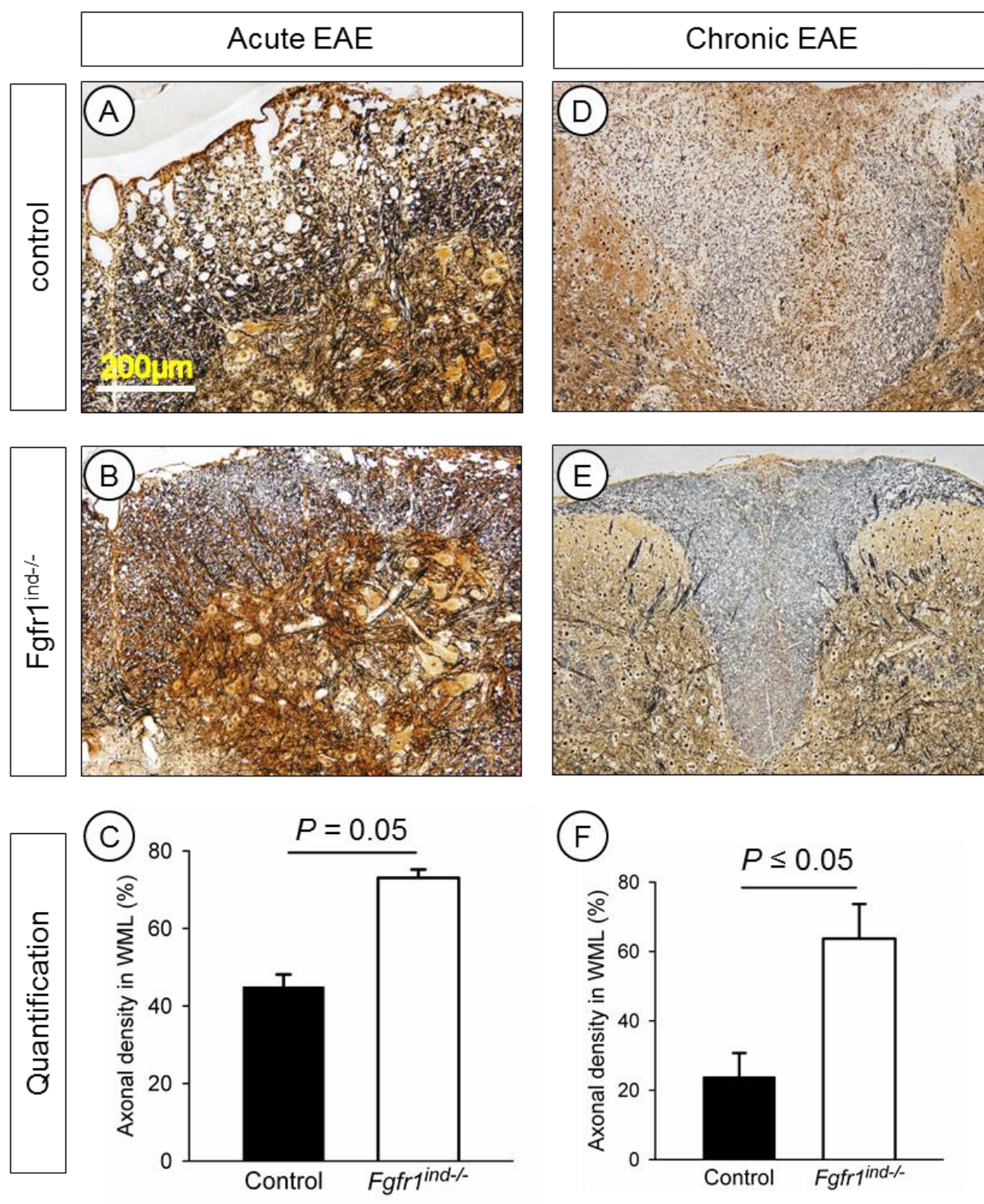


Figure 25 Histopathological analysis of acute and chronic EAE (Silver staining).

Axonal density in the spinal cord sections of acute (A, B and C) and chronic (D, E and F) EAE in controls (A, D) and *Fgfr1*^{ind/-} mice (B, E). Representative images of spinal cord sections are shown. Percentage of axonal density (C and F) was higher in *Fgfr1*^{ind/-} mice compared to control. Bar: 200 µm. n = 3, data are presented as mean ± SEM.

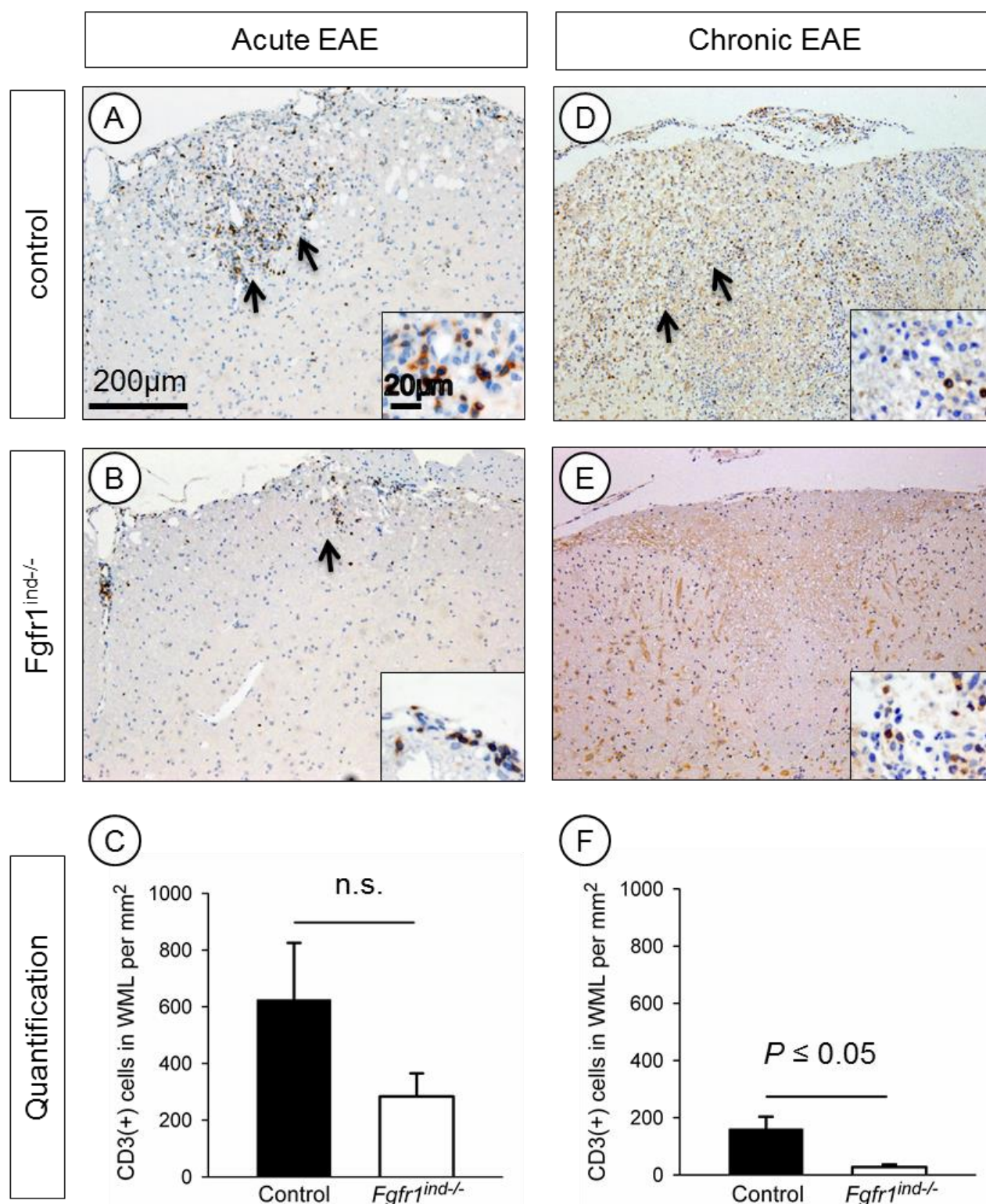


Figure 26 Immune cell infiltration in acute and chronic EAE spinal cord (T cells). CD3 (+) T cells in white matter lesions of spinal cord sections in acute (A, B and C) and chronic (D, E and F) EAE in controls (A, D) and *Fgfr1^{ind/-}* mice (B, E). Representative images of spinal cord sections are presented. The number of CD3 (+) T cells per mm² was less in *Fgfr1^{ind/-}* mice compared with controls in chronic EAE (F). Bar: 200 μ m, 20 μ m (insert). n = 3, data are presented as mean \pm SEM.

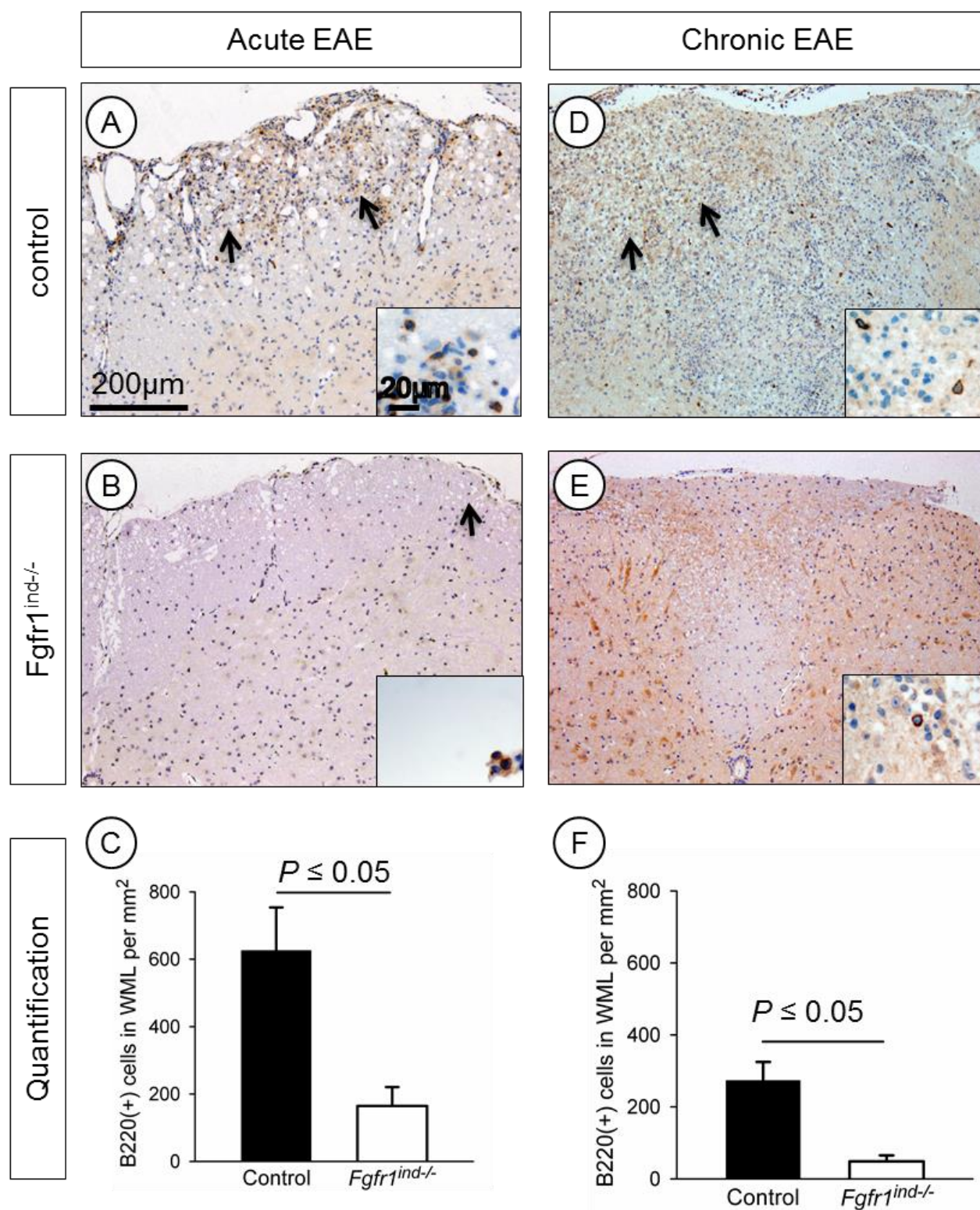


Figure 27 Immune cell infiltration in acute and chronic EAE spinal cord (B cells). B220 (+) B cells in white matter lesions of spinal cord sections in acute (A, B and C) and chronic (D, E and F) EAE in controls (A, D) and Fgfr1^{ind/-} mice (B, E). Representative images of spinal cord sections are presented. The number of B220 (+) B cells per mm² was less in Fgfr1^{ind/-} mice compared with controls in acute and chronic EAE (C and F). Bar: 200 μ m, 20 μ m (insert). n = 3, data are presented as mean \pm SEM.

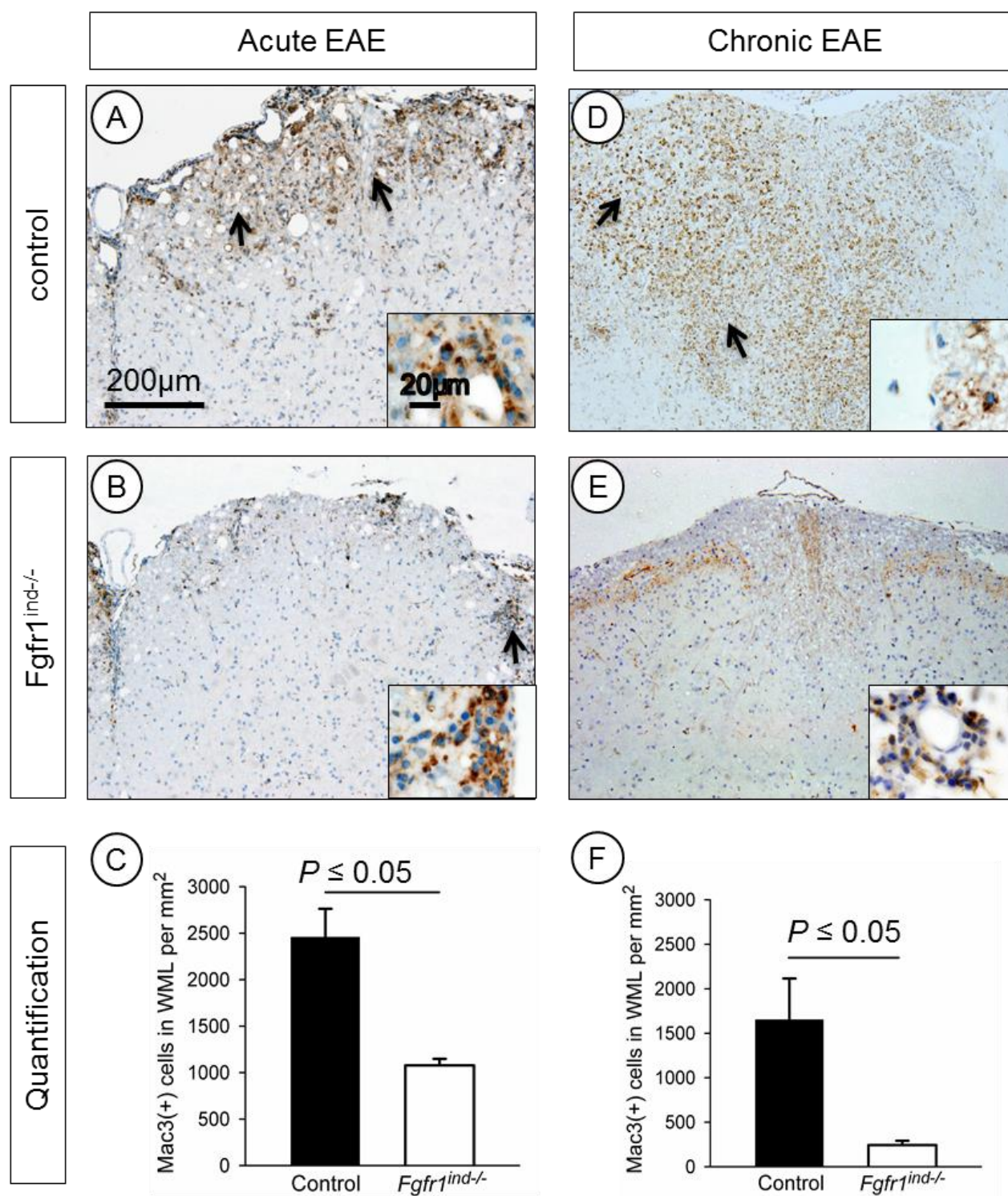


Figure 28 Immune cell infiltration in acute and chronic EAE spinal cord (Macrophages). Mac3 (+) Macrophages in white matter lesions of spinal cord sections in acute (A, B and C) and chronic (D, E and F) EAE in controls (A, D) and *Fgfr1*^{ind-/-} mice (B, E). Representative images of spinal cord sections are presented. The number of Mac3 (+) macrophage cells per mm² was less in *Fgfr1*^{ind-/-} mice compared with controls in acute and chronic EAE (C and F). Bar: 200 µm, 20 µm (insert). n = 3, data are presented as mean ± SEM.

4.2.5 Altered pattern of cytokines expression in Fgfr1^{ind/-} mice spinal cord

To characterize the underlying molecular mechanisms of cellular activation, proinflammatory cytokine mRNA was analyzed in the spinal cord in the acute and chronic phase (Figure 29 and 30). In the acute phase Fgfr1^{ind/-} mice showed decreased expression of TNF- α ($P < 0.001$), IL-1 β ($P \leq 0.05$) and IL-6 ($P < 0.001$) compared with controls (Figure 29 A, B, C respectively). Expression of inducible NOS (iNOS) and IL-12, however, was not changed in Fgfr1^{ind/-} mice (Figure 30 A and B). In the chronic phase no differences in proinflammatory cytokine expression for TNF- α , IL-1 β , IL-6 (Figure 29 D, E and F respectively), iNOS and IL-12 (Figure 30 C and D) were observed.

4.2.6 Altered pattern of cytokine expression in Fgfr1^{ind/-} mice spleen

To analyze whether relation with the reduced clinical score of Fgfr1^{ind/-} mice and peripheral immune response, we measured proinflammatory cytokine levels in the spleen. Spleen from Fgfr1^{ind/-} and controls of acute and chronic EAE mice were used for RNA isolation and DNA were reverse transcribed. The proinflammatory cytokines IL-1 β , IL-6, IL-12, TNF- α and iNOS expression were measured (Figure 31 and 32).

Proinflammatory cytokine TNF- α which mediate demyelination was significantly reduced in spleen of Fgfr1^{ind/-} on day 22 p.i. ($P = 0.0121$) and 62 p.i. ($P = 0.0475$) (Figure 31 A and D). In addition, reduced expression of IL-1 β in spleen of Fgfr1^{ind/-} mice in acute and chronic phase was observed but not statistically significant (Figure 31 B and E). IL-6 level was increased in Fgfr1^{ind/-} spleen in both time points but not significant (Figure 31 C and F). IL-12 and iNOS expression were not altered in control and Fgfr1^{ind/-} spleen (Figure 32).

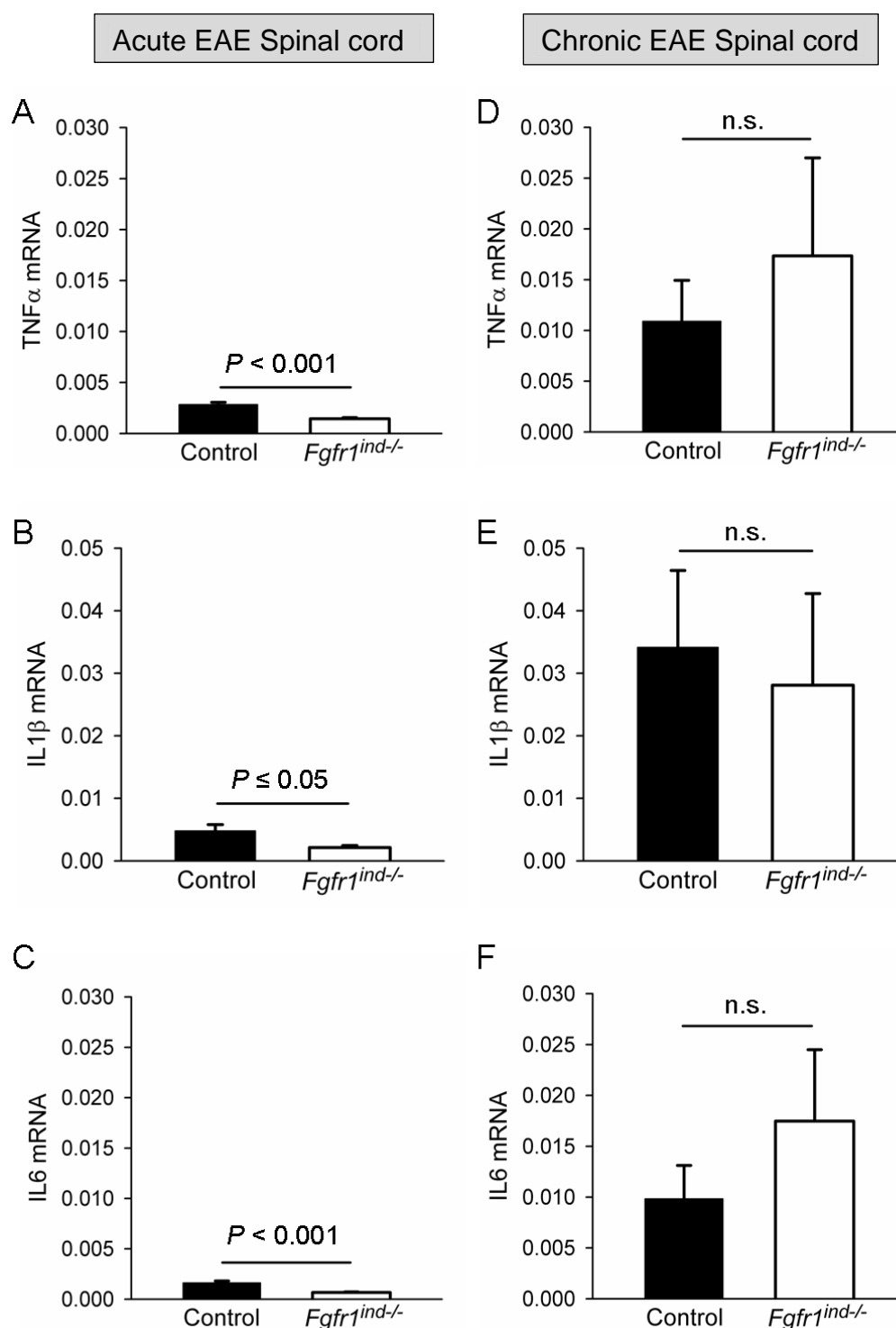


Figure 29 Gene expression of proinflammatory cytokine levels in the spinal cord of controls and *Fgfr1^{ind/-}* mice. Findings at the acute phase (A, B, C) and the chronic phase (D, E, F) are shown. At the acute phase decreased mRNA expression of TNF-α, IL-1β and IL-6 was observed in *Fgfr1^{ind/-}* mice compared with controls. In chronic phase the cytokines TNF-α, IL-1β, IL-6 were not different between *Fgfr1^{ind/-}* mice and controls. $n = 9$ (acute phase) and $n = 6$ (chronic phase), data are presented as mean \pm SEM.

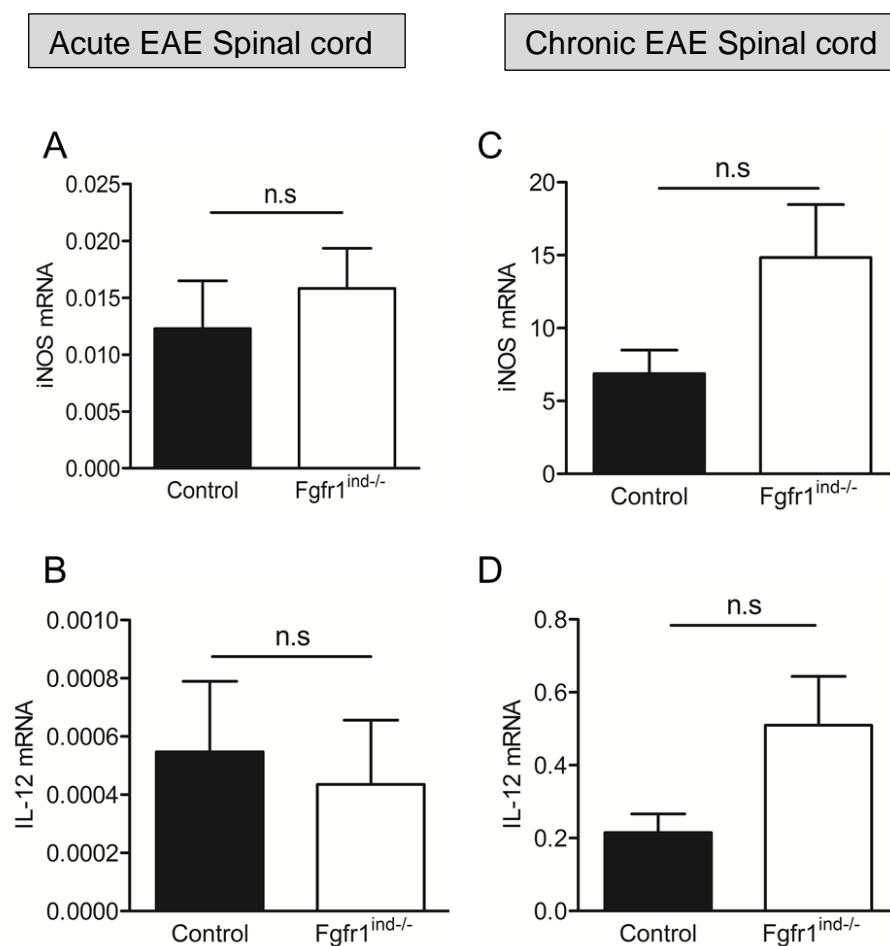


Figure 30 Gene expression of proinflammatory cytokine levels in the spinal cord of controls and Fgfr1^{ind-/-} mice. Findings at the acute phase (A, B) and the chronic phase (C, D) are shown. No differences in mRNA expression were seen for IL-12 and iNOS. At the chronic phase the cytokines IL-12, iNOS were not different between Fgfr1^{ind-/-} mice and controls. n = 9 (acute phase) and n = 6, data are presented as mean ± SEM.

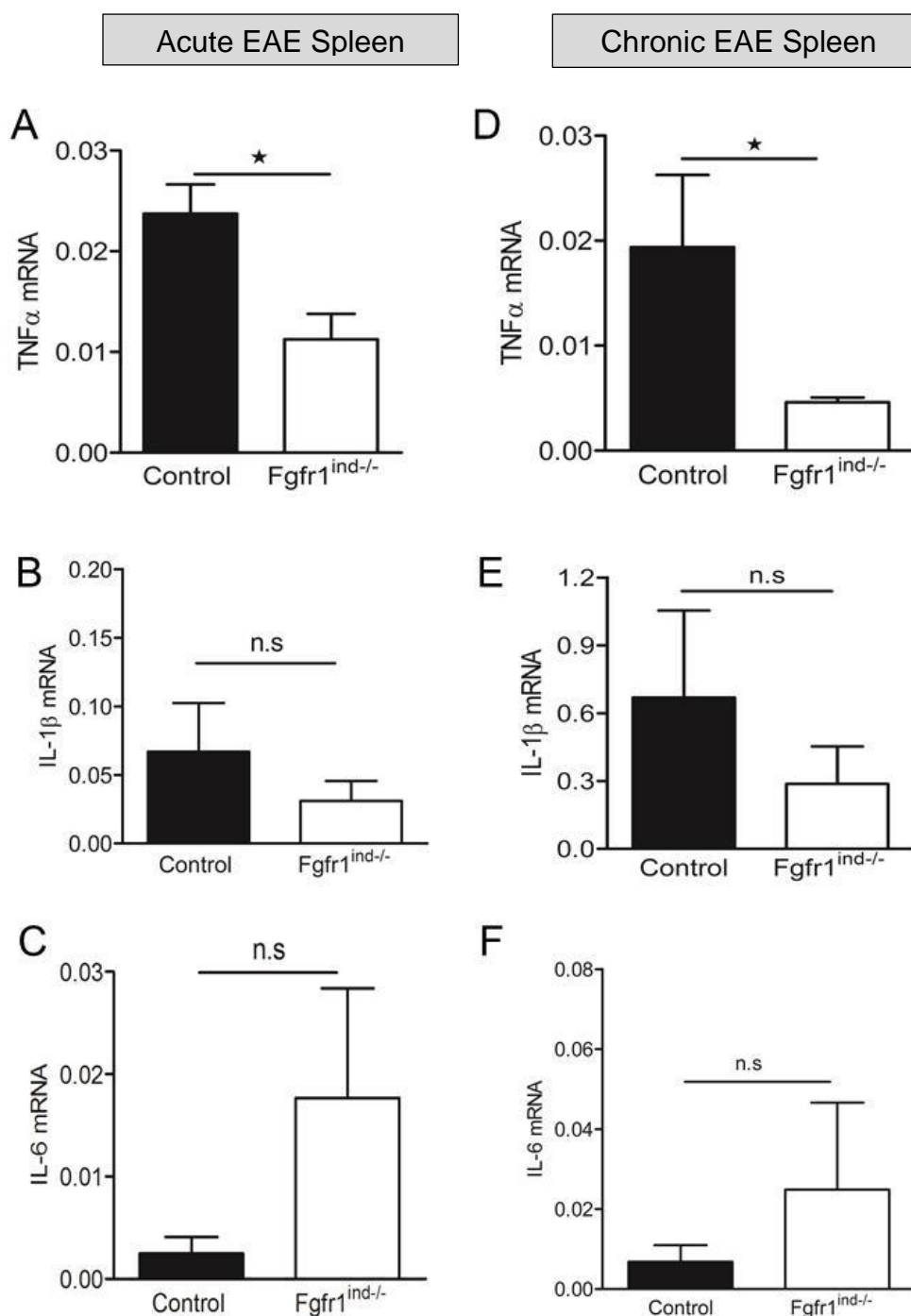


Figure 31 Relative mRNA expression level of proinflammatory cytokines in acute (A-E) and chronic (F-J) EAE spleen of control and *Fgfr1^{ind-/-}* mice. There were no significant changes in the expression of proinflammatory cytokines IL-1 β (A and F), IL-6 (B and G), IL-12 (C and H), inducible NOS (D and I) in spleen of both group in acute and chronic EAE. $n = 9$ (acute phase) and $n = 6$, data are presented as mean \pm SEM.

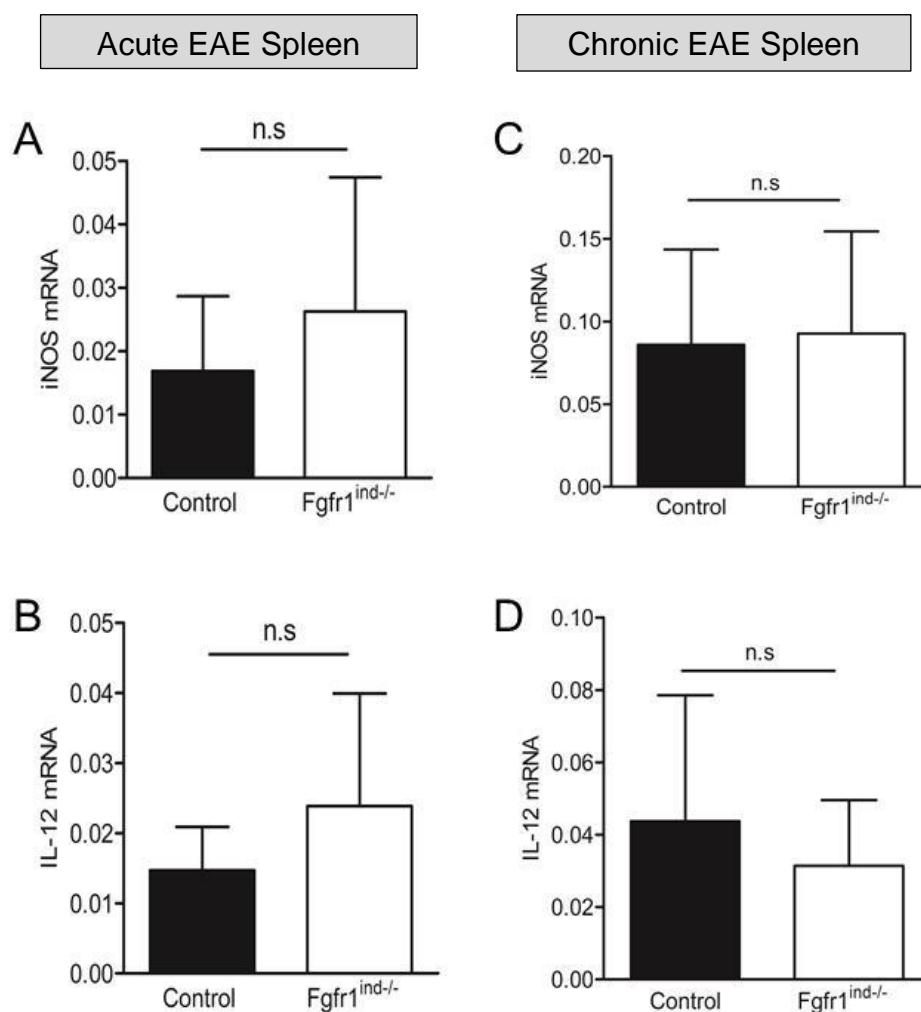


Figure 32 Relative mRNA expression level of proinflammatory cytokines in acute (A-E) and chronic (F-J) EAE spleen of control and *Fgfr1*^{ind-/-} mice. There were no significant changes in the expression of proinflammatory cytokines iNOS (A and C) and IL-12 (B and D) in spleen of both group in acute and chronic EAE. $n = 9$ (acute phase) and $n = 6$, data are presented as mean \pm SEM.

4.2.7 Chemokine and its receptor expression in *Fgfr1*^{ind-/-} mice spinal cord

In addition, to define further molecular mechanisms of cellular activation, the expression of the chemokine CX3CL1 and its receptor CX3CR1 in the spinal cord were studied in the acute and chronic phase (Figure 33). In the acute phase no effect of *Fgfr1* deletion on mRNA expression of CX3CL1 or CX3CR1 was seen (Figure 33 A and B). In the chronic phase CX3CL1 ($P \leq 0.05$) and CX3CR1 ($P \leq 0.05$) mRNA was decreased compared with controls (Figure 33 C and D).

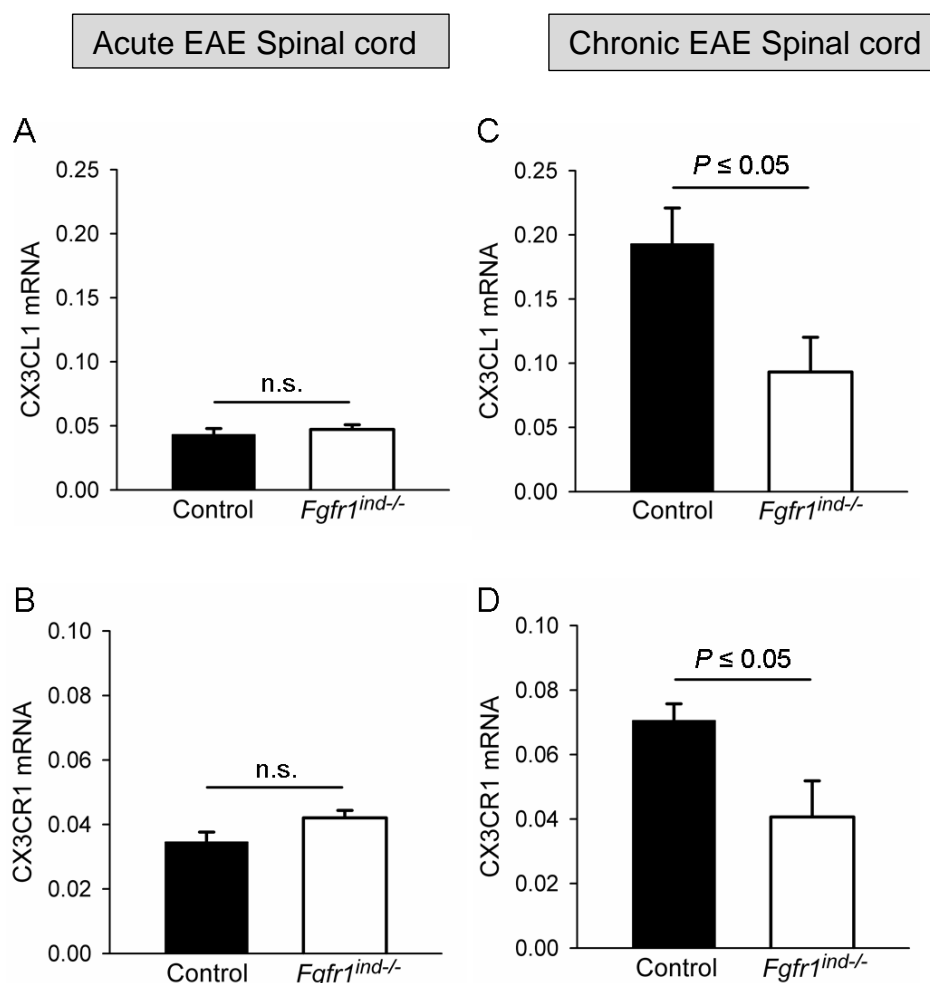


Figure 33 Gene expression of the chemokine CX3CL1 and the receptor CX3CR1 in the spinal cord of controls and *Fgfr1^{ind/-}* mice. Findings at the acute phase (A, B) and the chronic phase (C, D) are presented. At the acute phase no differences between *Fgfr1^{ind/-}* mice compared with controls were seen. At the chronic phase CX3CL1 and CX3CR1 were reduced in *Fgfr1^{ind/-}* mice. $n = 9$ (acute phase) and $n = 6$, data are presented as mean \pm SEM.

4.2.8 Increased ERK and AKT phosphorylation in chronic EAE *Fgfr1^{ind/-}* mice spinal cord

Spinal cord lysate from chronic EAE mice were analyzed by western blot to investigate the downstream signalling of *Fgfr1* pathway. *Fgfr1^{ind/-}* mice spinal cord showed increased expression of ERK ($P = 0.017$) and AKT ($P = 0.027$) phosphorylation during chronic EAE (Figure 34 B) and there were no regulation of ERK ($P = 0.246$) or AKT ($P = 0.327$) phosphorylation in acute phase (Figure 34 A).

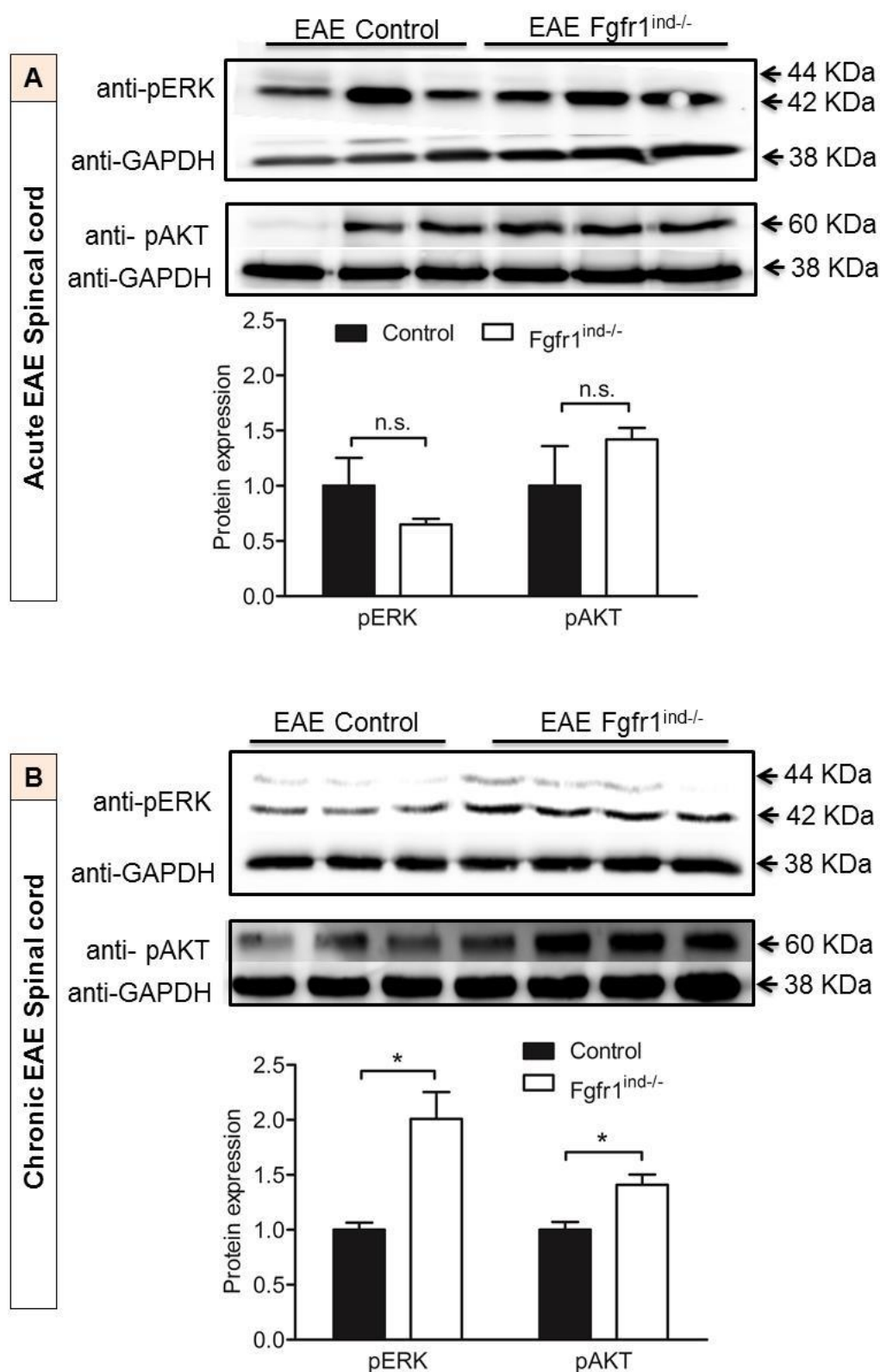


Figure 34 ERK and AKT phosphorylation in chronic EAE mice spinal cord. Increased phosphorylation of ERK and AKT was seen in chronic EAE spinal cord (B). There was no regulation of ERK and AKT phosphorylation in acute EAE spinal cord (A). GAPDH act as the internal loading control. P values of * $P < 0.05$, ** $P < 0.005$, *** $P < 0.001$ were considered as significant. Values are expressed as mean \pm standard error of mean. n.s. = not significant.

4.2.9 Deletion of Fgfr1 causes changes in BDNF and TrkB receptor expression

To investigate whether demyelination and axonal damage in the spinal cord was accompanied by changes in BDNF synthesis, the effect of oligodendroglial ablation of Fgfr1 on the neurotrophin BDNF and its receptor TrkB was studied on mRNA and protein levels in the acute (Figure 35) and chronic phase (Figure 36). In the acute phase BDNF (Figure 35 B) and TrkB receptor protein (Figure 35 D and E) expression was similar between Fgfr1^{ind-/-} mice and controls. In the chronic phase BDNF protein ($P \leq 0.05$) (Figure 36 B and E) and mRNA expression ($P \leq 0.05$) (Figure 36 A) was increased in Fgfr1^{ind-/-} mice when compared with controls. Also, in chronic phase TrkB receptor protein was increased in Fgfr1^{ind-/-} mice ($P < 0.01$) (Figure 36 D and E).

4.2.10 Deletion of Fgfr1 in oligodendrocytes mediates the milder disease course of chronic EAE through upregulation of PLP

To analyze the corresponding effect of Fgfr1 deletion in oligodendrocytes on myelin related protein expression in EAE, we studied the expression of PLP and MBP (Figure 37, 38 and 39). PLP expression is not regulated in Fgfr1^{ind-/-} compared to control in acute phase of the disease ($P = 0.678$) (Figure 37 A and C). Whereas PLP expression in Fgfr1^{ind-/-} were upregulated in MOG induced chronic EAE spinal cord (day 62 p.i, $P = 0.0209$, Figure 38 A and C). Myelin basic protein expression was not influenced by Fgfr1 deletion in oligodendrocytes in acute (Figure 37 B and D) and chronic EAE spinal cord in protein (Figure 38 B and D) and tissue level (Figure 39).

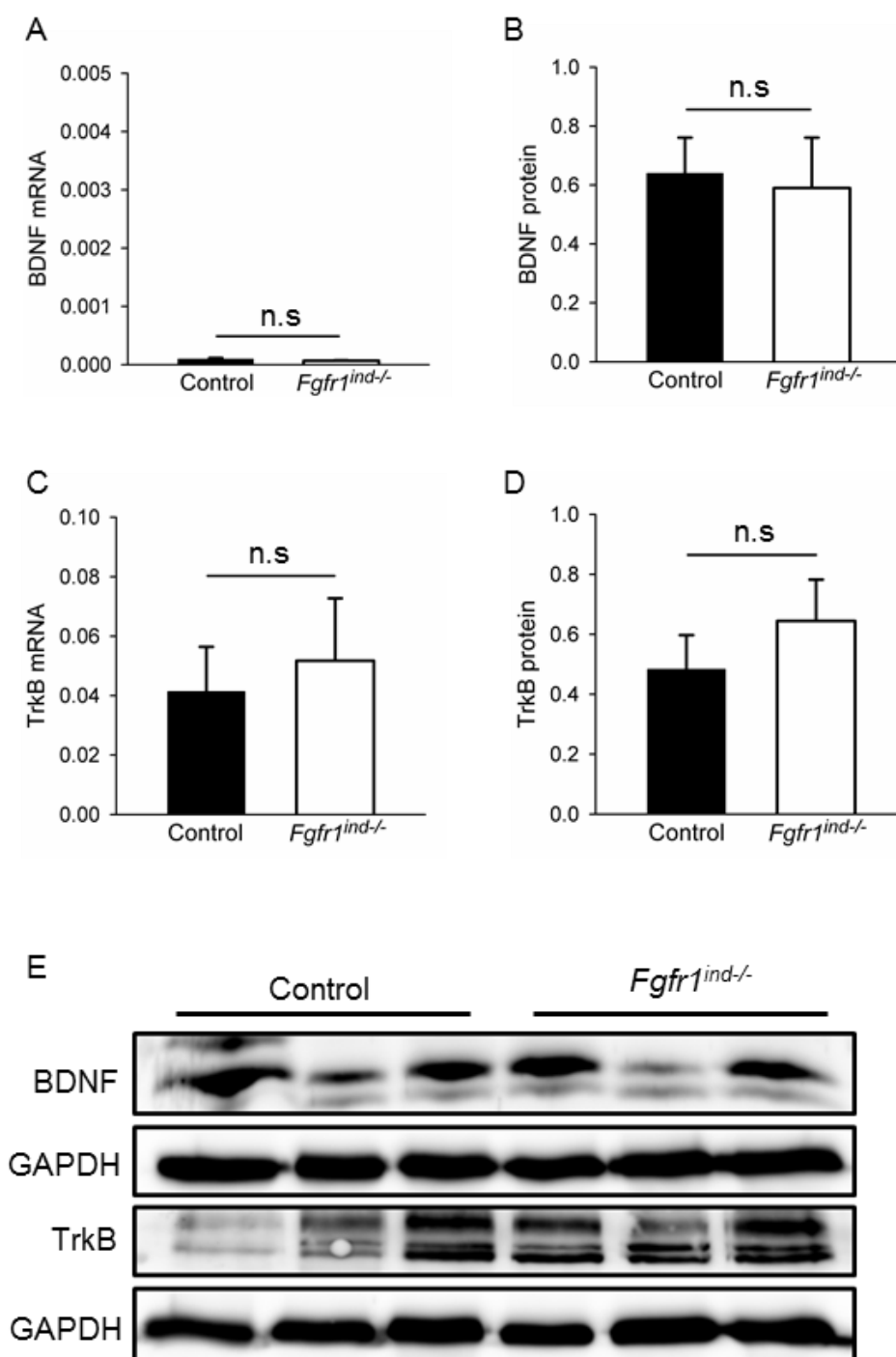


Figure 35 Gene expressions and protein quantification of brain-derived neurotrophic factor (BDNF) and the TrkB receptor in spinal cord lysates of acute EAE controls and *Fgfr1^{ind/-}* mice. At the acute phase no effect of *Fgfr1* deletion on BDNF mRNA (A) or protein expression (B) and no effect on TrkB receptor mRNA (C) or protein expression (D) were seen. Representative western blot images were shown (E). $n = 6$ (mRNA) and $n = 3$ (protein), data are presented as mean \pm SEM.

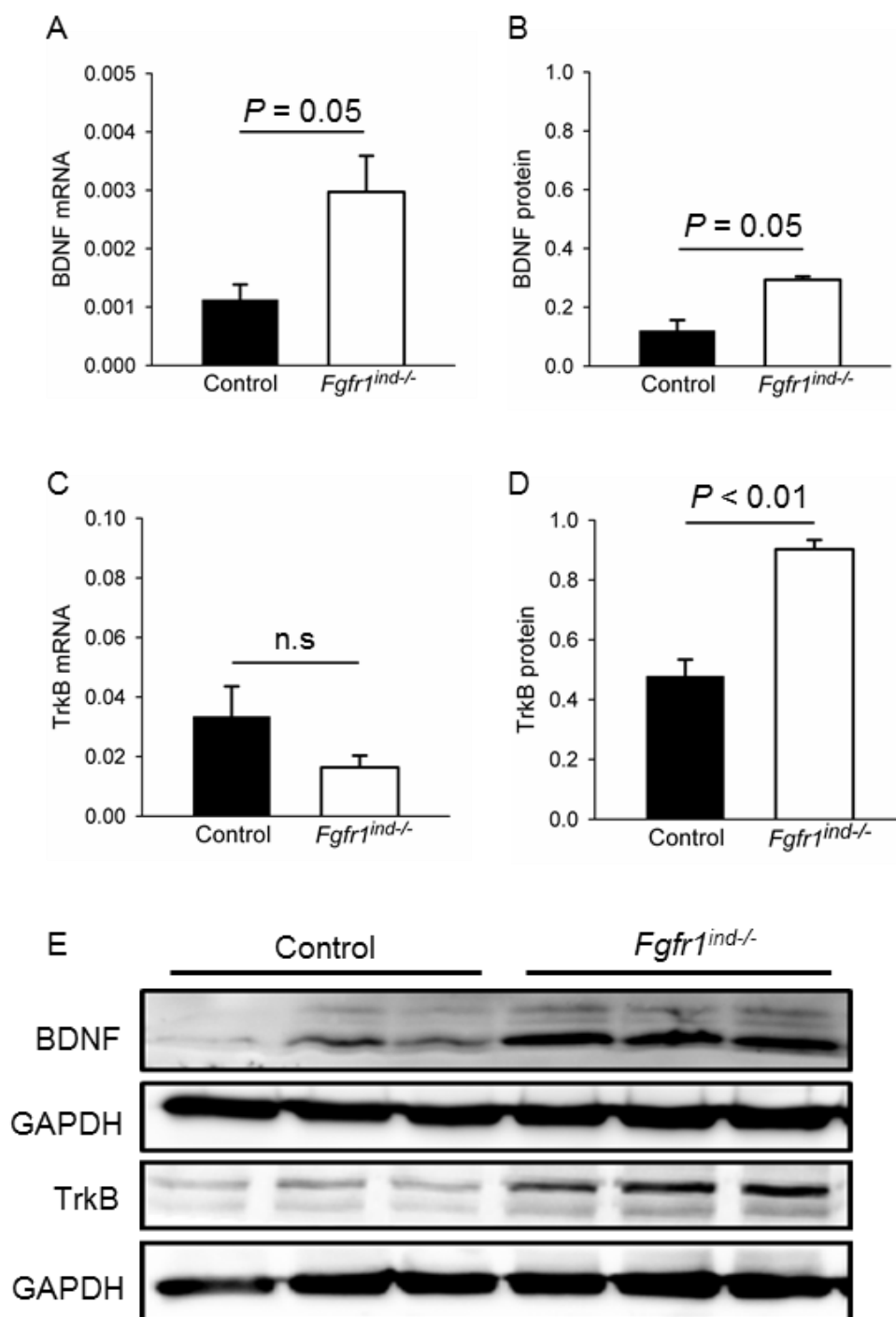


Figure 36 Gene expressions and protein quantification of brain-derived neurotrophic factor (BDNF) and the TrkB receptor in spinal cord lysates of chronic EAE controls and *Fgfr1*^{ind/-} mice. At the chronic phase increased BDNF mRNA (A) and protein expression (B) were found in *Fgfr1*^{ind/-} mice. TrkB receptor protein expression was upregulated in *Fgfr1*^{ind/-} mice (D). Representative western blots for BDNF and TrkB receptor are shown (E). $n = 6$ (mRNA) and $n = 3$ (protein), data are presented as mean \pm SEM.

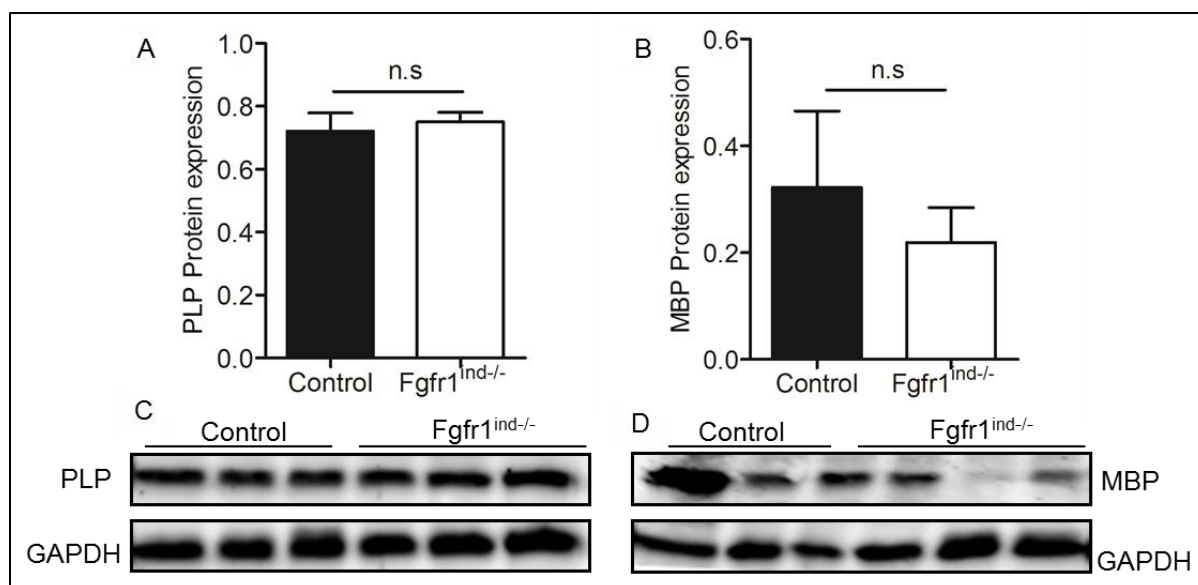


Figure 37 Effect of oligodendrocyte specific Fgfr1 ablation in the expression of proteo lipid protein and myelin basic protein in spinal cord of C57Bl/6J in acute phase of MOG EAE. MOG induced EAE was achieved in 10-12 weeks old female control and Fgfr1 conditional knockout (specific to oligodendrocytes) mice. Spinal cords were removed from acute EAE mice and the spinal cord lysates were analyzed for myelin proteins PLP and MBP. In acute EAE protein expression of PLP (A), MBP (B) was not altered by Fgfr1 deletion in oligodendrocyte lineage. Representative blots were shown (C and D). n.s. = not significant.

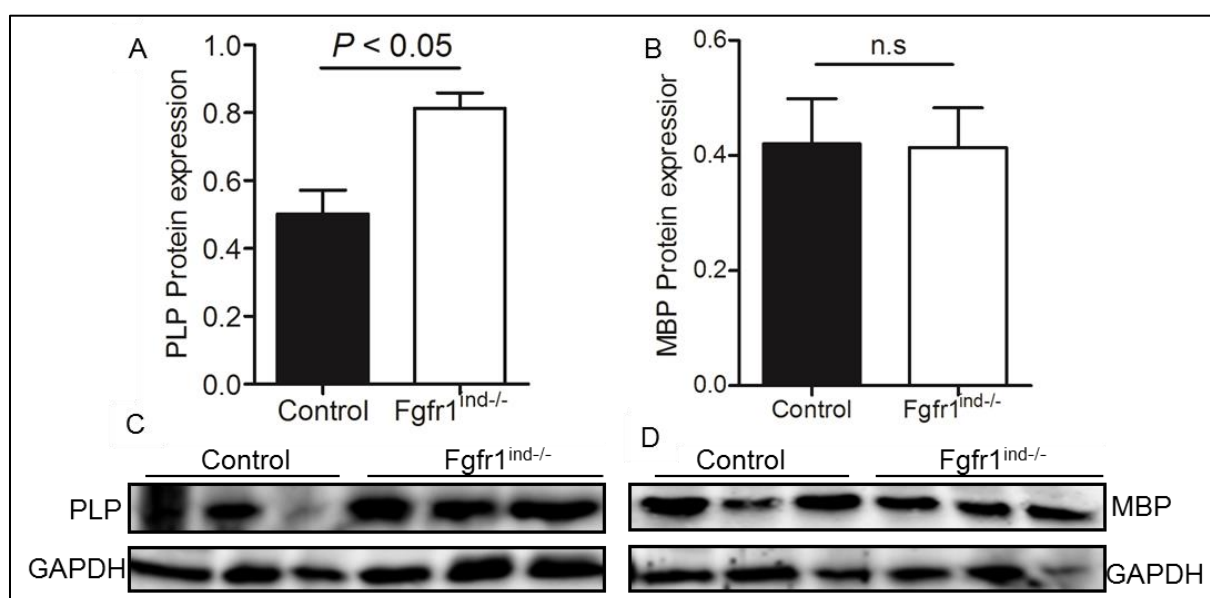


Figure 38 Effect of oligodendrocyte specific Fgfr1 ablation in the expression of proteo lipid protein and myelin basic protein in spinal cord of C57Bl/6J in chronic phase of MOG EAE. Proteolipid protein expression was significantly upregulated in oligodendrocyte specific Fgfr1 conditional knockout mice spinal cord in chronic EAE (A). MBP protein expression was not altered in Fgfr1^{ind/-} mice spinal cord in chronic EAE (B). n.s. = not significant.

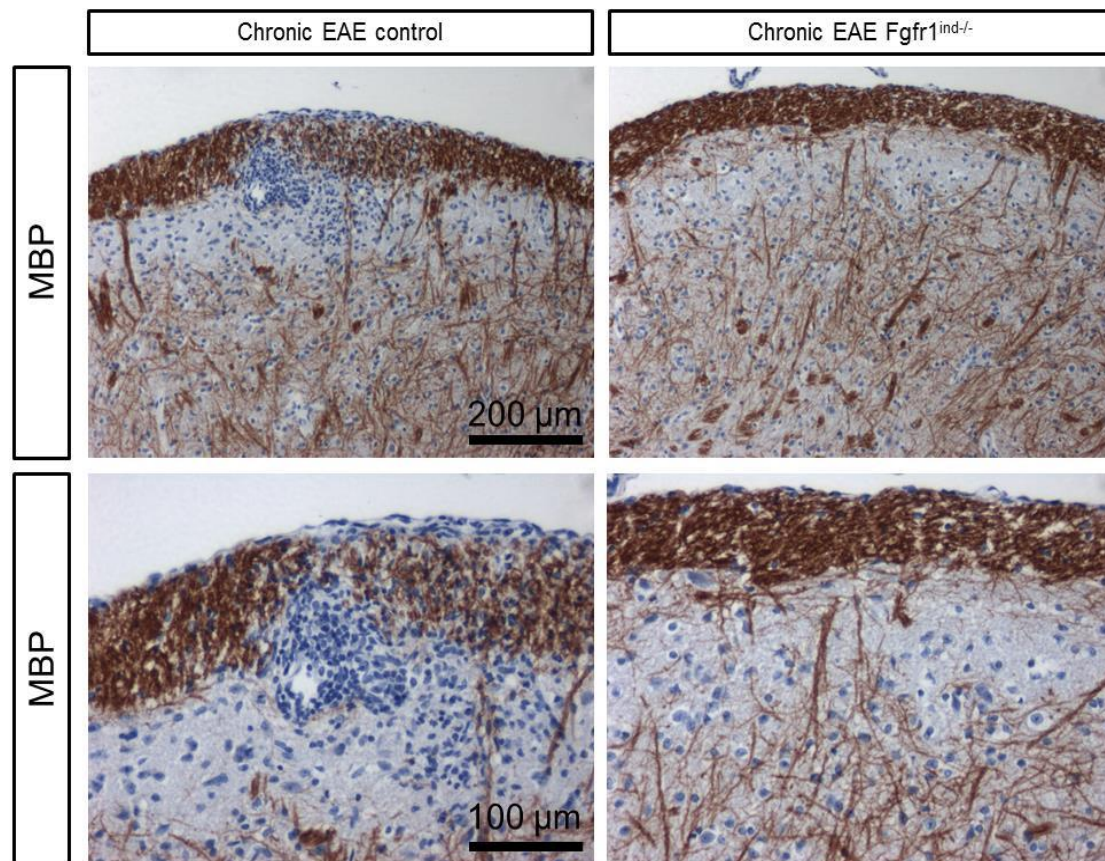


Figure 39 Myelin basic protein expression in chronic EAE control and $Fgfr1^{ind/-}$ mice spinal cord. Immunohistochemistry analysis of MBP level in spinal cord tissue shows no significant differences. Two respective magnifications were shown.

4.2.11 Ablation of $Fgfr1$ affects remyelination inhibitor expression

To analyze the expression of $Fgfr1$ in spinal cord of control and $Fgfr1^{ind/-}$ mice in acute and chronic phase of EAE, mRNA expression was analyzed by real time PCR (Figure 40). Reduced expression of $Fgfr1$ mRNA level was seen in acute ($P = 0.013$; Figure 40 A) and chronic ($P = 0.017$; Figure 40 B) EAE spinal cord of $Fgfr1^{ind/-}$.

To study whether differences in myelin damage in the spinal cord were accompanied by changes in inhibition of remyelination, the effect of $Fgfr1$ on remyelination inhibitors such as Lingo-1, FGF2, TGF β and SEMA3A were studied on mRNA level (Figure 41). In the acute phase no differences for Lingo-1 (Figure 41 A), FGF2 (Figure 41 G), TGF β (Figure 41 E) and SEMA3A (Figure 41 C) expression were seen between $Fgfr1^{ind/-}$ mice and controls. In the chronic phase mRNA expression of Lingo-1 (Figure 41 B) was decreased in $Fgfr1^{ind/-}$ mice ($P \leq 0.05$), a trend towards reduced mRNA expression of FGF2 (Figure 41 H) was seen in $Fgfr1^{ind/-}$ mice ($P = 0.071$). No differences were found for TGF β and SEMA3A (Figure 41 F and D).

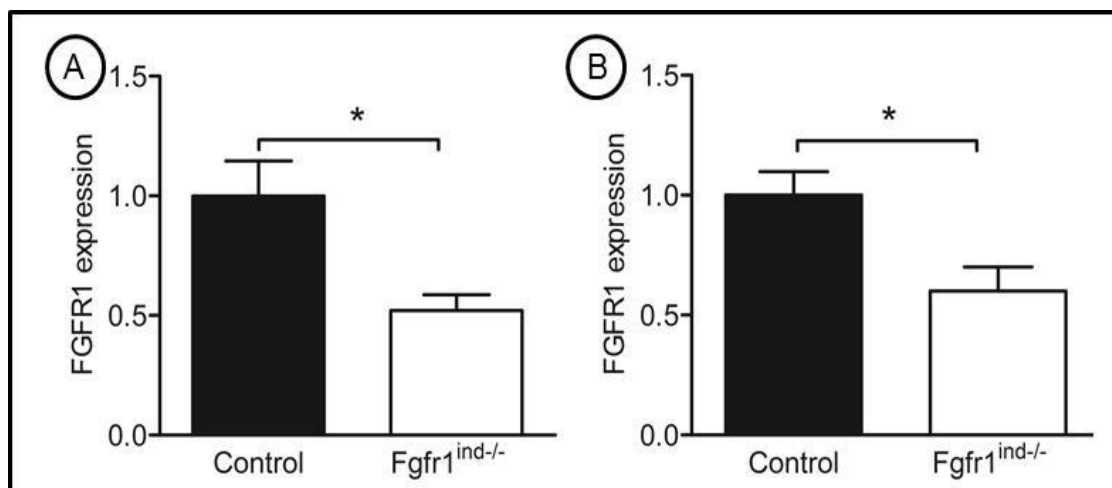


Figure 40 Fgfr1 mRNA expression in spinal cord of control and Fgfr1^{ind/-} mice in acute and chronic EAE. Reduced level of Fgfr1 expression was seen in mRNA level in acute (A) and chronic (B) EAE spinal cord of Fgfr1^{ind/-} mice.

4.2.12 Deletion of Fgfr1 does not affect oligodendrocyte lineage cells

In mouse CNS, olig2 (Kitada und Rowitsch 2006) and nogo-A (Kuhlmann *et al.* 2007) is expressed by oligodendrocyte lineage cells. To answer the question whether deletion of oligodendroglial Fgfr1 affects oligodendrocyte lineage cells in EAE the number of olig2 (+) and nogoA (+) oligodendrocytes was studied in spinal cord white matter lesions in the acute (Figure 42) and chronic phase (Figure 43). There was no effect of Fgfr1 deletion on the number of these cells at both time points. A trend towards an increased number of nogoA (+) oligodendrocytes in Fgfr1^{ind/-} mice was found both in the acute phase ($P = 0.124$) and the chronic phase ($P = 0.118$) (Table 7; Figure 42 and 43 respectively).

Table 7 Oligodendrocyte lineage cell population in EAE spinal cord.

Oligodendrocyte lineage	Acute EAE			Chronic EAE		
	control	Fgfr1 ^{ind/-}	P- value	control	Fgfr1 ^{ind/-}	P- value
olig2 (+) cells	395 ± 91	530 ± 23	$P = 0.229$	491 ± 105	480 ± 39	$P = 0.927$
nogoA (+) cells	386 ± 72	530 ± 16	$P = 0.124$	394 ± 80	528 ± 24	$P = 0.188$

Semiquantitative analysis of oligodendrocyte lineage cell population were shown. There were no differences in the number of olig2 and nogoA positive cells in the spinal cord of control and Fgfr1^{ind/-} mice during acute and chronic phase of EAE.

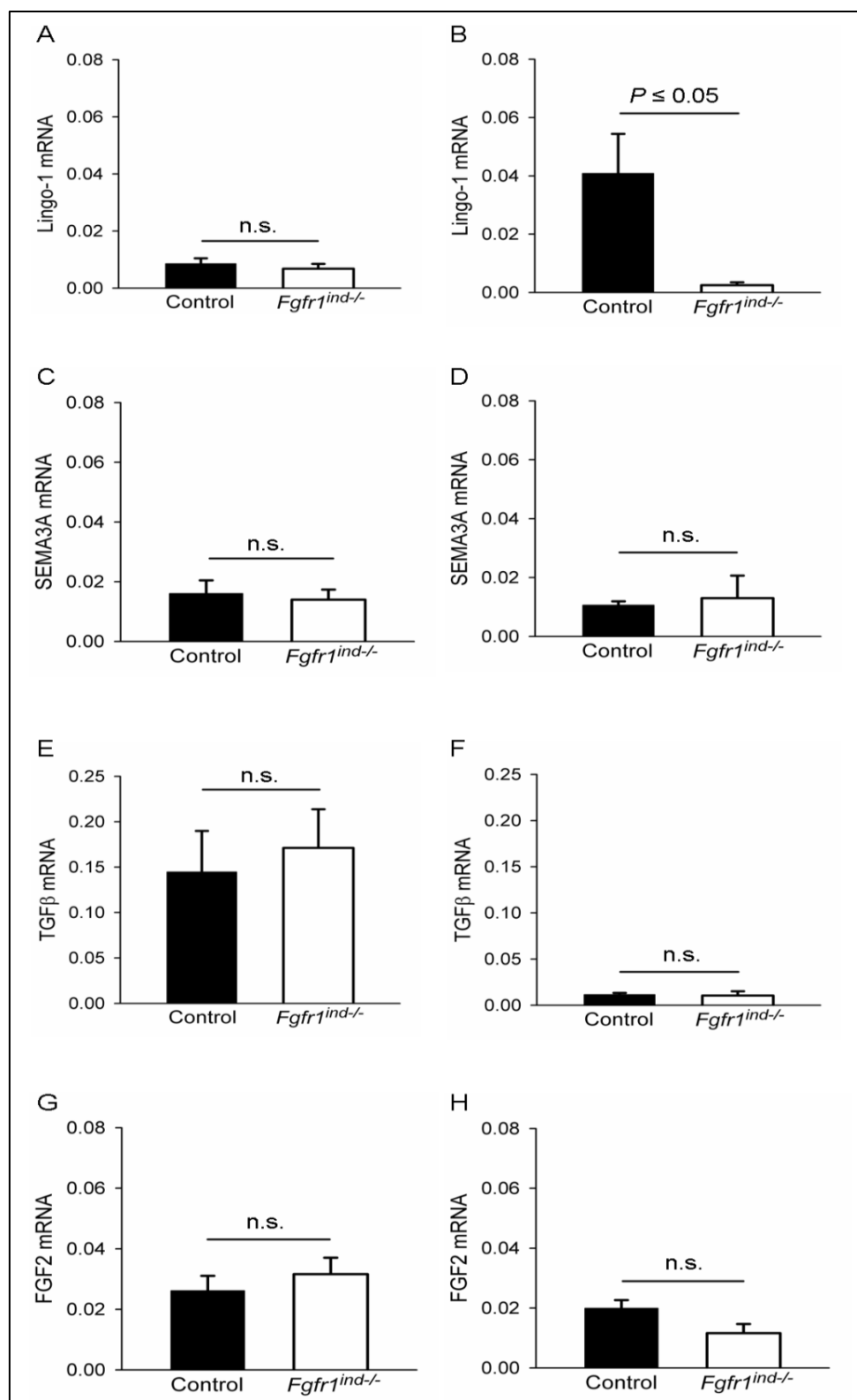


Figure 41 Gene expressions of the remyelination inhibitors Lingo-1, SEMA3A, TGFβ and FGF2 in the spinal cord of controls and *Fgfr1^{ind/-}* mice. Findings at the acute phase (A, C, E, G) and the chronic phase (B, D, F, H) are shown. At the acute phase Lingo-1, SEMA3A, TGFβ and FGF2 expression was not different between *Fgfr1^{ind/-}* mice and controls. In the chronic phase both Lingo-1 (B) was reduced in *Fgfr1^{ind/-}* mice, furthermore a trend towards a reduced expression of FGF2 was seen (H). $n = 6$, data are presented as mean \pm SEM.

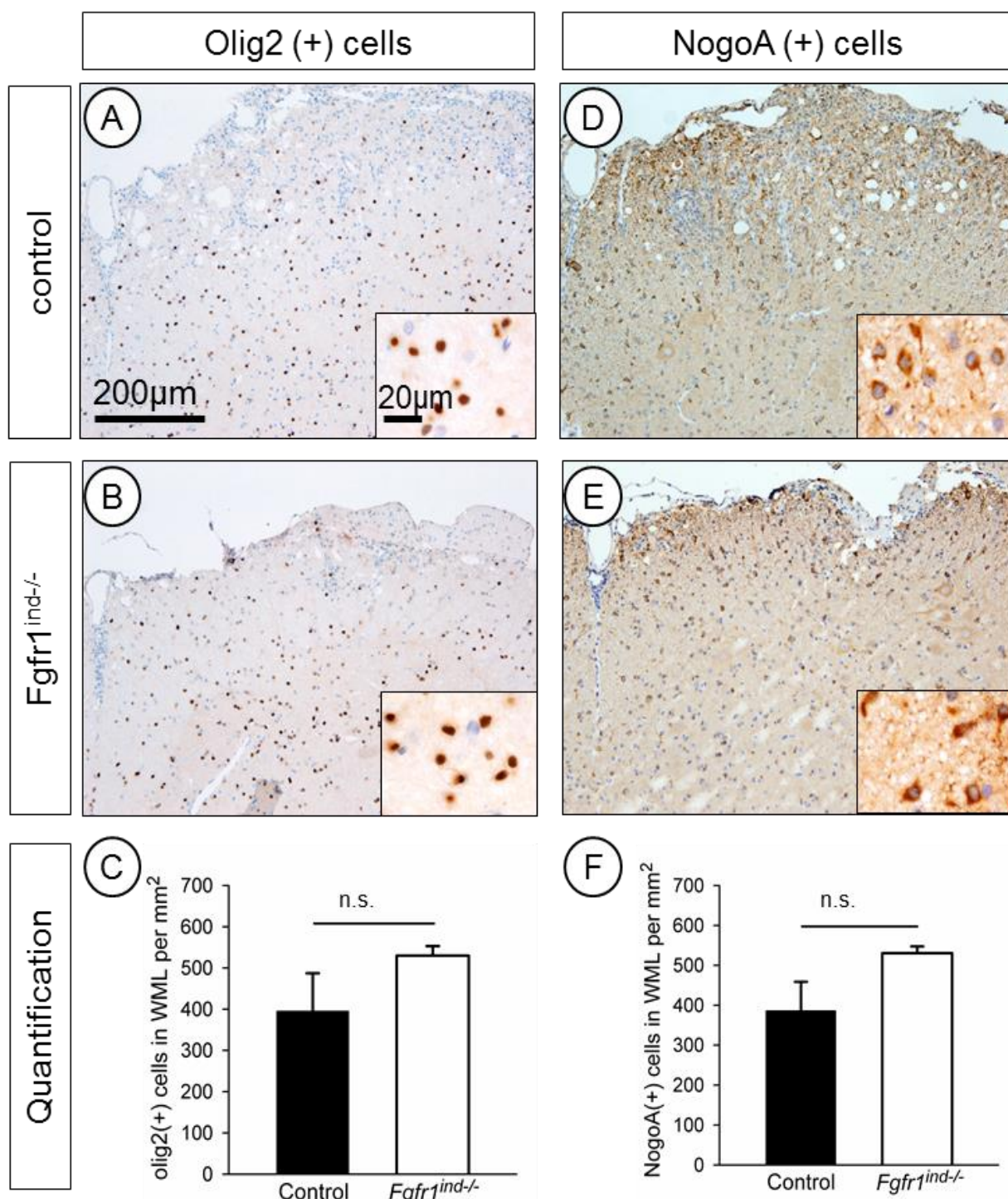


Figure 42 Oligodendrocyte lineage cell populations in control and *Fgfr1*^{ind/-} mice spinal cord in acute EAE. Olig2 and nogoA positive oligodendrocyte lineage cell populations in controls and *Fgfr1*^{ind/-} mice spinal cord. There were no differences in the population of olig2 (A, B and C) and nogo A (D, E and F) positive cells in *Fgfr1*^{ind/-} mice spinal cord. n = 3 mice, data are presented as mean ± SEM.

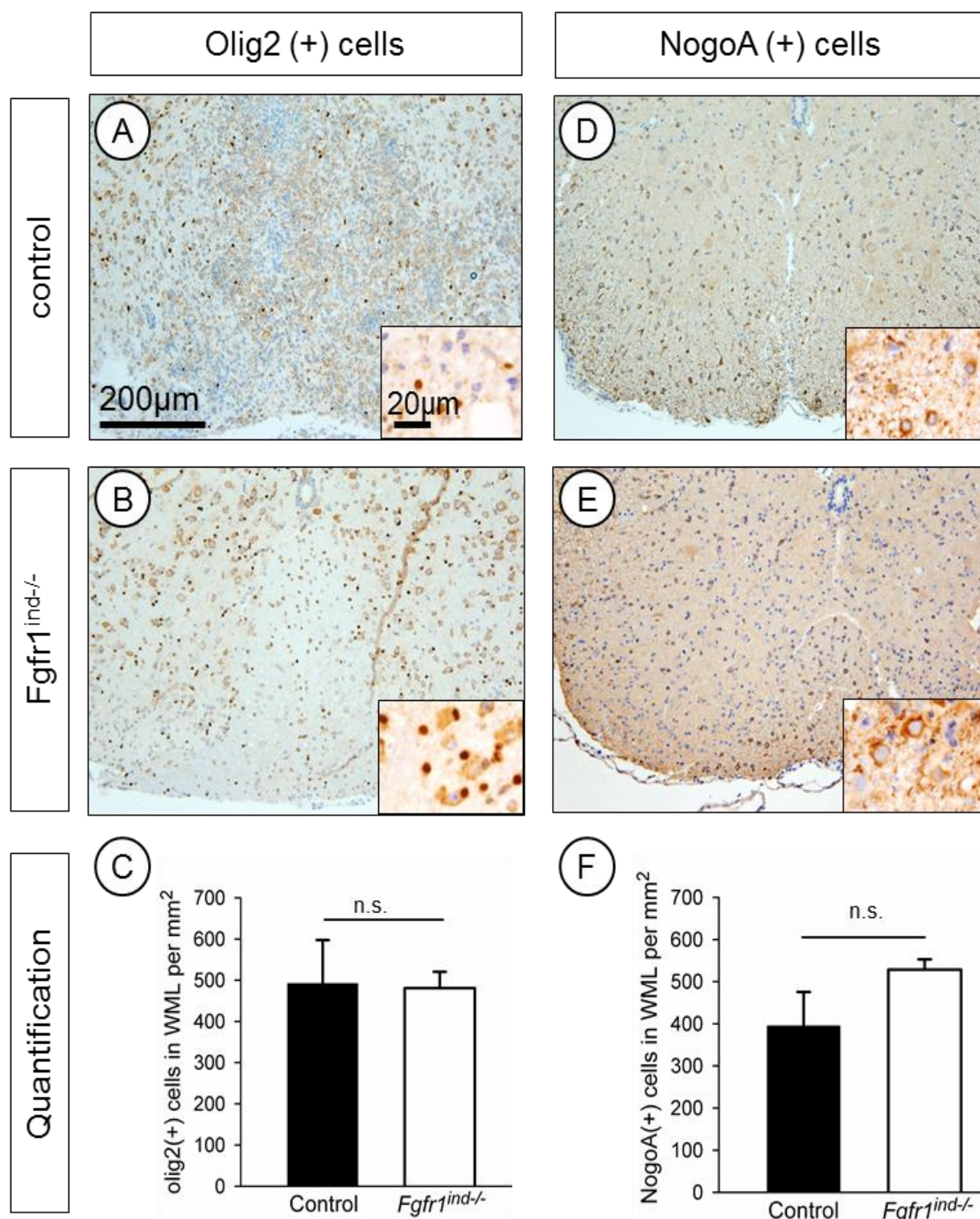


Figure 43 Olig2 (+) and nogoA (+) oligodendrocytes in spinal cord sections in chronic EAE controls and *Fgfr1*^{ind/-} mice. Representative images of spinal cord sections at the chronic phase are shown. There were no differences in the number of olig2 (+) oligodendrocytes (A, B and C). A trend towards an increased number of nogoA (+) oligodendrocytes in *Fgfr1*^{ind/-} mice was seen at the chronic phase (D, E and F). *n* = 3 mice, data are presented as mean \pm SEM.

4.3 Milder EAE score in IFN β -1a treated Fgfr1^{ind/-} mice

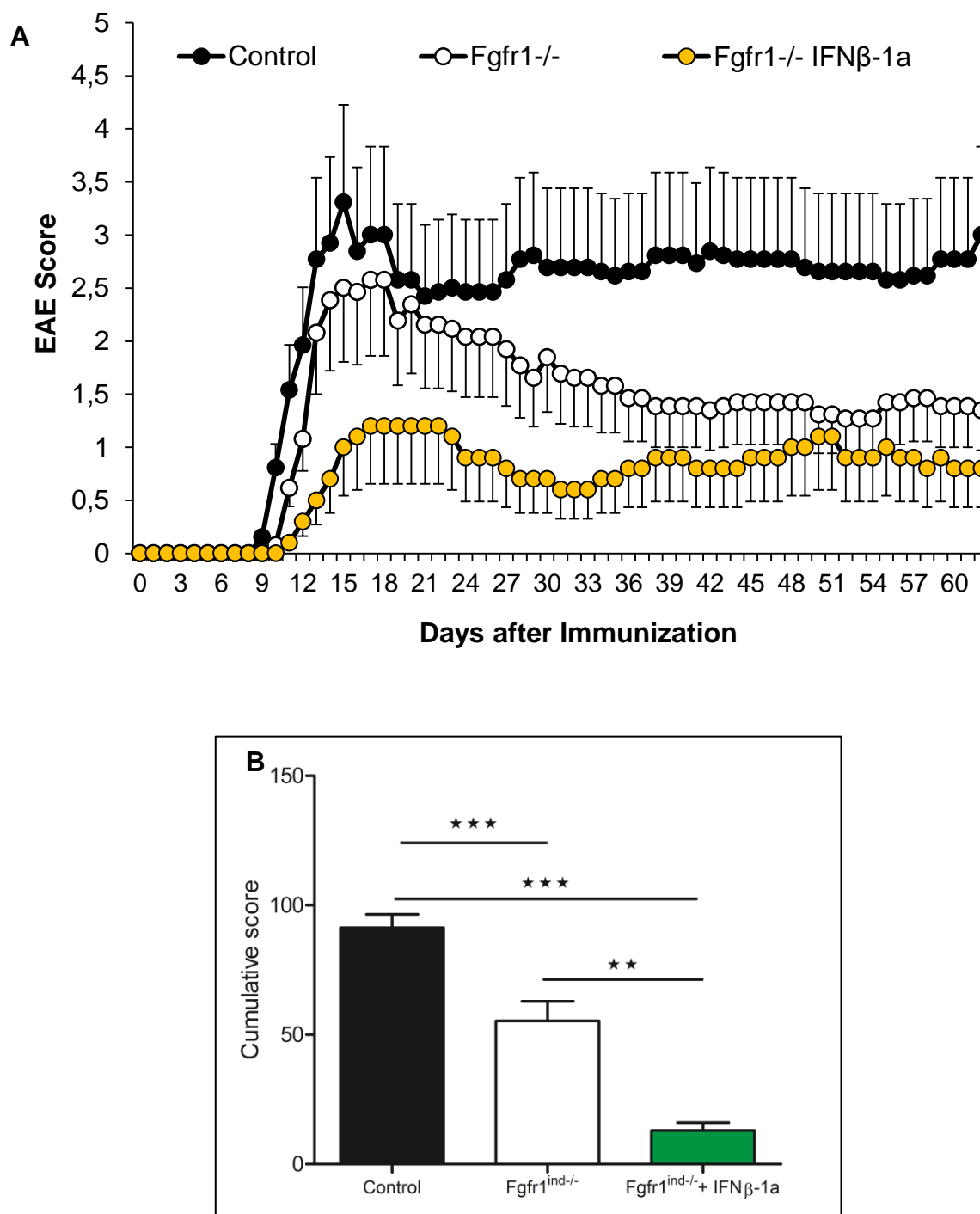


Figure 44 Effects of Interferon β -1a treatment in chronic EAE. Chronic EAE was induced in control and Fgfr1^{ind/-} mice and IFN β -1a was treated from day 0 till day 7 post immunization. EAE score were monitored till day 62. A) IFN β -1a treated Fgfr1^{ind/-} mice showed milder EAE disease course (70 % milder). B) Cumulative EAE score of control, Fgfr1^{ind/-} and Fgfr1^{ind/-} mice treated with IFN β -1a. Significant milder score was seen in Fgfr1^{ind/-} and IFN β -1a treated Fgfr1^{ind/-} mice.

Mice with oligodendroglial Fgfr1 deletion ($Fgfr1^{ind/-}$) were analyzed for their susceptibility to MOG₃₅₋₅₅ peptide EAE induction (Figure 8). To investigate IFN β -1a treatment effect in $Fgfr1^{ind/-}$ mice during chronic EAE, EAE was induced in eight to twelve-week-old female $Fgfr1^{ind/-}$ mice and compared with age- and sex-matched controls. Following IFN β -1a treatment from day 0 till day 7 p.i. mice were assessed for clinical symptoms (Figure 44 A). The onset of clinical symptoms was on day 11 p.i. in control and $Fgfr1^{ind/-}$ mice treated with IFN β -1a. The mean maximum disease score was 2.7 in control and 1.5 in IFN β -1a treated $Fgfr1^{ind/-}$ mice ($P \leq 0.001$). IFN β -1a treated $Fgfr1^{ind/-}$ mice showed a milder disease course than controls ($P \leq 0.001$). In this disease phase, $Fgfr1^{ind/-}$ mice presented with a mild paraparesis whereas controls still suffered from a severe paraparesis. Also, the cumulative EAE score was higher in controls ($P \leq 0.001$; Figure 44 B). Disease incidence was 100%. No effect of gene deletion on mortality was observed. There were no differences in body weight between $Fgfr1^{ind/-}$ and control mice.

4.4 *In vitro* experiments

4.4.1 The effects of Fgfr1 inhibition and IFN β -1a in oli-neu oligodendrocytes

PD166866 is a potent Fgfr1 inhibitor which is used to analyze *in vitro* role of Fgfr1 in oligodendrocyte cells oli-neu. Fgfr1 inhibitor PD166866 showed significant reduced proliferation in oli-neu cells. There was no proliferation effect of IFN β -1b treatment in oli-neu cells. Combined treatment of IFN β -1b and PD166866 reduce the proliferation effect of oli-neu cells (Figure 45). There was no effect of Fgfr1 inhibition and IFN β -1b on cytotoxicity in oli-neu cells (Figure 46). ERK1/2 phosphorylation was decreased by Fgfr1 inhibition in oli-neu cells and there was no effect of IFN β -1b on ERK1/2 phosphorylation (Figure 47). Combination of Fgfr1 inhibition and IFN β -1b treatment does not reduce the ERK1/2 phosphorylation as in either Fgfr1 inhibition or IFN β -1b treatment alone (Figure 47). IFN β -1b enhances STAT1 phosphorylation and Fgfr1 does not influence STAT1 phosphorylation (Figure 47).

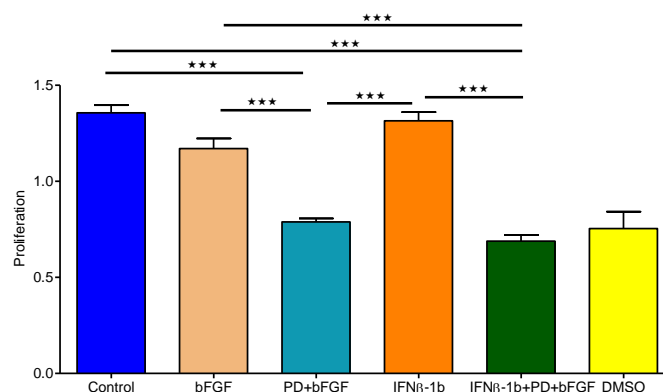


Figure 45 Proliferation effects of Fgfr1 inhibition and IFN β -1b treatment in oligodendrocyte oli-neu cell line by WST assay. Oli-neu cells were incubated with PD166866 to inhibit Fgfr1 and IFN β -1b was treated and proliferation was estimated. Fgfr1 inhibition decrease the proliferation and IFN β -1b treatment does not affect the proliferation. *** represent < 0.001 .

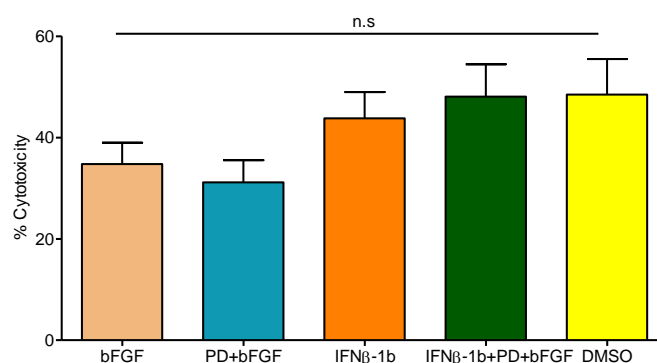


Figure 46 Cytotoxicity effects of Fgfr1 inhibition and IFN β -1b treatment in oligodendrocyte oli-neu cell line by LDH assay. Oli-neu cells were incubated with PD166866 to inhibit Fgfr1 and IFN β -1b was treated and cytotoxicity was estimated. There is no effect of Fgfr1 inhibition and IFN β -1b on cytotoxicity of oli-neu cells. n.s = not significant.

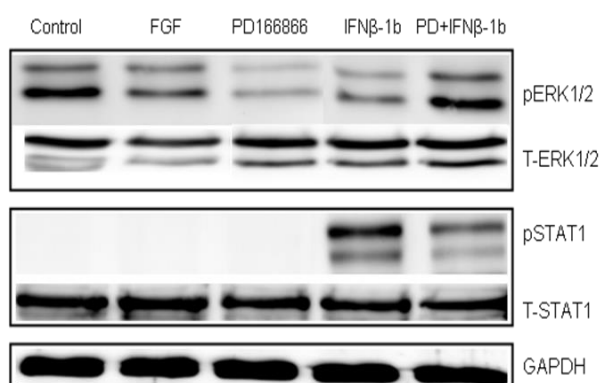


Figure 47 Expression of ERK1/2 and STAT1 phosphorylation upon Fgfr1 inhibition and IFN β -1b on oli-neu cell line. Upon Fgfr1 inhibition and IFN β -1b treatment, ERK1/2 and STAT1 phosphorylation were checked by western blotting. ERK phosphorylation decreases after Fgfr1 inhibition and no effect in IFN β -1b treatment. pSTAT1 is upregulated after IFN β -1b treatment in oli-neu cells.

5 DISCUSSION

Fibroblast growth factors and its receptors (FGF/FGFR) play a major role in embryogenesis and development of organs, and contribute to the development of CNS. In the present study the *in vivo* function of FGF receptor 1 was characterized using an oligodendrocyte-specific genetic approach. We have seen milder disease course in $Fgfr1^{ind/-}$ mice in MOG₃₅₋₅₅-induced EAE which is contrasting to our hypothesis. $Fgfr1^{ind/-}$ mice showed a milder the disease course. The pathological analysis showed decreased lymphocyte and macrophage/microglia infiltration, and myelin and axon degeneration in $Fgfr1^{ind/-}$ mice. In addition, in acute EAE down regulation of proinflammatory cytokines such as TNF- α , IL-1 β and IL-6 and in chronic EAE down regulation of the CX3CL1/CX3CR1 was seen in $Fgfr1^{ind/-}$ mice. Furthermore, increased expression of TrkB/BDNF and decreased expression of Lingo-1 was found in $Fgfr1^{ind/-}$ mice.

5.1 Oligodendrocyte specific $Fgfr1$ knock out in C57Bl/6J mice

5.1.1 $Fgfr1$ deletion in oligodendrocytes does not result in phenotypic changes

FGF/ $Fgfr1$ signalling has been involved in numerous cellular processes, including proliferation, differentiation and survival (Knights and Cook 2010). It was shown that complete or partial loss of $Fgfr1$ resulted in lethality at embryonic days 7-12.5. Xu *et al.* developed $Fgfr1$ conditional knockout allele using the Cre-loxP system (Xu *et al.* 2002). The $Fgfr1$ knockout in keratinocytes caused progressive loss of skin appendages, cutaneous inflammation (Yang *et al.* 2010). Moreover, $Fgfr1$ deficient embryos displayed severe growth retardation and died prior to or during gastrulation because of intrinsic blocks in mesoderm differentiation, and mice with targeted deletion of $Fgfr1$ in mesenchymal cells leads to the death of mice at birth and mice that lack the Frs-binding site on $Fgfr1$ died during late embryogenesis (Su *et al.* 2014). Furthermore, Smith *et al.* (2014) showed reduced number of perivascular positive cortical interneurons in conditional knockout of $Fgfr1$ in neuron ($Fgfr1^{fl/fl}; Nestin-Cre^{+}$ mice) and astrocytes ($Fgfr1^{fl/fl}; hGFAP-Cre^{+}$ mice) under nestin and GFAP promoters respectively. Recently, Zhou *et al.* (2012) showed the conditional deletion of $Fgfr1$ in oligodendrocyte lineage cells by Tamoxifen inducible Cre

mediated system and reduced Fgfr1 expression. Here we used a Tamoxifen inducible system of cre mediated Fgfr1 deletion in oligodendrocyte lineage cells in C57BL/6J mice line. The principle conclusion that emerges from our results in Fgfr1^{ind/-} mice phenotype is that conditional deletion of Fgfr1 in oligodendrocytes under Plp promoter does not show phenotypic changes.

5.1.2 Increased ERK and AKT phosphorylation in Fgfr1^{ind/-} mice

Spinal cord and cortex whole lysates of control and Fgfr1^{ind/-} mice showed no differences in the expression of Fgfr1 or Fgfr2, because the conditional knockout system allows the deletion of Fgfr1 specifically in oligodendrocyte lineage cells. We demonstrated that the loss of Fgfr1 in oligodendrocyte lineage cells resulted in an increased phosphorylation of ERK, AKT and TrkB receptors in spinal cord. Fgfr1 autophosphorylation internally activates ERK and AKT pathways which lead to proliferation, survival and differentiation of oligodendrocyte lineages. Hence, we expected that conditional deletion of Fgfr1 in oligodendrocyte lineage will decrease the ERK and AKT signalling pathways. However, an increased phosphorylation of ERK and AKT was detected in Fgfr1^{ind/-} mice cortex and spinal cord whole lysates. The influence of oligodendrocyte specific Fgfr1 in ERK and AKT expression in whole lysates of spinal cord and cortex is not understood well. It has been shown that increased AKT expression mediate enhanced myelination in CNS (Flores *et al.* 2008). This increase that is observed in Fgfr1^{ind/-} mice might be due to compensatory mechanisms through other growth factor receptors such as Fgfr 3 or 4. Moreover, the variation in the response of oligodendrocyte Fgfr1 to whole lysate downstream pathways, both within CNS tissues and between CNS tissues, is likely to reflect combination of unknown factors, including the response of individual oligodendrocytes on site.

The study of the Fgfr1 signalling pathway initiated by conditional knockout system is currently an emerging field of investigation. Fgfr signalling permits or promotes olig2 gene transcription (Easin *et al.* 2010). Fgfr signalling maintains a basal level of MAPK phosphorylation, which is essential for olig2 expression. Mechanisms behind oligodendrocyte progenitor cell generation through Fgfr are not well understood.

However, Fgfr1 is a tyrosine kinase receptor that initiates a number of well characterized signalling pathways such as Shc-Ras-Erk (MAPK/ERK), PI3K/AKT, and PLC- γ pathways (Turner and Grose 2010). Some of these pathways have been implicated in regulating myelination. The expression of constitutively active AKT in oligodendrocyte progenitor cells and oligodendrocytes (via the PLP promoter) exerted no influence on oligodendrocyte number, but dramatically increased myelin thickness (Flores *et al.* 2008, Narayanan *et al.* 2009). ERK1/2 MAPK pathway has been shown to be a major contributor leading to the induction of oligodendrocyte progenitors in spinal cord. Besides, inhibition of ERK1/2 MAPK by chemical inhibitor also inhibits the induction of olig2 cells in cultures of spinal cord *in vitro*. It is difficult to interpret these findings in the aspect of oligodendrocyte specific Fgfr1 in whole spinal cord as little is known about the molecular events in oligodendrocyte Fgfr1 in altering signalling pathway in whole lysate.

On top of those Furusho *et al.* (2011) shown that loss of Fgfr1 or Fgfr2 in oligodendrocytes does not affect the proliferation or cell death of oligodendrocyte progenitor cells. They examined oligodendrocyte proliferation and cell death in forebrains of Fgfr1^{-/-} mutants and their littermate controls on E12.5 day. They measured the proliferation of oligodendrocyte progenitors in cultures initiated from E12.5 day control and Fgfr1 mutant forebrains and showed no differences in the number of oligodendrocyte progenitor cells either *in vivo* or *in vitro*.

5.1.3 Increased TrkB expression in Fgfr^{ind/-} mice spinal cord

In our study, Fgfr1^{ind/-} cortex and spinal cord showed increased expression of TrkB, brain stem and cerebellum showed there was no difference in TrkB expression. Brain-derived neurotrophic factor (BDNF) belongs to the neurotrophin family of growth factors and signals via two distinct classes of receptors: tropomyosin-related kinase (Trk) B and p75. *In vitro* studies have identified that BDNF exerts direct effects on oligodendroglia, variously promoting OPC proliferation and differentiation, as well as myelination via activation of endogenous TrkB receptors on oligodendroglia (Xiao *et al.* 2010). BDNF/TrkB clearly exerted a positive effect on myelination; however, it remained unclear whether this was primarily a neuronal or oligodendroglial-mediated effect. Also, BDNF and its receptor TrkB are expressed in macrophages (Artico *et al.*

2008) and play autocrine and paracrine roles in the modulation of regeneration and angiogenesis following nerve injury (Kermani and Hempstead 2007). The reason for this diversity in response of oligodendrocytes to TrkB *in vivo* is unclear, but could be due to regional differences and heterogeneity of progenitor populations of the cells in the specific tissues. Thus the molecular substrates present in the Fgfr1 mediated BDNF/TrkB expression remains unknown and several other negative feedback mechanisms that may exist to control the adverse effect of oligodendrocyte Fgfr1 over activation need to be further investigated.

5.2 Oligodendrocyte specific Fgfr1 inhibition reduces chronic EAE

In our present study the *in vivo* function of Fgfr1 was characterized using an oligodendrocyte-specific genetic approach, which allowed defining the function of this receptor in a cell-specific and inducible fashion. Impaired signalling via oligodendroglial Fgfr1 resulted in a milder disease course. Recent studies suggest that Fgfr1 plays a role in multiple sclerosis and its model EAE. Fgfr1 is up regulated in oligodendrocyte precursor cells within active and around chronic multiple sclerosis brain lesions (Clemente *et al.* 2011). In EAE, Fgfr1 is expressed on effector cells such as macrophages and activated microglia (Liu *et al.* 1998).

The key clinical finding of our study is that Fgfr1^{ind/-} mice showed a milder disease course in the chronic phase of EAE. Furthermore, Fgfr1^{ind/-} mice is presented with a delay in onset of symptoms and less maximum disease severity. This pattern of milder EAE disease course during chronic phase is particularly interesting. These clinical findings are in contrast to those obtained after systemic deletion of its key ligand FGF2. FGF2^{-/-} mice are more severely affected in the chronic phase of EAE (Rottlaender *et al.* 2011), a finding, which is supported by data from a FGF2 gene therapy study (Ruffini *et al.* 2001). In addition, intrathecal injection of a HSV multigene vector engineered with the human FGF2 gene at day 20 after EAE induction also resulted in a milder disease course.

5.2.1 Reduced immune cells in $Fgfr1^{ind/-}$ mice

In both acute and chronic phases of EAE, impaired signalling via $Fgfr1$ was associated with a decreased number of macrophages/activated microglia and B220 (+) B cells in the spinal cord. Macrophages are the dominant effector cell population in the acute phase of EAE (Gold *et al.* 2006). Activated macrophages and microglia release a number of soluble factors such as nitric oxide (NO), excitotoxins and proteases, which cause structural damage in the CNS (Gold *et al.* 2006). In $Fgfr1^{ind/-}$ mice a significant reduction of CD3 (+) T cells was observed only in the chronic phase of EAE. In EAE, myelin specific T cells, which are activated in the periphery migrate into the CNS. In the CNS these T cells are reactivated resulting in the release of proinflammatory cytokines and chemokines (Fletcher *et al.* 2010). Data on oligodendrocyte-specific $Fgfr1$ ablation and immune cell infiltration into the CNS are not available from the toxic demyelination model (Zhou *et al.* 2012). In contrast to our findings, in $FGF2^{-/-}$ mice the number of macrophages and T cells are increased in acute EAE (Rottlaender *et al.* 2011). B220 (+) cell infiltration is regulated by oligodendroglial $Fgfr1$ in our study. The contradicting findings that we observed in the disease course and cellular infiltration between $Fgfr1^{ind/-}$ and $FGF2^{-/-}$ mice may be explained by alternative binding of other ligands to $Fgfr1$ or activation of other FGFRs by FGF2 (Reuss and von Bohlen 2003). Our data indicate that oligodendrocyte $Fgfr1$ exerts important and independent effects that directly or indirectly influence immune cell infiltration and perhaps more importantly in chronic phase of EAE.

In vitro data suggest that the deleterious effects of $Fgfr1$ activation by FGF2 on differentiated oligodendrocytes are associated with a downregulation of myelin proteins (Fortin *et al.* 2005). Myelin sheaths play an important role in protecting axons from degeneration (Irvine and Blakemore 2008). Our findings suggest that impaired signalling via oligodendroglial $Fgfr1$ results in decreased demyelination. Oligodendroglial $Fgfr1$ did not affect the number of oligodendrocyte lineage cells in our model. In the model of toxic demyelination reduced $Fgfr1$ expression is associated with increased oligodendrocyte repopulation (Zhou *et al.* 2012). $Fgfr1^{ind/-}$ mice showed enhanced axonal density in our study, which is in accordance with findings in the model of toxic demyelination (Zhou *et al.* 2012).

5.2.2 Decreased cytokines in Fgfr1^{ind/-} mice

In the acute phase of EAE, impaired signalling via Fgfr1 was associated with decreased secretion of proinflammatory cytokines such as TNF- α , IL1- β and IL-6. Microglia produces TNF- α , IL-6 and IL-1 β in response to IFN- γ (Rodgers and Miller 2012). Signalling via Fgfr1 did not change expression levels of these cytokines in the chronic phase of EAE. Myelin degeneration and axon remyelination failure in oligodendrocytes, which are associated with differentiation dysfunction, are pathological hallmarks of MS. It is known that cytokines affect the permeability of the blood brain barrier, oligodendrocyte progenitor differentiation, activation of microglia and astrocytes to participate in disease progression and remyelination. Several lines of evidence indicate that TNF- α is one of the most relevant cytokines involved in the pathogenesis of this disease (Bonora *et al.* 2014). TNF- α is a key mediator of inflammation in multiple sclerosis (Caminero *et al.* 2011, Lock *et al.* 2002) and EAE (Hidaka *et al.* 2014, Lock *et al.* 2002).

In our study, Fgfr1^{ind/-} mice showed less TNF- α compared to control mice which is associated by disease recovery of Fgfr1^{ind/-} mice. TNF α is produced by infiltrating immune cells and activated glia (astrocytes and microglia) in multiple sclerosis (Caminero *et al.* 2011, Rodgers and Miller 2012) and EAE (Gold *et al.* 2006). *In vitro* TNF- α inhibits oligodendrocyte progenitor cell proliferation and differentiation through a mitochondria-dependent process (Bonora *et al.* 2014). The Th1 cytokines, IFN- γ and TNF- α , were both higher in MS patients, but only the TNF- α levels were statistically significant (Lovett-Racke *et al.* 2011). TNF- α signalling mediates cell death cascades through activating one or more of the three pathways such as nuclear factor (NF) κ B, MAPK and caspases. TNF- α inhibits oligodendrocyte progenitor cell proliferation and differentiation and also induces mature oligodendrocyte apoptosis (Rodgers and Miller 2012).

IL-1 β promotes pathogenic Th17 differentiation, T cell trafficking, and CNS tissue damage. There is also evidence that suggests that IL-1 β causes disruption in inhibitory connections in the cerebellum during EAE and MS (Rodgers and Miller 2012). Both IL-6 (Quintana *et al.* 2009, Steinman 2008) and IL-1 β (Prins *et al.* 2013, Rossi *et al.* 2012) are mediators of inflammatory responses in the white matter and

contribute to the development of brain lesions in multiple sclerosis and EAE. It is known that IL-1 β plays a role in demyelination, breakdown of blood-brain barrier (BBB), microglia activation and promotion of IL-17 expression (Inoue and Shinohara 2013). In our results, *Fgfr1*^{ind-/-} mice showed increased expression of BDNF and reduced IL-1 β expression in spinal cord which is in agreement with one alternative hypothesis that BDNF primarily reduce IL-1 β expression, thereby attenuating astrogliosis (Lin *et al.* 2006) and microgliosis (Basu *et al.* 2002).

5.2.3 Decreased chemokines in *Fgfr1*^{ind-/-} mice

More specifically, we asked how target removal of *Fgfr1* in oligodendrocytes affects the immune cell infiltration. Chemokine mediated immune cell infiltration through *Fgfr1* has been reported (Reed *et al.* 2012). There is evidence for a role of the CX3CL1/CX3CR1 pathway in multiple sclerosis and EAE. Molecular signalling through fractalkine (CX3CL1), a nociceptive chemokine, via its receptor (CX3CR1) is thought to be associated with MS. CX3CR1 is present on astrocytes and oligodendrocytes in active and silent multiple sclerosis lesions (Omari *et al.* 2005). Increased expression of serum CX3CL1 is observed in patients with multiple sclerosis (Kastenbauer *et al.* 2003). Data from a genetic study suggest that the CX3CR1 I249T280 haplotype may protect from switch to secondary progressive multiple sclerosis (Stojkovic *et al.* 2012). In rats CX3CL1 and CX3CR1 are expressed by neurons, astrocytes and microglia (Sunnemark *et al.* 2005). In the chronic phase of EAE we observed that impaired signalling via oligodendroglial *Fgfr1* was associated with decreased immune cell infiltration through the CX3CL1/CX3CR1 pathway, *Fgfr1* does not seem to affect this pathway in the acute phase. CX3CR1-deficient mice have been shown to have a more severe disease course, and increased IFN- γ expression (Garcia *et al.* 2013).

Treatment with an anti-CX3CL1 antibody resulted in reduced clinical disease severity and less lymphocyte infiltration in acute EAE. In addition, in EAE model of MS, Zhu *et al.* (2013) showed significant increases in mRNA and the protein expression of CX3CL1 and CX3CR1 in the dorsal root ganglia (DRG) and spinal cord 12 days after EAE induction compared to controls. Furthermore, this increased expression

correlated with the peak neurological disability caused by EAE induction. In inflammatory state, increased expression of CX3CL1 occurs in neurons and also in astrocytes in the dorsal horn of the spinal cord. CX3CL1 is usually expressed in the normal rodent CNS tissue by different neuronal cell subtypes (Harrison *et al.* 1998). In addition, it is also expressed in monocytes, natural killer (NK) cells, and smooth muscle cells (Linde *et al.* 2005). The CX3CL1 receptor, CX3CR1, is constitutively expressed in microglia of the brain and spinal cord and is significantly increased as a result of microglial activation (Harrison *et al.* 2005).

Following inflammation, injured neurons release adenosine triphosphate (ATP), which binds to the P2X7 receptor on microglia that subsequently causes the release of the protease Cathepsin S (Coddou *et al.* 2011). CX3CL1 is bound to the neuronal membrane and is cleaved by the Cathepsin S (Clark *et al.* 2010). Soluble CX3CL1 binds to the CX3CR1 on microglia resulting in the increased synthesis and release of proinflammatory mediators such as IL-6 and nitric oxide. TNF- α also involved in the post transcriptional regulation of CX3CL1 and TNF- α is a critical upstream factor that regulates CX3CL1 production (Isozaki *et al.* 2010). Up-regulation of TNF- α in spinal cord may be a critical early step in regard to the regulation of MS induction via CX3CL1/CX3CR1 signalling pathway. However, further studies are also required to study the effect of TNF- α on CX3CL1 expression in spinal cord oligodendrocytes.

Our findings suggest that the CX3CL1/CX3CR1 pathway is controlled by oligodendroglial Fgfr1 in the chronic phase of EAE. The cell migration mechanism was explained with IL-1 β and IL-18, which are processed by the inflammasome and up-regulate expression of chemokines and their receptors in both in T cells and antigen presenting cells (Inoue and Shinohara 2013). It is our belief that the oligodendrocyte specific Fgfr1 and CX3CL1/CX3CR1 signalling crosstalk in spinal cord may be involved in the underlying pathology in EAE.

5.2.4 Increased neuronal growth factors in *Fgfr1^{ind/-}* mice

BDNF is a neurotrophic factor involved in neuronal survival and differentiation as well as axonal growth (Chao 2003). Oligodendrocytes produce BDNF that promote the survival of neurons, advancing oligodendrocyte differentiation and myelination, especially during CNS myelin lesion and repair (Bankston *et al.* 2013). However, how BDNF expression is regulated in oligodendrocyte is much less understood. It has been proven that BDNF is a suppressing factor for macrophage migration and infiltration and may play a detrimental role after spinal cord injury (Wong *et al.* 2010) and intracerebroventricular administration of BDNF has been reported to significantly reduce blood brain barrier breakdown. In multiple sclerosis immune cells are a major source of BDNF (Kerschensteiner *et al.* 1999). More BDNF (+) cells are found in active demyelinating lesions compared with inactive lesions (Stadelmann *et al.* 2002). Furthermore, neurons around active lesions and reactive astrocytes within lesions express high levels of its high affinity receptor gp145trkB (Stadelmann *et al.* 2002).

In EAE (Lee *et al.* 2012, Linker *et al.* 2010) and other lesion models (Markus *et al.* 2002) BDNF is expressed by activated immune cells and it is also associated with axonal protection (Linker *et al.* 2010). In the present study we observed increased BDNF or TrkB levels in the chronic phase of EAE in *Fgfr1^{ind/-}* mice suggesting that expression of these molecules is regulated by oligodendroglial *Fgfr1*. In post-mortem tissue from patients different inhibitors of oligodendrocyte precursor cell differentiation have been detected (Kotter *et al.* 2011). Ultimately CNS myelination is orchestrated by an unknown number of extracellular factors and the removal of the *Fgfr1* in oligodendrocytes may be sufficient to enhance the intracellular signalling cascades that regulate the remyelination. Taken together, these results suggest that inhibition of oligodendrocyte *Fgfr1* can promote both the expression of BDNF and its receptor TrkB in chronic phase of EAE, hence promoting an enhanced recovery of *Fgfr1^{ind/-}* mice in chronic EAE.

TrkB activation leads to an enhanced PI3K/AKT and ERK1/2 signalling in the retinal ganglion cells (RGCs), ERK1/2 in particular appears to be responsible for promoting the survival of RGCs (Gupta *et al.* 2013). Blocking Lingo-1 in retina enhances AKT signalling in increased intra-ocular pressure animal models and thus plays a neuroprotective role (Gupta *et al.* 2013).

5.2.5 Decreased myelin inhibitors in Fgfr1^{ind-/-} mice

A molecule correlating with the extent of oligodendrocyte maturation and myelination is Lingo-1, a transmembrane protein with leucine rich repeats and an immunoglobulin domain expressed in neurons and oligodendrocytes. The nogo receptor-interacting protein (Lingo-1) is a key inhibitor of oligodendrocyte precursor cell differentiation and myelination *in vitro* (Mi *et al.* 2005) and *in vivo* (Mi *et al.* 2007). Deletion of Lingo-1 causes a less severe EAE disease course, improved axonal integrity, promoted axon remyelination (Mi *et al.* 2007), increased myelination, whereas its overexpression inhibits myelin formation (Bradl and Lassmann 2010). An anti-Lingo-1 antagonist applied before and after onset of symptoms results in less disease activity in acute EAE (Mi *et al.* 2007). In our study impaired signalling via oligodendroglial Fgfr1 was associated with downregulated Lingo-1 expression in the chronic phase of EAE suggesting that this inhibitor is controlled by oligodendroglial Fgfr1 as well. Collectively, these data suggest a mechanism wherein FGF, signalling through oligodendrocyte-expressed Fgfr1, could be a key factor influencing inflammation through mediating chemokines and neuronal growth factors and receptors. In addition, data showed that inhibition of Lingo-1 activity *in vitro* and *in vivo* promotes outgrowth of oligodendrocyte processes and leads to highly developed myelinated axons (Zhou *et al.* 2012a).

Our finding that signalling via oligodendroglial Fgfr1 modulates clinical disease activity and inflammation gives the opportunity for a targeted molecular therapy. Selective and multikinase FGFR inhibitors are currently being tested in patients with genetically selected tumors with promising efficacy in some of these trials (Dienstmann *et al.* 2014). Tyrosine kinase inhibitors are active against kinases such as VEGFR or PDGFR. Luzitanib, a VEGFR/FGFR inhibitor has been applied successfully in FGFR1-amplified breast tumors (Dienstmann *et al.* 2014). In addition, monoclonal antibodies such as FP-1039 binding to the extracellular domain of FGFRs are used in clinical testings (Dienstmann *et al.* 2014). Signalling via oligodendroglial Fgfr1 also modulates Lingo-1 expression suggesting that Lingo-1 inhibition could be a promising approach to further decrease the effects of the receptor. A Lingo-1 antagonist has been used successfully to promote remyelination in EAE (Mi *et al.* 2007) and inhibition of Lingo-1 is has been tested in a Phase I clinical multiple sclerosis trial (NCT01244139).

Lingo-1 is the co-receptor of Nogo-66 receptor (NgR1) and lack of Lingo-1 will significantly decrease the activity of the NgR1 signalling pathway. Binding of Lingo-1 with NgR1 can activate the NgR1 signalling pathway, leading to inhibition of oligodendrocyte differentiation and myelination in the central nervous system (Zhou *et al.* 2012a). Lingo-1 has also been found to bind with epidermal growth factor receptor (EGFR) and induce down regulation of the activity of EGFR–PI3K–AKT signalling (Zhou *et al.* 2012a), whereas the interaction of Lingo-1 with FGFR1 is not known. We provided evidence for Lingo-1 downregulation and increased AKT phosphorylation in *Fgfr1^{ind/-}* mice.

Our data clearly point to a key role for *Fgfr1* expressed by oligodendrocytes in MOG₃₅₋₅₅ induced EAE. Importantly, our strategy to selectively delete *Fgfr1* from oligodendrocytes is the first to unequivocally identify a clear role for *Fgfr1* in mediating CNS repair in EAE. Other studies have implicated *Fgfr1* in CNS myelination; for example, targeted deletion of *Fgfr1* in oligodendrocyte lineage cells by the PLP promoter showed significantly enhanced axonal density and number of oligodendrocytes in cuprizone mediated toxic demyelination model (Zhou *et al.* 2012).

5.3 IFN β -1a treatment causes a milder disease course in *Fgfr1^{ind/-}* mice

Interferon β -1a treated *Fgfr1^{ind/-}* mice showed delayed onset of disease and milder disease course of EAE. Type 1-interferons (IFN-1) such as IFN- α and IFN- β , are involved in various aspects of immune responses. IFN- β has been used for more than 15 years as a first-line treatment for MS, and also markedly attenuates EAE development. The mechanisms of action of IFN- β involves multiple immunoregulatory functions, including blocking the trafficking of lymphocytes to the CNS (Floris *et al.* 2002), reducing expression of major histocompatibility class II molecules (Jiang *et al.* 1995), attenuating T cell proliferation and altering the cytokine milieu from pro-inflammatory to anti-inflammatory (Ramgolam *et al.* 2009). The combination of *Fgfr1* knockdown and selective preventive treatment with IFN β -1a in our EAE model confirms that *Fgfr1* is an attractive target for therapeutic intervention.

In vitro, PD166866, a potent Fgfr1 inhibitor does not show enhanced oli-neu oligodendrocyte cell proliferation. Fgfr1 regulates proliferation and differentiation through ERK and AKT pathways. Inhibition of Fgfr1 *in vitro* down regulates oli-neu cell proliferation. The reason for this diversity in response of oligodendrocytes to Fgfr1 *in vivo* is the cross talk and heterogeneity of progenitor populations of the cells in the specific tissues. Although we do not fully understand the mechanism of action of the Fgfr1 inhibition and IFN β -1b combination in oli-neu cells, future studies are needed to clarify the mechanisms behind the regulation. Considering that FGFR inhibitors are used in cancer trials, the oligodendroglial Fgfr1 pathway may provide a new target for therapy in multiple sclerosis.

FGFR pathway plays a distinct and major role in cancer as it directly promotes the endothelial cell proliferation and tumor neoangiogenesis and having complementary and synergistic effects with the vascular endothelial cell growth factor (VEGF) signalling (Dienstmann *et al.* 2014). Recent knock down and selective pharmacological inhibition of FGFR studies promote FGFR as a target for cancer treatment. Different FGFR pathway aberrations have been identified in cancer. (i) receptor overexpression by gene amplification or post-transcriptional regulation; (ii) mutated FGFR produces constitutively active or exhibit reduced dependence on ligand binding for activation; (iii) constitutive FGFR kinase activity with the expression of FGFR-fusion protein; (iv) alternative splicing of FGFR and isoform switching, which substantially alters ligand specificity increasing the range of FGFs that can stimulate tumor cells; and (v) up-regulation of FGF expression in cancer or stromal cells and the enhanced release of FGFs from the extracellular matrix, resulting in paracrine/autocrine activation of the pathway (Dienstmann *et al.* 2014).

In conclusion, the present study provides first evidence that inhibition of Fgfr1 in oligodendrocytes enhanced recovery of chronic EAE through controlling of immune cell infiltration. This effect may be caused by a reduction of activated immune cells and decreased cytokine and chemokine levels. Therefore, oligodendroglial Fgfr1 may represent an interesting therapeutic target for MS. The detailed molecular mechanism(s) will have to be explored in the future.

6 SUMMARY

Fibroblast growth factor and receptors play an important role in various cellular processes in CNS. Role of Fgfr1 in Multiple sclerosis and EAE is not understood, a recent study on toxic demyelination oligodendroglial Fgfr1 knockout mice showed increased axonal density and remyelination.

The current study focuses on the oligodendroglial Fgfr1 in EAE, an animal model for Multiple sclerosis. There were no phenotypic differences in the Fgfr1^{ind-/-} mice. Impaired signalling via oligodendroglial Fgfr1 had a beneficial effect on MOG₃₅₋₅₅-induced EAE. Ablation of oligodendroglial Fgfr1 reduced the disease course, cellular inflammation, demyelination and increased axonal density. Cellular inflammation was regulated by the proinflammatory cytokines TNF- α , IL-1 β and IL-6, and the chemokine CX3CL1-CX3CR1 pathway in our model. Increased BDNF and TrkB receptor expression was seen in Fgfr1^{ind-/-} mice in our model associated with disease recovery. Myelin inhibitor Lingo-1 expression was less in Fgfr1^{ind-/-} mice in chronic EAE. IFN β -1a prevention treatment caused the milder EAE disease course in Fgfr1^{ind-/-} mice. Ablation of Fgfr1 in oligodendrocytes showed an increased expression of ERK and AKT phosphorylation and TrkB and BDNF expression in the spinal cord. Considering that FGFR inhibitors are used in cancer trials, the oligodendroglial Fgfr1 pathway may provide a new target for therapy in multiple sclerosis.

ZUSAMMENFASSUNG

Der Fibroblasten-Wachstumsfaktor und seine Rezeptoren spielen eine wichtige Rolle in verschiedenen Zellprozessen im ZNS. Welche Rolle Fgfr1 bei MS (*Multiple Sklerose*) und EAE (*Experimentelle autoimmune Enzephalomyelitis*) spielt, ist unbekannt. Eine Studie zur Funktion des Oligodendrozyten-spezifischen Fgfr1 in dem Cuprizone-Modell ergab, dass das Fehlen von FGFR1 zu einem axonalen Dichteverlust führt.

Die vorliegende Studie richtet ihren Fokus auf das Oligodendrozyten-spezifische Fgfr1 bei EAE, einem Tiermodell für MS. Es gab keine Unterschiede im Phänotyp von Fgfr1^{ind/-}-Mäusen. Der Signalweg, der durch oligodendrozytäres Fgfr1 vermittelt wird, führt zu einem mildereren Krankheitsverlauf, geringerer zellulärer Inflammation und weniger Degeneration von Myelinscheiden und Axonen. Die zelluläre Inflammation wird durch die proinflammatorischen Zytokine TNF- α , IL-1 β und IL-6 und den Pathway der Chemokine CX3CL1-CX3CR1 reguliert. Präventive Behandlung mit IFN β -1a mildert den Krankheitsverlauf von EAE in Fgfr1^{ind/-} Mäusen ab. Die Entfernung von Fgfr1 in Oligodendrozyten führt zu einer vermehrten Expression von ERK und AKT-Phosphorylierung sowie TrkB- und BDNF-Expression. Unter der Annahme, dass Fgfr1-Inhibitoren in der Krebstherapie eingesetzt werden, könnte der oligodendrozytäre Fgfr1-Signalweg ein Ziel für eine Therapie der Multiplen Sklerose darstellen.

REFERENCES

- Artico M, Bronzetti E *et al* (2008) Neurotrophins and their receptors in human lingual tonsil: an immunohistochemical analysis. *Oncol Rep* 20: 1201-1216.
- Bachis A, Major EO, Mocchetti I (2003) Brain-derived neurotrophic factor inhibits human immunodeficiency virus-1/gp120-mediated cerebellar granule cell death by preventing gp120 internalization. *J Neurosci* 23: 5715-5722.
- Bankston AN, Mandler MD, Feng Y (2013) Oligodendroglia and neurotrophic factors in neurodegeneration. *Neurosci Bull* 29(2): 216-228.
- Bansal and Pfeiffer (1997) FGF-2 converts mature oligodendrocytes to a novel phenotype. *Journal of Neurosci Res* 50: 215-228.
- Bansal *et al* (1996) Regulation of FGF receptors in the oligodendrocyte lineage. *Mol and Cell Neurosci* 7: 263-275.
- Bansal R (2002) Fibroblast growth factors and their receptors in oligodendrocyte development: implications for demyelination and remyelination. *Dev Neurosci* 24: 35-46.
- Basu A, Krady JK, O'Malley M, Styren SD, DeKosky ST, Levison SW (2002) The type 1 interleukin-1 receptor is essential for the efficient activation of microglia and the induction of multiple proinflammatory mediators in response to brain injury. *J Neurosci* 22: 6071-6082.
- Beenken A and Mohammadi M (2009) The FGF family: biology, pathophysiology and therapy. *Nature Reviews Drug Discovery* 8(3): 235-253.
- Belov and Mohammadi (2013) Molecular mechanisms of fibroblast growth factor signalling in physiology and pathology. *Cold Spring Harb Perspect Biol* 5(6): doi:10.1101/cshperspect.a015958.
- Bittner S, Afzali AM, Wiendl H, Meuth SG (2014) Myelin Oligodendrocyte Glycoprotein (MOG35-55) Induced Experimental Autoimmune Encephalomyelitis (EAE) in C57BL/6 Mice. *J Vis Exp* (86), e51275, doi:10.3791/51275.
- Bø L, Esiri M, Evangelou N, Kuhlmann T (2013) Demyelination and remyelination in multiple sclerosis. In: Duncan ID, Franklin RJM (eds) *Myelin Repair and Neuroprotection in Multiple Sclerosis*. New York: Springer. pp. 23-45, doi: 10.1007/978-1-4614-2218-1_2.
- Bohrer LR, Schwertfeger KL (2012) Macrophages promote fibroblast growth factor receptor-driven tumor cell migration and invasion in a Cxcr2-dependent manner. *Molecular Cancer Research* 10(10): 1294-1305.

- Bonora M, De ME, Patergnani S *et al.* (2014) Tumor necrosis factor- α impairs oligodendroglial differentiation through a mitochondria-dependent process. *Cell Death and Differentiation* 1-11.
- Bradl M and Lassmann H (2010) Oligodendrocytes: biology and pathology. *Acta Neuropathol* 119:37-53.
- Brück *et al.* (2012) Therapeutic decisions in multiple sclerosis moving beyond efficacy. *JAMA Neurology* 70(10): 1315-1324.
- Butt AM and Dinsdale J (2005) Fibroblast growth factor 2 induces loss of adult oligodendrocytes and myelin *In vivo*. *Exp Neurology* 192: 125-133.
- Caminero A, Comabella M, Montalban X (2011) Tumor necrosis factor alpha (TNF- α), anti-TNF- α and demyelination revisited: an ongoing story. *J Neuroimmunol* 234: 1-6.
- Chao MV (2003) Neurotrophins and their receptors: a convergence point for many signalling pathways. *Nature Review Neuroscience* 4: 299-309.
- Clark AK *et al.* (2010) P2X7-dependent release of interleukin-1 β and nociception in the spinal cord following lipopolysaccharide. *The Journal of Neuroscience* 30(2): 573-582.
- Clemente D, Ortega MC, Arenzana FJ, de CF (2011) FGF-2 and Anosmin-1 are selectively expressed in different types of multiple sclerosis lesions. *J Neurosci* 31: 14899-14909.
- Clemente *et al.* (2013) The effect of glia–glia interactions on oligodendrocyte precursor cell biology during development and in demyelinating diseases. *Frontiers in Cellular Neuroscience* 7: 268.
- Coddou C, Stojilkovic SS, Huidobro-Toro JP (2011) Allosteric modulation of ATP-gated P2X receptor channels. *Reviews in the Neurosciences* 22(3): 335-354.
- Compston A *et al.* (2005) The story of multiple sclerosis. In: Compston A *et al.* (eds) *McAlpines's Multiple sclerosis*. Fourth edition, Churchill Livingstone, Elsevier publication.
- Constantinescu CS *et al.* (2011) Experimental autoimmune encephalomyelitis (EAE) as a model for multiple sclerosis (MS). *British J of Pharmacology* 164: 1079-1106.
- Daniele G *et al.* (2012) FGF receptor inhibitors: role in cancer therapy. *Curr Oncol Rep* 14: 111-119.
- Dienstmann R, Rodon J, Prat A *et al.* (2014) Genomic aberrations in the FGFR pathway: opportunities for targeted therapies in solid tumors. *Ann Oncol* 25: 552-563.
- Doherty and Walsh (1996) CAM-FGF receptor interactions: a model for axonal growth. *Mol and Cell Neuroscience* 8: 99-111.

- Dutta R, Trapp BD (2011) Mechanisms of neuronal dysfunction and degeneration in multiple sclerosis. *Prog Neurobiol* 93(1): 1-12.
- Esain V, Postlethwait JH, Charnay P, Ghislain J (2010) FGF-receptor signalling controls neural cell diversity in the zebrafish hindbrain by regulating Olig2 and sox9. *Development* 137: 33-42.
- Fletcher JM, Lalor SJ, Sweeney CM, Tubridy N, Mills KH (2010) T cells in multiple sclerosis and experimental autoimmune encephalomyelitis. *Clin Exp Immunol* 162: 1-11.
- Flores AI, Narayanan SP, Morse EN, Shick HE, Yin X, Kidd G, Avila RL, Kirschner DA, Macklin WB (2008) Constitutively active Akt induces enhanced myelination in the CNS. *J Neurosci* 28: 7174 -7183.
- Floris S, Ruuls SR, Wierinckx A, Van Der Pol SM, Dopp E, Van Der Meide PH, Dijkstra CD, De Vries HE (2002) Interferon-beta directly influences monocyte infiltration into the central nervous system. *J Neuroimmunol* 127: 69-79.
- Fortin D, Rom E, Sun H, Yayan A, Bansal R (2005) Distinct fibroblast growth factor (FGF)/FGF receptor signaling pairs initiate diverse cellular responses in the oligodendrocyte lineage. *J Neurosci* 25: 7470-7479.
- Furdui *et al.* (2006) Autophosphorylation of FGFR1 kinase is mediated by a sequential and precisely ordered reaction. *Mol Cell* 21(5): 711-717.
- Furusho M, Kaga Y, Ishii A, Hebert JM, Bansal R (2011) Fibroblast growth factor signaling is required for the generation of oligodendrocyte progenitors from the embryonic forebrain. *J Neurosci* 31: 5055–5066.
- Galvez-Contreras AY, Gonzalez-Castaneda RE, Luquin S, Gonzalez-Perez O (2012) Role of fibroblast growth factor receptors in astrocytic stem cells. *Curr Signal Transduct Ther* 7: 81-86.
- Garcia JA, Pino PA, Mizutani M *et al.* (2013) Regulation of adaptive immunity by the fractalkine receptor during autoimmune inflammation. *J Immunol* 191: 1063-1072.
- Goetz R, Mohammadi M (2013) Exploring mechanisms of FGF signalling through the lens of structural biology. *Nat Rev Mol Cell Biol* 14: 166-180.
- Gold R, Linington C, Lassmann H (2006) Understanding pathogenesis and therapy of multiple sclerosis via animal models: 70 years of merits and culprits in experimental autoimmune encephalomyelitis research. *Brain* 129: 1953-1971.
- Goldenberg MM (2012) Multiple sclerosis review. *Pharmacy and Therapeutics* 37: 175-184

- Gudi V, Skuljec J *et al.* (2011) Spatial and temporal profiles of growth factor expression during CNS demyelination reveal the dynamics of repair priming. *PLoS One* 6: e22623.
- Guillemot and Zimmer (2011) From cradle to grave: the multiple roles of fibroblast growth factors in neural development. *Neuron* 71(4): 574-588.
- Gupta VK, You Y *et al.* (2013) TrkB receptor signalling: implications in neurodegenerative, psychiatric and proliferative disorders. *Int J Mol Sci* 14: 10122-10142.
- Harirchian MH, Tekieh AH, Modabbernia A *et al.* (2012) Serum and CSF PDGF-AA and FGF-2 in relapsing-remitting multiple sclerosis: a case-control study. *Eur J Neurol* 19: 241-247.
- Harrison JK, Jiang Y, Chen S *et al.* (1998) Role for neuronally derived fractalkine in mediating interactions between neurons and CX3CR1-expressing microglia. *Proceedings of the National Academy of Sciences of the US* 95(18): 10896-10901.
- Hartmann JT, Haap M, Kopp HG, Lipp HP (2009) Tyrosine kinase inhibitors - a review on pharmacology, metabolism and side effects. *Curr Drug Metab.* 10(5): 470-81.
- Hidaka Y, Inaba Y, Matsuda K *et al.* (2014) Cytokine production profiles in chronic relapsing-remitting experimental autoimmune encephalomyelitis: IFN-gamma and TNF-alpha are important participants in the first attack but not in the relapse. *J Neurol Sci* 340: 117-122.
- Hoglund AR and Maghazachi AA (2014) Multiple sclerosis and the role of immune cells. *World J Exp Med* 4(3): 27-37.
- Inoue H, Lin L, Lee X *et al.* (2007) Inhibition of the leucine-rich repeat protein LINGO-1 enhances survival, structure, and function of dopaminergic neurons in Parkinson's disease models. *Proc Natl Acad Sci* 104: 14430-14435.
- Inoue M and Shinohara ML (2013) The role of interferon-b in the treatment of multiple sclerosis and experimental autoimmune encephalomyelitis – in the perspective of inflammasomes. *Immunology* 139: 11-18.
- Irvine KA, Blakemore WF (2008) Remyelination protects axons from demyelination-associated axon degeneration. *Brain* 131: 1464-1477.
- Isozaki T, Kasama T, Takahashi R *et al.* (2008) Synergistic induction of CX3CL1 by TNF alpha and IFN gamma in osteoblasts from rheumatoid arthritis: involvement of NF-kappa B and STAT-1 signaling pathways. *J Inflamm Res* 1: 19-28.
- Itoh N and Ornitz DM (2008) Functional evolutionary history of the mouse Fgf gene family. *Developmental dynamics* 237: 18-27.

- Itoh N *et al* (1990) The complete amino acid sequence of the shorter form of human basic fibroblast growth factor receptor deduced from its cDNA. *Biochem Biophys Res Commun* 169(2): 680-685.
- Jiang H, Milo R, Swoveland P, Johnson KP, Panitch H, Dhib-Jalbut S (1995) Interferon beta-1b reduces interferon gamma-induced antigen-presenting capacity of human glial and B cells. *J Neuroimmunol* 61: 17-25.
- Johnson DE and Williams LT (1993) Structural and functional diversity in the FGF receptor multigene family. *Adv Cancer Res* 60: 1-41.
- Jones M, Tussey L, Athanasou N, Jackson DG (2000) Heparan sulfate proteoglycan isoforms of the CD44 hyaluronan receptor induced in human inflammatory macrophages can function as paracrine regulators of fibroblast growth factor action. *J Biol Chem* 275: 7964-7974.
- Kastenbauer S, Koedel U, Wick M, Kieseier BC, Hartung HP, Pfister HW (2003) CSF and serum levels of soluble fractalkine (CX3CL1) in inflammatory diseases of the nervous system. *J Neuroimmunol* 137: 210-217.
- Kermani P, Hempstead B (2007) Brain-derived neurotrophic factor: a newly described mediator of angiogenesis. *Trends Cardiovasc Med* 17: 140-143.
- Kerschensteiner M, Gallmeier E, Behrens L *et al.* (1999) Activated human T cells, B cells, and monocytes produce brain-derived neurotrophic factor *In vitro* and in inflammatory brain lesions: a neuroprotective role of inflammation? *J Exp Med* 189: 865-870.
- Knights V and Cook SJ (2010) De-regulated FGF receptors as therapeutic targets in cancer. *Pharmacology and Therapeutics* 125: 105-117.
- Kotter MR, Stadelmann C, Hartung HP (2011) Enhancing remyelination in disease--can we wrap it up? *Brain* 134: 1882-1900.
- Kuhlmann T, Miron V, Cui Q, Wegner C, Antel J, Bruck W (2008) Differentiation block of oligodendroglial progenitor cells as a cause for remyelination failure in chronic multiple sclerosis. *Brain* 131: 1749-1758.
- Lee DH, Geyer E, Flach AC *et al.* (2012) Central nervous system rather than immune cell-derived BDNF mediates axonal protective effects early in autoimmune demyelination. *Acta Neuropathol* 123: 247-258.
- Lin HW, Basu A, Druckman C, Cicchese M, Krady JK, Levison SW (2006) Astrogliosis is delayed in type 1 interleukin-1 receptor-null mice following a penetrating brain injury. *J Neuroinflammation* 3: 15.
- Lindia JA, McGowan E, Jochowitz N, Abbadie C (2005) Induction of CX3CL1 expression in astrocytes and CX3CR1 in microglia in the spinal cord of a rat model of neuropathic pain. *Journal of Pain* 6(7): 434-438.

- Linker RA, Lee DH, Demir S *et al.* (2010) Functional role of brain-derived neurotrophic factor in neuroprotective autoimmunity: therapeutic implications in a model of multiple sclerosis. *Brain* 133: 2248-2263.
- Liu X, Mashour GA, Webster HF, Kurtz A (1998) Basic FGF and FGF receptor 1 are expressed in microglia during experimental autoimmune encephalomyelitis: temporally distinct expression of midkine and pleiotrophin. *Glia* 24: 390-397.
- Lock C, Hermans G, Pedotti R *et al.* (2002) Gene-microarray analysis of multiple sclerosis lesions yields new targets validated in autoimmune encephalomyelitis. *Nat Med* 8: 500-508.
- Lovett-Racke AE, Yang Y, Racke MK (2011) Th1 versus Th17: Are T cell cytokines relevant in multiple sclerosis? *Biochimica et Biophysica Acta* 1812: 246-251.
- Markus A, Patel TD, Snider WD (2002) Neurotrophic factors and axonal growth. *Curr Opin Neurobiology* 12: 523-31.
- Mi S, Hu B, Hahm K *et al.* (2007) LINGO-1 antagonist promotes spinal cord remyelination and axonal integrity in MOG-induced experimental autoimmune encephalomyelitis. *Nat Med* 13: 1228-1233.
- Mi S, Miller RH, Lee X *et al.* (2005) LINGO-1 negatively regulates myelination by oligodendrocytes. *Nat Neurosci* 8: 745-751.
- Mills JH, Alabanza LM, Mahamed DA, Bynoe MS (2012) Extracellular adenosine signaling induces CX3CL1 expression in the brain to promote experimental autoimmune encephalomyelitis. *J Neuroinflammation* 9: 193.
- Milo R and Miller A (2014) Revised diagnostic criteria of multiple sclerosis. *Autoimmunity Reviews* 13: 518-524.
- Mirshafiey A, Ghalamfarsa G, Asghari B, Azizi G (2014) Receptor tyrosine kinase and tyrosine kinase inhibitors: new hope for success in multiple sclerosis therapy. *Innov Clin Neurosci* 11(7-8): 23-36.
- Narayanan SP, Flores AI, Wang F, Macklin WB (2009) Akt signals through the mammalian target of rapamycin pathway to regulate CNS myelination. *J Neurosci* 29: 6860-6870.
- Omari KM, John GR, Sealton SC, Raine CS (2005) CXC chemokine receptors on human oligodendrocytes: implications for multiple sclerosis. *Brain* 128: 1003-1015.
- Patel J and Balabanov R (2012) Molecular mechanisms of oligodendrocyte injury in multiple sclerosis and experimental autoimmune encephalomyelitis. *Int J Mol Sci* 13: 10647-10659.

- Pollinger B, Krishnamoorthy G, Berer K, Lassmann H, Bosl MR, Dunn R *et al.* (2009) Spontaneous relapsing-remitting EAE in the SJL/J mouse: MOG-reactive transgenic T cells recruit endogenous MOG-specific B cells. *J Exp Med* 206: 1303-16.
- Polman CH, Reingold SC, Banwell B, Clanet M, Cohen JA, Filippi M *et al.* (2011) Diagnostic criteria for multiple sclerosis: 2010 revisions to the McDonald criteria. *Ann Neurol* 69(2): 292-302.
- Prins M, Eriksson C, Wierinckx A *et al.* (2013) Interleukin-1beta and interleukin-1 receptor antagonist appear in grey matter additionally to white matter lesions during experimental multiple sclerosis. *PLoS One* 8: e83835.
- Quintana A, Muller M, Frausto RF *et al.* (2009) Site-specific production of IL-6 in the central nervous system retargets and enhances the inflammatory response in experimental autoimmune encephalomyelitis. *J Immunol* 183: 2079-2088.
- Ramgolam VS, Sha Y, Jin J, Zhang X, Markovic-Plese S (2009) IFN-beta inhibits human Th17 cell differentiation. *J Immunol* 183: 5418-5427.
- Rangachari M and Kuchroo VK (2013) Using EAE to better understand principles of immune function and autoimmune pathology. *J of Autoimmunity* 45: 31-39.
- Reed JR, Stone MD, Beadnell TC, Ryu Y, Griffin TJ *et al.* (2012) Fibroblast Growth Factor Receptor 1 Activation in Mammary Tumor Cells Promotes Macrophage Recruitment in a CX3CL1-Dependent Manner. *PLoS ONE* 7(9): e45877. doi:10.1371/journal.pone.0045877
- Reuss B, Dono R, Unsicker K (2003) Functions of fibroblast growth factor (FGF)-2 and FGF-5 in astroglial differentiation and blood-brain barrier permeability: evidence from mouse mutants. *J Neurosci* 23: 6404-6412.
- Reuss B, von Bohlen und HO (2003) Fibroblast growth factors and their receptors in the central nervous system. *Cell Tissue Res* 313: 139-157.
- Robin JM Franklin (2002) Why does remyelination fail in multiple sclerosis? *Nature Reviews Neuroscience* 3: 705-714.
- Rodgers JM, Miller SD (2012) Cytokine control of inflammation and repair in the pathology of multiple sclerosis. *Yale J Biol Med* 85(4): 447-68.
- Rossi S, Furlan R, De CV *et al.* (2012) Interleukin-1beta causes synaptic hyperexcitability in multiple sclerosis. *Ann Neurol* 71: 76-83.
- Rottlaender A, Villwock H, Addicks K, Kuerten S (2011) Neuroprotective role of fibroblast growth factor-2 in experimental autoimmune encephalomyelitis. *Immunology* 133: 370-378.

- Ruffini F, Furlan R, Poliani PL *et al.* (2001) Fibroblast growth factor-II gene therapy reverts the clinical course and the pathological signs of chronic experimental autoimmune encephalomyelitis in C57BL/6 mice. *Gene Ther* 8: 1207-1213.
- Sanders VJ *et al.* (2000) Fibroblast Growth Factor Modulates HIV Coreceptor CXCR4 Expression by Neural Cells. *Journal of Neuroscience Research* 59: 671-679.
- Sarchielli P, Di FM, Ercolani MV *et al.* (2008) Fibroblast growth factor-2 levels are elevated in the cerebrospinal fluid of multiple sclerosis patients. *Neurosci Lett* 435: 223-228.
- Smith KM, Maragnoli ME, Phull PM, Tran KM, Choubey L *et al.* (2014) Fgfr1 inactivation in the mouse telencephalon results in impaired maturation of interneurons expressing parvalbumin. *PLoS ONE* 9(8): e103696. doi:10.1371/journal.pone.0103696
- Stadelmann C, Kerschensteiner M, Misgeld T, Bruck W, Hohlfeld R, Lassmann H (2002) BDNF and gp145trkB in multiple sclerosis brain lesions: neuroprotective interactions between immune and neuronal cells? *Brain* 125: 75-85.
- Stadelmann C, Wegner C, Brück W (2011) Inflammation, demyelination, and degeneration-recent insights from MS pathology. *Biochimica et Biophysica Acta* 1812: 275-282.
- Steinman L (2008) Nuanced roles of cytokines in three major human brain disorders. *J Clin Invest* 118: 3557-3563.
- Steinmann and Zamvil (2003) Transcriptional analysis of targets in multiple sclerosis. *Nature Reviews Immunology* 3: 483-492.
- Stojkovic L, Djuric T, Stankovic A *et al.* (2012) The association of V249I and T280M fractalkine receptor haplotypes with disease course of multiple sclerosis. *J Neuroimmunol* 245: 87-92.
- Su *et al.* (2014) Role of FGF/FGFR signaling in skeletal development and homeostasis: learning from mouse models. *Bone research* 2: 14003.
- Sunnemark D, Eltayeb S, Nilsson M *et al.* (2005) CX3CL1 (fractalkine) and CX3CR1 expression in myelin oligodendrocyte glycoprotein-induced experimental autoimmune encephalomyelitis: kinetics and cellular origin. *J Neuroinflammation* 2: 17.
- Takeo Isozaki, Tsuyoshi Kasama, Ryo Takahashi *et al.* (2008) Synergistic induction of CX3CL1 by TNF alpha and IFN gamma in osteoblasts from rheumatoid arthritis: involvement of NF-kappa B and STAT-1 signaling pathways. *Journal of Inflammation research* 1: 19-28.
- Turner N, Grose R (2010) Fibroblast growth factor signalling: from development to Cancer. *Nature Neuroscience* 10: 116-129.

- Wingerchuk M and Carter JL (2014) Multiple Sclerosis: current and emerging disease-modifying therapies and treatment strategies. *Mayo Clin Proc* 89(2): 225-240.
- Wong I, Liao H, Bai X, Zaknic A, Zhong J, Guan Y, Li HY, Wang YJ, Zhou XF (2010) ProBDNF inhibits infiltration of ED1+ macrophages after spinal cord injury. *Brain Behav Immun* 24: 585-597.
- Xiao J, Wong AW, Willingham MM, van den Buuse M, Kilpatrick TJ, Murray SS (2010) Brain-derived neurotrophic factor promotes central nervous system myelination via a direct effect upon oligodendrocytes. *Neurosignals* 18:186-202.
- Xu X *et al.* (2002) Generation of Fgfr1 conditional Knockout mice. *Genesis* 32: 85-86.
- Yang *et al.* (2010) Fibroblast growth factor receptors 1 and 2 in keratinocytes control the epidermal barrier and cutaneous homeostasis. *J Cell Biol* 188(6): 935-952.
- Zhang *et al.* (2006) Receptor Specificity of the Fibroblast Growth Factor Family: the complete mammalian FGF family. *J Biol Chem* 281(23): 15694-15700.
- Zhou YX, Pannu R, Le TQ, Armstrong RC (2012) Fibroblast growth factor 1 (FGFR1) modulation regulates repair capacity of oligodendrocyte progenitor cells following chronic demyelination. *Neurobiol Dis* 45: 196-205.
- Zhou ZD, Sathiyamoorthy S, Tan EK (2012a) LINGO-1 and Neurodegeneration: Pathophysiologic Clues for Essential Tremor? Tremor and Other Hyperkinetic Movements Tremor Other Hyperkinet (NY) 2: tre-02-51-249-1.
- Zhu W, Acosta C, MacNeil B *et al.* (2013) Elevated Expression of Fractalkine (CX3CL1) and Fractalkine Receptor (CX3CR1) in the Dorsal Root Ganglia and Spinal Cord in Experimental Autoimmune Encephalomyelitis: Implications in Multiple Sclerosis-Induced Neuropathic Pain. *Bio Med Research International*. Article ID 480702. doi:10.1155/2013/480702



ACKNOWLEDGEMENTS

My first and foremost thankful goes to my advisor, **PD Dr. Martin Berghoff**, my supervisor supporting me during these past four years. Dr. Berghoff is the cool advisor and one of the smartest people I know. I hope that I could be as lively, cool and energetic as Dr. Berghoff. He has been supportive and has given me the freedom to pursue various projects without objection. He has also provided insightful support to expose me to various pharmaceutical industries representatives. A good support system is important to surviving and staying sane in graduation time. I was lucky to be a person who had the support from Dr. Berghoff in my graduation.

I am also very grateful to **Prof. Dr. Reinhard Lakes-Harlan** who accepted as my first supervisor for my Dr.rer.nat thesis. He provided the opportunity to present and discuss my research work in his laboratory.

I like to extend my grateful to **Dr. Mario Giraldo Velazguz**, who formed the project and recruited me as Dr.rer.nat student in our research group. Upon my application within one day he called me for the interview and on first meeting he confirmed me that you are my research scholar. I am also very grateful to him for his scientific advice and knowledge and many insightful discussions and suggestions. He is my primary resource for getting my science questions answered and was instrumental in helping me cranked out this thesis successful. Presently he is alumni in our group and working in Socialstiftung Bambug, Germany.

I will forever be thankful to my former research advisor, **PD Dr. Gero Benckiser**. He has been helpful in providing advice many times during my graduate career. He was and remains my best role model for a scientist, mentor, teacher and personnel adviser. He was the reason gave opportunity to start my research in international laboratory. I am very grateful to him and his wife for their love.

I also thank our collaborator **Prof. Dr. Christina Stadelmann**, Institute for Neuropathology, Göttingen, Germany, for her help in arranging technical assitenship in her lab and valuable discussions in my research. She´s a great neuropathologist and has taught me various points on histology and immunostaining. She treated me as her own student and gave valuable suggestions.

I would like to extend my sincere thanks to the “Giessen Graduate school of Life Sciences” (GGL), where I had the opportunity to acquire scientific knowledge and got the grant for lab rotation in Harvard University, Boston, USA.

I thank my fellow graduate Salar Kamali (formerly Esmaeil Kamali) who helped me in beginning of my research in our lab and we discuss about both of our projects till the end. I thank my other fellow graduates Backialakshmi, Liza for research discussion and our colleagues Helga, Cornelia, Edith and Marita for the wonderful time in our lab. I thank Dr. Daniel Zahner, animal facility in charge for his help.

I also thanks **my friends (too many to list here but you know who you are!!!)**, for providing support and friendship that I needed. Especially Balaji, Vijith, Bala, Balaprabu, Srikanth, Kishore.

I especially thank my grandmother, dad, mom and brother. My hard-working grandmother have sacrificed her life for me and my brother and provided unconditional love and care. I love them so much, and I would not have made it this far without them. My brother Vinoth has been my best friend all my life and I love him dearly and thank him for all his advice and support. I know I always have my family to count on when times are rough. Special thanks to the newest additions to our family, Priya, my better half, my wife as well as her wonderful family who all have been supporting and caring.

I also have to thank the members of my Dr.rer.nat committee for their helpful career advice and suggestions in general.

I grateful to **Merck Serono GmbH** and **Novartis Pharmaceutical** who sponsored my thesis and supported me to attend international conferences in Denmark and Chicago, USA.

PUBLICATIONS

1. **Ranjithkumar Rajendran**, Mario Giraldo, Martin Berghoff (2011) Expression pattern of FGF/FGFR signal cascade in FGFR1^{-/-} mice. Poster. 5th GGL international conference, Giessen, Germany.
2. **Ranjithkumar Rajendran**, Mario Giraldo, Martin Berghoff (2012) Targeting FGFR1 in oligodendrocytes decreases the severity of MOG₃₅₋₅₅ induced EAE. Poster. 6th GGL international conference, Giessen, Germany.
3. **Ranjithkumar Rajendran**, Mario Giraldo, Martin Berghoff (2013) Impact of FGFR1 ablation and IFN β -1b treatment on Oli-neu oligodendrocytes. 29th Congress of the European Committee for Treatment and Research in Multiple Sclerosis, Oct 2-5, 2013, Copenhagen, Denmark. Multiple Sclerosis Journal. 19: (S1) 74-558.
4. **Ranjithkumar Rajendran**, Mario Giraldo, Martin Berghoff (Nov. 2013) Interaction of FGFR1 ablation and IFN β -1b treatment on oligodendrocytes. Research Day MS and Oppenheim Förderprises für MS, Novartis Pharmaceuticals, Nuremberg, Germany.
5. **Ranjithkumar Rajendran**, Mario Giraldo, Christine Stadelmann, Martin Berghoff (2014) Fgfr1 ablation in oligodendrocytes reduces disease severity and inflammation in the CNS in MOG₃₅₋₅₅ induced EAE. Neurology. Vol. 82 (10), Supplement P1.167.
6. **Ranjithkumar Rajendran**, Mario Giraldo, Christine Stadelmann, Martin Berghoff (2014) Oligodendroglial fibroblast growth factor receptor 1 is a key modulator of experimental autoimmune encephalomyelitis. Submitted in Acta Neuropathologica. 2014.
7. Mario Giraldo, Mathias Bähr, **Ranjithkumar Rajendran**, Walter Stühmer, Sabine Martin (2011) DCLK and its splicing variants could work like a possible switch protein regulating the neuronal regeneration potential in the retinal gene expression after optical nerve axotomy and in the retinal development. Poster. 19–22 October 2011, 5th Joint Triennial Congress of ECTRIMS and ACTRIMS, Amsterdam, The Netherlands.